The intracellular signaling pathway mediating the role of Nogo-A in regulating functional plasticity in the adult mouse hippocampus

Von der Fakultät für Lebenswissenschaften
der Technischen Universität Carolo-Wilhelmina zu Braunschweig
zur Erlangung des Grades
einer Doktorin der Naturwissenschaften
(Dr. rer. nat.)
genehmigte
Dissertation

von Cristina Iobbi
aus San Benedetto del Tronto / Italien

1. Referent:	Prof. Dr. Martin Korte
2. Referent:	Prof. Dr. Reinhard Köster
eingereicht am:	17.02.2016
mündliche Prüfung (Disputation) am:	29.04.2016

Druckjahr 2016

Vorveröffentlichungen der Dissertation

Teilergebnisse aus dieser Arbeit wurden mit Genehmigung der Fakultät für Lebenswissenschaften, vertreten durch den Mentor der Arbeit, in folgenden Beiträgen vorab veröffentlicht.

Publikationen

Berto GE, **Iobbi C**, Camera P, Scarpa E, Iampietro C, Bianchi F, Gai M, Sgrò F, Cristofani F, Gärtner A, Dotti CG, Di Cunto F. *The DCR protein TTC3 affects differentiation and Golgi compactness in neurons through specific actin-regulating pathways.* Plos One. 2014 Apr 2;9(4):e93721

Kempf A, Tews B, Arzt ME, Weinmann O, Obermair FJ, Pernet V, Zagrebelsky M, Delekate A, **Iobbi C**, Zemmar A, Ristic Z, Gullo M, Spies P, Dodd D, Gygax D, Korte M, Schwab ME. *The Sphingolipid Receptor S1PR2 is a Receptor for Nogo-A Repressing Synaptic Plasticity.* PLoS Biol. 2014 Jan;12(1):e1001763

Kellner Y, Fricke S, Kramer S, **Iobbi C**, Wierenga CJ, Schwab ME, Korte M, Zagrebelsky M. *Nogo-A controls structural plasticity at dendritic spines by rapidly modulating actin dynamics.* Hippocampus. 2016; 10.1002/hipo.22565

Iobbi C, Korte M, Zagrebelsky M. *Nogo-66 restricts synaptic strengthening via Lingo1 and the ROCK2-Cofilin pathway to control actin dynamics.* Cerebral Cortex. 2016; 10.1093/cercor/bhw122

Tagungsbeiträge

Iobbi C, Schwab ME, Zagrebelsky M, Korte M. *Nogo-A signaling modulates activity-dependent functional plasticity in the mouse hippocampus.* 9th FENS forum of European Neuroscience, Milan 2014

Iobbi C, Korte M, Zagrebelsky M. *Nogo-A influences structural dynamics of mossy fiber synapses.* 11th Göttingen Meeting of the German Neuroscience Society, Göttingen 2015

Abstract

In the developing and adult brain synaptic connections between neurons are plastic, allowing the acquisition of new information and their integration within existing memory traces, but at the same time they have to be stable to a certain extent in order to maintain old stored memories. It is now clear that specific molecular mechanisms come into play in order to regulate the tight balance between stability and plasticity processes, raising the question of how stability is achieved to limit plasticity events in the adult brain. In this context, Nogo-A has been described as a negative regulator of synaptic plasticity in the adult mouse hippocampus, a structure remaining plastic throughout the entire life. In particular, Nogo-A restricts long-term potentiation (LTP) at the Schaffer collateral-CA1 pathway via two extracellular domains, Nogo-A-Δ20 and Nogo-66. Although it has been shown that Nogo-66 signals via the Nogo Receptor 1 (NgR1) to regulate synaptic function, whether the NgR1 co-receptors, Lingo1 and p75^{NTR}, are involved in the signalling in this context is still not known. Moreover, the intracellular cascade mediating the activity of Nogo-66 and Nogo-A-Δ20 domains in restricting LTP is unexplored.

Here I combined electrophysiological and biochemical approaches in acute hippocampal slices to address these questions. First, I demonstrated that a loss-of-function approach for the NgR1 co-receptor Lingo1 results in a significant increase in LTP levels at the Schaffer collateral-CA1 pathway, and that Lingo1 is the NgR1 co-receptor mediating the role of Nogo-66 in restricting LTP. Moreover, these data show that while p75^{NTR} is not involved in mediating the Nogo-66 effect, it is required to mediate the role of NgR1 in attenuating LTD independently on Nogo-66. Finally, these results indicate that Nogo-66 signalling limits the magnitude of LTP by activating the intracellular ROCK2-Cofilin pathway to control the dynamics of the actin cytoskeleton, and these data suggest that also the Nogo-A-Δ20 domain-dependent signalling converge on the same intracellular cascade activated by Nogo-66 domain.

Functional and structural changes at synapses are correlated and together mediate long-lasting synaptic plasticity. In addition to the role of Nogo-A in restricting LTP, it has been shown to be involved in negatively regulating the morphological changes at dendritic spines. However, it remains an open question if Nogo-A controls these modifications at the presynaptic compartment. Here, I showed that Nogo-A modulates the structural remodelling of the presynaptic mossy fiber synapses. Indeed, while the acute neutralization of Nogo-A does not affect their motility, its chronic neutralization leads to a reduction of the size of the main terminal and of the length of the filopodial extensions.

Taken together, these data contribute to the understanding of how Nogo-A stabilizes neural circuits to limit plasticity events in the mature hippocampus.

Zusammenfassung

Das sich entwickelende, aber auch das adulte Gehirn ist in seinen synaptischen Verbindungen zwischen den Nervenzellen plastisch um die Übernahme von neuen Informationen und deren Integration in bestehende Gedächtnisspuren zu gewährleisten. Jedoch ist auch eine gewisse Stabilität erforderlich um schon vorhandenen Erinnerungen aufrecht zu halten. Bestimmte Moleküle spielen dabei eine Rolle. Sie regulieren das feine Gleichgewicht zwischen Stabilitäts- und Plastizitätsprozessen. Dies wirft die Frage auf wie Stabilität erreicht wird um die plastischen Vorgänge im Gehirn zu begrenzen. In diesem Zusammenhang wurde Nogo-A als negativer Regulator der synaptischen Plastizität im adulten Hippokampus der Maus beschrieben, eine Gehirnstruktur welche im gesamten Leben plastisch bleibt. Nogo-A schränkt hierbei die Langzeitpotenzierung (LTP) an der Schaffer Kollateral-CA1 Verbindung über zwei extrazelluläre Domänen, Nogo-A-Δ20 und Nogo-66, ein. Es konnte gezeigt werden, dass der Nogo-66 Signalweg über den Nogo Rezeptor 1 (NgR1) erfolgt um synaptische Plastizität zu regulieren. Jedoch ist unklar, ob die NgR1 Korezeptoren, Lingo1 und $p75^{NTR}$, auch in diesem Prozess beteiligt sind. Darüber hinaus ist die intrazelluläre Kaskade, welche die Aktivität der Nogo-66 und Nogo-A-Δ20 Domänen vermitteln um LTP zu beeinträchtigen, unerforscht.

Ich habe elektrophysiologische und biochemische Methoden in akuten Schnitten des Hippocampus kombiniert angewandt um dieser Fragestellung nachzugehen. Zuerst habe ich gezeigt, dass ein Verlust der Funktion des NgR1 Korezeptors Lingo1 zu einem signifikant erhöhten Level des LTPs an der Schaffer Kollateralen-CA1 Verbindung führt und dass Lingo-1 als Korezeptor des NgR1 die Rolle von Nogo-66 im Rahmen der LTP Beschränkung vermittelt. Darüber hinaus zeigen diese Daten, dass $p75^{NTR}$ nicht bei der Vermittlung der Nogo-66 Wirkung beteiligt ist, es aber erforderlich ist, um den Effekt von NgR1 beim Verminderten des LTDs unabhängig von Nogo-66 zu vermitteln. Schließlich zeigen diese Ergebnisse, dass der Nogo-66 Signalweg die Stärke des LTPs limitieren kann, indem der intrazelluläre Signalweg ROCK2-Cofilin aktiviert wird und dieser die Dynamik des Aktincytokeletts kontrolliert. Zusätzlich zeigen die Daten, dass auch der Nogo-A-Δ20 abhängige Signalweg dieselben intrazellulären Kaskaden aktiviert.

Funktionellen und strukturellen Veränderungen an den Synapsen korrelieren und vermitteln zusammen die langanhaltende synaptische Plastizität. Zusätzlich zu der Funktion von Nogo-A in Begrenzung des LTPs, konnte gezeigt werden, dass es auch in der negativen Regulierung der morphologischen Veränderungen der dendritischen spines beteiligt ist. Jedoch bleibt die Frage offen ob Nogo-A diese Modifikationen auf der präsynaptischen Seite steuert. In dieser Arbeit habe ich gezeigt, dass Nogo-A die strukturellen Modifikationen auf den präsynaptischen Moosfasern, abhängig der App-

likationsdauer, kontrolliert. Die akute Neutralisierung von Nogo-A zeigt keinen Einfluss auf die kurzzeitige Motilität der Synapsen, während die chronische Neutralisierung zu einer Verringerung der Synapsengröße führt.
Zusammenfassend tragen die hier vorgestellten Daten zu einem besseren Verständnis bei, wie Nogo-A die neuronalen Verschaltungen stabilisiert um die Plastizität im adulten Hippokampus zu begrenzen.

Acknowledgment

Gratitude is not only the greatest of
virtues, but the parent of all others.

Marcus Tullius Cicero

The 1st October 2012 a new adventure started in my life, and now after three years I am at the end of my PhD work and it is time to thank all the people who helped to make this happen.
I would like to thank Prof. Dr. Martin Korte and Dr. Marta Zagrebelsky, without their advice and assistance I could probably not have achieved my goal. Thank you, for taking me in the lab three year ago, giving me the the opportunity to know the dynamic and fascinating field of brain plasticity and the not trivial chance to live a new experience in a foreign country. Thank you, Martin, for the patience, support and encouragement that you always had with me. Thank you, Marta, you always encouraged me for doing my best and you never denied your help. I still remember the first time I met you, I was impressed by your energy and determination.
I would like to thank Prof. Reinhard Köster and Dr. Florian Bittner for reviewing my thesis and being part of my thesis committee.
Over these years I met many people, and all in different ways have contributed to my experience. Thank you, Kristin, for your scientific help and suggestions whenever I needed and for our conversations in the canteen. Thank you, Anita, for your nice translation of my abstract from English to German. Thank you, Andreas, for your comments about my project and for speaking with me in Italian. Thank you, Gayane, for your suggestions about electrophysiology. Thank you, Martin Rothkegel, for your precise suggestions about biochemical problems. Thank you, Reinhard, for your excellent technical support and for our friendly conversation in the canteen. Thank you, Tania, for your technical support on biochemical experiments and for loving my shoes. Thank you, Diane, for picking up the mice whenever I needed. Thank you, Eva, for ordering the antibodies for my experiments. I thank all my colleagues for sharing with me their experiences: Qin, Yves, Ulrike, Sabine, Stefanie, Shirin, Marianna, Nina, Franziska, Jan, Susann, Steffen, Jonas, Niklas. Thank you, Qin, for our friendly conversations about various topics of the life. Thank you, Shirin, for your energy, positivity and friendship.
I would like to thank my family and my Italian friends for their psychological support, it is hard to live far from you but I keep you with me in my heart.
Thank you, Andrea, for believing in this new adventure with me, and more than anything else thank you for your love, because *"Chi ama riesce a vincere il mondo", Paulo Coelho.*

Contents

List of Abbreviations

ACSF Artificial cerebral spinal fluid

AMPA α-amino-3-hydroxy-5-methyl-4-isoxazolepropionic acid

ATP Adenosine triphosphate

BDNF Brain-derived neurotrophic factor

BSA Bovine serum albumin

$CaCl_2$ Calcium chloride

CNS Central nervous system

CO_2 Carbon dioxide

CSPGs chondroitin sulfate proteoglycans

DIV Days in vitro

DMSO Dimethyl sulfoxide

EPSPs Excitatory postsynaptic potentials

fEPSP Field excitatory postsynaptic potential

FV Fiber volley

GBSS Gey's balanced salt solution

GFP Green fluorescent protein

GPCR G protein-coupled receptors

HRP Horseradish peroxidase

IEG Immediate early gene

IPSPs Inhibitory postsynaptic potentials

ISI Inter-stimulus interval

KCl Potassium chloride

KH_2PO_4 Monopotassium phosphate

LFS Low-frequency stimulation

LIMK LIM kinase

LTD Long-term depression

LTP Long-term potentiation

MAG Myelin-associated glycoprotein

mEPSC Miniature excitatory postsynaptic current

Mg^{2+} Magnesium

$MgCl_2$ Magnesium chloride

mGlu Metabotropic glutamate

$MgSO_4$ Magnesium sulfate

MI Motility index

NA Numerical aperture

NaCl Sodium chloride

NaH_2PO_4 Monosodium phosphate

$NaHCO_3$ Sodium bicarbonate

NgR1 Nogo receptor 1

NMDA N-methyl-D-aspartate

O_2 Oxygen

OHCs Organotypic hippocampal slice cultures

OMgp Oligodendrocyte-myelin glycoprotein

$p75^{NTR}$ p75 neurotrophin receptor

PFA Paraformaldehyde

PP-LFS Paired-pulse low-frequency stimulation

PPF Paired-pulse facilitation

PVDF Polyvinylidene difluoride

ROCK Rho-associated protein kinase

S1P Sphingosine-1-phosphate

S1PR2 Sphingosine-1-phosphate receptor-2

SEM Standard error of the means

SHH Slingshot phosphatase

TBS Theta-burst stimulation

TBS-T Tris buffered saline-Tween

List of Figures

List of Tables

In the beginning God created the heavens and the earth.
The earth was formless and void, and darkness was over the surface of the deep,
and the Spirit of God was moving over the surface of the waters.
Then God said, "Let there be light"; and there was light.
Genesis 1,1-3

To you Andrea, the light of my life

1 | Introduction

1.1 Learning and memory

> We are who we are in good measure because of what we have learned and what we remember and forget.
>
> *Kandel*
> *Nobel lecture 2000*

During life, the knowledge and information that we acquire through our experiences are in part forgotten and in part retained over time in form of memories. Learning and memory processes continuously alter our behaviour, as they address one of the fundamental feature of human activity, that is learn from experience and retain the learned information in memory. This requires that neuronal networks in the brain change in response to the environment throughout life. Interestingly, synaptic connections between neurons are plastic responding to alterations in neuronal activity and experience to integrate new knowledge, but at the same time they have to be stable in a certain extent to preserve previously acquired information. Thus, a balance between plasticity and stability of neuronal circuitry is required to ensure proper acquisition as well as the maintenance of memories in the brain. In this context, molecules come into play. In this thesis, I analysed the role of Nogo-A protein in regulating synaptic plasticity in the hippocampus, a crucial structure of the brain for learning and memory processes.

1.1.1 The role of the hippocampus in memory

The hippocampus has been demonstrated to be the locus for episodic memory, encoding information about events and personal experiences (Vargha Khadem et al., 1997). Indeed, studies on patients have revealed that removal of the hippocampus with its subcortical connections leads to specific deficit in episodic memory, leading to amnesia. Interestingly, these patients showed anterograde amnesia, retaining the memory for events happened before but not after the injury (Scoville and Milner, 1957). Accordingly, later on it has been demonstrated that the hippocampus is a temporal store implicated in transforming new memory, or short-term memory, into long-term memory by a selective transfer to the neocortical system store (Squire and Zola-Morgan, 1991). Furthermore, studies on animals have clarified that the hippocampus is also involved in encoding spatial information (Eichenbaum, 2015). Indeed, when the animals move, individual hippocampal pyramidal neurons, or place cells, fire encoding a map of the environment (O'Keefe and Dostrovsky, 1971). Interestingly, in humans it has been demonstrated that the right hippocampus is involved in spatial learning (Smith

et al., 1981), while the left one is implicated in episodic memory (Frisk and Milner, 1990), (Burgess et al., 2002). Moreover, the hippocampus is critical for learning the context of events or experience, by creating context-specific representations (Eichenbaum, 2004). Hence, the hippocampus is responsible for encoding and consolidation of episodic, spatial and contextual memory (Burgess et al., 2002).
The information reaches the hippocampus from the entorhinal cortex via the perforant pathway making synapses onto dentate gyrus granule cells. In turn, the axons of dentate gyrus neurons, the mossy fibers project onto CA3 pyramidal neurons. Finally, the Schaffer collaterals, the axons of CA3 neurons contact the CA1 pyramidal cells (Fig. 1.1). Interestingly, this trisynaptic circuit is organized in a series of lamellae along the longitudinal axis of the hippocampus, make it suitable for studies of synaptic transmission.

1.2 Synaptic plasticity and stability

Synaptic plasticity, the ability of synapses to change the strength of their connection in response to specific activity patterns, is considered to be the cellular correlate of learning and memory processes. Indeed, synapses which are the sites of connections between neurons can modify either their shape (structural plasticity) and their function (functional plasticity) in response to stimuli (Bailey et al., 2000). Synaptic plasticity is prominent in the juvenile brain within so called critical periods when neuronal circuits in the brain are particularly prone to be modified in response to sensory stimulation and changes in neuronal activity. Indeed, learning and novel sensory experiences elicited by the interaction with the environment, e.g. visual or auditory stimuli, shape the neural circuitry leading to remodelling of the neuronal network for the development of a proper behaviour, e.g. visual or auditory ability. After the closure of the critical

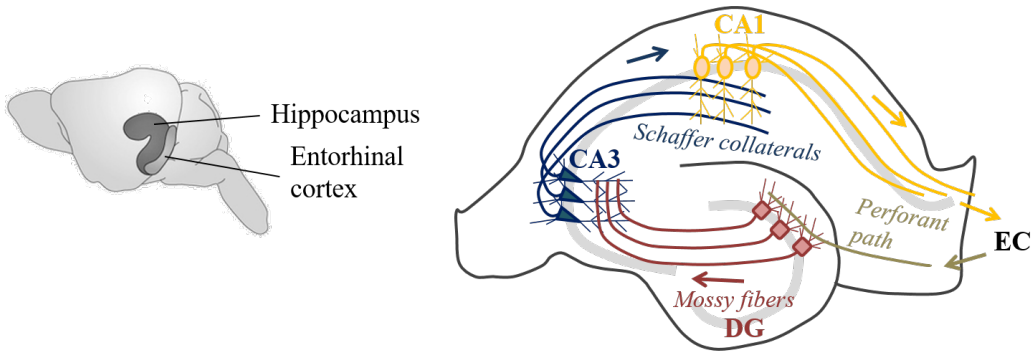

Figure 1.1: Left panel: the localization of the hippocampus and entorhinal cortex in the mouse brain. Right panel: the organization of the hippocampus. The perforant pathway from the entorhinal cortex (EC) project to the dentate gyrus (DG). The axons of DG neurons, the mossy fibers, project to the CA3 pyramidal neurons. The axons of CA3 cells, the Schaffer collaterals, project to the CA1 pyramidal neurons. CA1 cells send back projections into the EC. CA: cornu Ammonis.

periods, plasticity is reduced and neuronal networks in the adult brain become progressively more stable so that the circuits sculpted by experience during development are maintained (Hübener and Bonhoeffer, 2014), (Hensch, 2005). Accordingly, long-term in vivo imaging studies revealed that the organization of neurons connection within several areas of the adult brain is remarkably stable (Holtmaat and Svoboda, 2009). This is because the intrinsic ability of certain areas of the adult brain to be plastic is dampened by cellular and molecular mechanisms e.g. memory suppressor genes (Abel et al., 1998). In particular, the molecular "triggers" promote plasticity, while the molecular "brakes" limit plasticity supporting stability. Thus, a tight regulated balance of these molecular mechanisms is fundamental to integrate new experiences into existing memories in the adult brain (Takesian and Hensch, 2013).

1.2.1 Dendritic spines

Most glutamatergic-excitatory neurons carry dendritic spines, small membrane protrusions emerging from their dendritic branches. Spines receive inputs from the presynaptic axonal varicosities (or boutons) containing synaptic vesicles. Dendritic spines are formed by a head and by a neck connecting them to the dendrite. They have been proposed to function as an independent electrical rather than structural or biochemical compartment, being more depolarized than the dendritic shafts (Yuste, 2013). Moreover, it has been shown that the morphology of spine neck determines the extent of depolarization during post-synaptic potential, allowing a precise control of synaptic strength (Yuste, 2013).

1.2.2 Functional plasticity

Specific activity patterns in the brain result in long-lasting changes in synaptic strength. In particular, the long-lasting enhancement or reduction in synaptic transmission, known as Long-Term Potentiation (LTP) (Bliss and Lomo, 1973) or Long-Term Depression (LTD) (Dudek and Bear, 1992) respectively, are considered to be the cellular correlates of learning and memory.
At the Schaffer collaterals-CA1 pathway of the hippocampus, under basal conditions excitatory synaptic transmission is mostly mediated by AMPA receptors (AMPARs) (Fig. 1.2A), which are permeable to Na^+ and K^+ ions. A brief high frequency activity pattern elicits LTP which is characterized by distinct stages:

- induction. The stimulation causes a post-synaptic depolarization which activates the NMDA receptors (NMDARs) by removing the Mg^{2+} block. The resulting high increase of Ca^{2+} influx leads to the activation of calcium - dependent cascades and the activation of protein kinases like Ca^{2+}/calmodulin - dependent protein kinase (CaMKII) and protein kinase C (PKC) (Fig. 1.2B);

- expression. This is a post-synaptic and post-translational stage depending on the insertion of new AMPARs by exocytosis into the post-synaptic membrane in order to increase the synaptic response (Fig. 1.2B);

- maintenance. This is a protein and mRNA synthesis - dependent stage. Indeed, local synthesis or transcription in the nucleus leads to structural modification of potentiated synapses, including the increase in the size of pre-existing spines or the growth of new ones.

Overall, two phases of LTP can be distinguished dependently on the time scale: an early-phase, representing functional changes and lasting minutes to hours, and a late-phase mRNA and protein synthesis - dependent, associated with structural modifications and lasting hours to days.

Prolonged low-frequency activity patterns induce LTD (Fig. 1.2C), characterized by the post-synaptic depolarization and by the activation of NMDARs leading to a small increase of Ca^{2+} influx. In turn, this activates the calcium - dependent protein phosphatases, like calcineurin and protein phosphatase 1 (PP1), promoting AMPARs endocytosis (Fig. 1.2C). The late synthesis - dependent phase leads to decrease spines size or number.

Thus, LTP and LTD can be considered as opposite phenomena sharing key elements. Indeed, following the NMDARs activation, is the amount in post-synaptic calcium rise that leads to the activation of protein kinases or phosphatases determining if LTP or

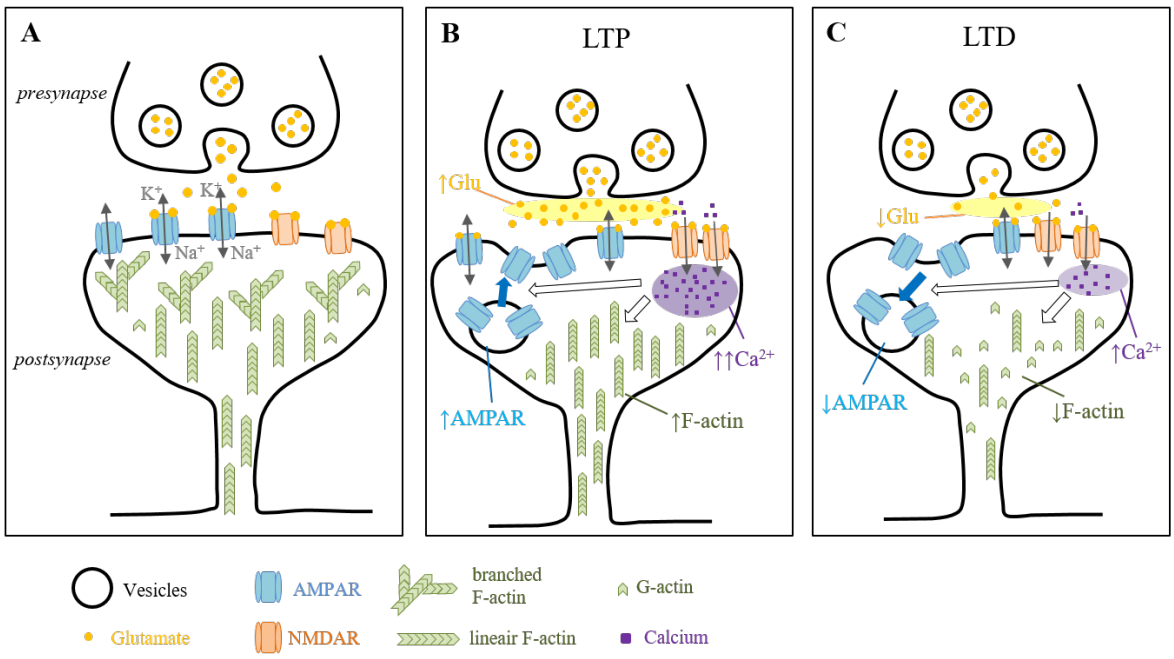

Figure 1.2: **(A)** During basal synaptic transmission released glutamate binds both to the ligand-gated ion channels NMDARs and AMPARs. As NMDARs are voltage - dependent and blocked by Mg^{2+}, only AMPARs contribute to the postsynaptic response. **(B)** LTP: tetanic stimulation leads to increase glutamate release from the presynaptic terminal and the depolarization of postsynaptic neuron activates NMDARs. This is followed by a high increase in Ca^{2+} influx through the NMDARs and by the activation of protein kinases - dependent cascades, leading to the insertion of new AMPARs in the plasma membrane and to increase the F-actin content into the postsynapse. **(C)** LTD: prolonged low frequency stimulation decreases glutamate release, and the low rise in Ca^{2+} concentration leads to the activation of phosphatase - dependent cascades, causing the activity - dependent endocytosis of AMPARs from the plasma membrane and the reduction of the F-actin content into the postsynapse.

LTD occur, respectively. Moreover, to be activated NMDARs require the concomitant release of glutamate from the activated pre-synapses (specificity) and the post-synaptic depolarization to relieve their Mg^{2+} block (cooperativity and associativity). Indeed, LTP and LTD are characterized by three properties:

- cooperativity. For LTP or LTD to occur many excitatory synapses belonging to different inputs have to be active and fire at the same time to provide the postsynaptic depolarization for the release of Mg^{2+} block from the NMDARs;
- input-specificity. Only active synapses belonging to different inputs are potentiated or depotentiated, while the inactive synapses are not;
- associativity. Synapses belonged to a weak input can undergo LTP when the weak input is paired with a strong one.

1.2.3 The function of LTP and LTD

The synaptic plasticity and memory (SPM) hypothesis asserts that the activity - dependent synaptic plasticity processes take place during memory formation, and that these are both necessary and sufficient for storing the memory (Martin et al., 2000). In order to confirm the SPM hypothesis, several hippocampal - dependent learning behavioural tasks have been developed. For instance, it has been shown that the pharmacological inhibition of NMDARs impairs both LTP induction in acute hippocampal slices and the learning performance of the animals during the water maze, a task used for evaluating spatial memory. This suggest that the same NMDARs - dependent mechanisms involved in LTP might also mediate the hippocampal - dependent memory formation (Morris et al., 1986). Recently, optical imaging, molecular-genetic and optogenetic techniques have been combined with behavioural tasks in order to directly prove that activity - dependent changes in the strength of synaptic connections are cellular mechanisms by which memory engrams are stored in the brain. Interestingly, a recent study in living animals shows that LTP and LTD induced by optogenetic stimulation cause memory formation or loss, respectively, thus demonstrating a causal link between synaptic plasticity processes and memory formation (Nabavi et al., 2014).

1.2.4 Structural plasticity

The combination of two-photon time-lapse imaging with glutamate uncaging techniques have facilitated the study of structural plasticity at spines (Kasai et al., 2003). Dendritic spines are dynamic structures which alter their shape, size and number under resting condition and in response to specific activity - dependent stimuli. This structural plasticity is prominent during development, while in the adult age spines become more stable and morphological changes are associated with learning (Fu and Zuo, 2011). Indeed, LTP has been correlated to the formation of new spines, with the enlargement of spine head (Matsuzaki et al., 2004) and the shortening of the spine neck resulting in reduced resistance (Nishiyama and Yasuda, 2015). Conversely, LTD is associated with spine shrinkage and pruning.

Interestingly, spines are not homogeneous, and can be subdivided in smaller or "learning spines" and larger or "memory spines" (Bourne and Harris, 2007). This categorization may explain the question of how both the maintenance and the rapid acquisition of new memory are achieved. Indeed, the lifetime of synaptic memory can vary widely depending on spine structure, with large stable spines being the structural basis for long-term memory, while small unstable spines generated during activity - dependent processes forming new memory (Kasai et al., 2003).

1.2.5 Synaptic plasticity at presynaptic compartments

While over the years many studies addressed activity - dependent plastic changes occurring at postsynaptic dendritic spines, it is now clear that synapse rearrangements involve postsynaptic remodelling with concomitant reorganization of presynaptic structures. Indeed, in the CA1 and CA3 regions of the hippocampus, persistent enlargement of dendritic spines upon LTP matches with a delayed increase of presynaptic boutons (Meyer et al., 2014), while LTD leads to shrinkage of presynaptic boutons reducing their association with spines (Becker et al., 2008).
The presynaptic mossy fiber synapses of the unmyelinated dentate gyrus granule cells axons represent an interesting system for investigating patterns of synaptic connection rearrangements. The mossy fiber synapses are large, with a diameter of 3-5 µm, establishing close to the soma few, sparse but powerful synaptic connections with excitatory CA3 pyramidal neurons (Fig. 1.3A). Indeed, each single terminal contains a high number of synaptic vesicles making synapses with postsynaptic thorny excrescences (Fig. 1.3B). Moreover, they are complex structures, as many terminals are connected through processes to satellite terminals (Galimberti et al., 2006). In addition they exhibit divergence and convergence of their local connectivity. Indeed, individual terminals establish contact with more than one CA3 pyramidal cells, and distinct terminals make inputs

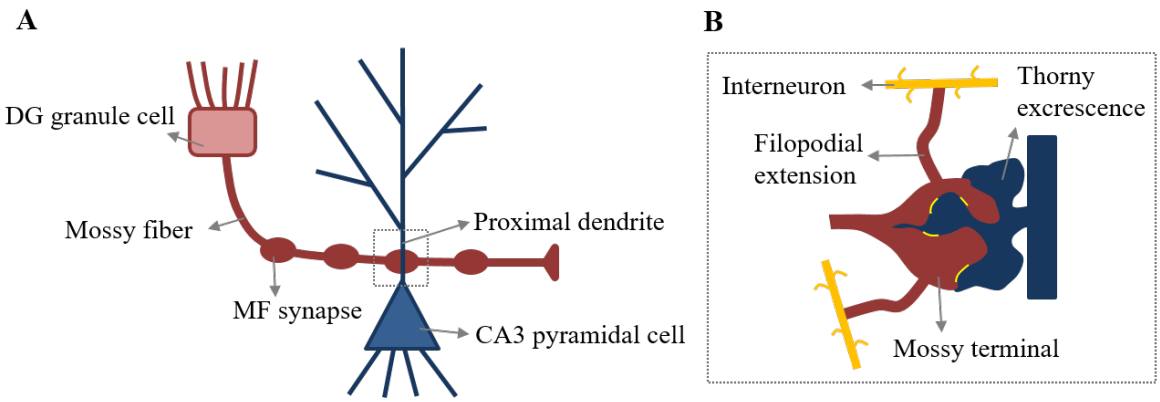

Figure 1.3: **(A)** The nonmyelinated mossy fibers of dentate gyrus (DG) granule cells travel within the stratum lucidum contacting the proximal dendrites of CA3 pyramidal cells. **(B)** Magnification of the dashed box in (A). The core of the terminal envelopes the postsynaptic thorny excrescences of an excitatory CA3 pyramidal cell, whereas their filopodial extensions contact the dendrites of inhibitory interneurons. Thus, the mossy fiber synapses regulate both synaptic excitation and inhibition of signal transduction to the CA3 circuitry of the hippocampus.

onto individual CA3 neurons (Galimberti et al., 2006). Interestingly, the filopodial extensions protruding from the terminal target the GABA-positive interneurons (Fig. 1.3B). Thus, the mossy fiber synapses regulate both synaptic excitation and inhibition of signal transduction to the CA3 circuitry of the hippocampus.

The mossy fiber synapses onto CA3 pyramidal cells display unique functional features in comparison to the other pathways of the hippocampus. Indeed, it has been described a presynaptic NMDARs - independent form of LTP, manifested as long-term changes in the probability of glutamate release from the terminals (Malenka and Kauer, 2007), (Nicoll and Schmitz, 2005). However, two recent studies have described a postsynaptic NMDA - dependent forms of LTP occurring at mossy fibers-CA3 pathway, suggesting that both forms of LTP (NMDAR - dependent and independent) may coexist at the same individual mossy fiber synapses (Kwon and Castillo, 2008), (Rebola et al., 2008). Moreover, the mossy fibers-CA3 pathway have been show to express also specific forms of LTD (Evstratova and Tóth, 2014).

In the adult hippocampus, the mossy fiber synapses have been demonstrated to be remarkably plastic (Galimberti et al., 2006), rearranging their structure and local connectivities in response to activity, experience and age. Fist of all, they have been shown to be highly dynamic structures in various extent, appearing and disappearing within days (De Paola et al., 2003). Interestingly, these dynamics are increased by activity, indicating that their reorganization is involved in changing the network connectivity in the hippocampus (De Paola et al., 2003). In addition, mossy fiber synapses are motile structures with the larger terminals more stable and the smaller showing higher motility (Chierzi et al., 2012). It has been shown that short-term activity suppression reduces the motility of the core terminal without affecting their volume, while long-term activity suppression leads to reduce their size, indicating that activity is needed to maintain the size of terminals. Interestingly, short- and long- term activity suppression does not affect structural remodelling of filopodial extensions, suggesting that the two presynaptic compartments remodel independently of each other (Chierzi et al., 2012). The complexity of the terminals increases in an experience-related manner. Indeed, terminals from mice housed under enriched environment establish a greater number of connection with satellite terminals and expand along the apical dendrite of pyramidal cells, thus increasing the number of synapses and of release sites (Gogolla et al., 2009), (Galimberti et al., 2006). Hippocampal mossy fiber synapses exhibit structural remodelling in response to age. Indeed, it has been shown that the volume of the terminals in organotypic slices cultures derived from young mice is smaller in comparison with that of the terminals in slices from adult mice (Galimberti et al., 2006). Moreover, the fraction of terminals containing satellites increases during development (Galimberti et al., 2006).

1.3 Actin cytoskeleton dynamics during synaptic plasticity

Actin cytoskeleton dynamics are critical for both structural and functional changes (Nishiyama and Yasuda, 2015), driving morphological remodelling (Matus, 2000), (Fis-

cher et al., 1998) and alterations in synaptic transmission at dendritic spines. Under basal conditions, the actin filaments or F-actin are parallel in the neck, while in the head the filaments form a lattice-twisted structure (Korobova and Tatyana, 2010) (Fig. 1.2A) with a dynamic pool at the tip and below the spine head and a stable pool at the base of the spine (Honkura et al., 2008). LTP induction leads to an early phase associated with the degradation of actin cytoskeleton to sustain trafficking of AMPAR (Gu et al., 2010) (Fig. 1.2B) and translocation of plasticity-related proteins into potentiated spines (Ouyang et al., 2005). Subsequently, actin cytoskeleton is rebuild and stabilized by processes that increase F-actin (Fig. 1.2B) and reorganize actin cytoskeleton into spines (Rudy, 2014). Indeed, LTP involves a rapid polymerization of actin within spines (Okamoto et al., 2004) and the establishment of a third pool of stable actin filaments at the core of spine head (Honkura et al., 2008). Accordingly, pharmacological inhibition of actin polymerization prevents LTP maintenance (Kim and Lisman, 1999), (Krucker et al., 2000), (Kramár et al., 2006) and impairs the formation of long-term memory (Motanis and Maroun, 2012), suggesting that actin remodelling is critical for these processes. Contrarily to LTP, LTD is associated with depolymerization of F-actin, thus increasing the content of G-actin into the depotentiated spines (Okamoto et al., 2004), (Fukazawa et al., 2003).

1.3.1 The Rho GTPases pathway

The actin-binding protein Cofilin is considered a key regulator of actin dynamics in response to plastic stimuli (Bosch et al., 2014), being involved in activity - dependent morphological and functional changes (Lappalainen et al., 2009), (Chen et al., 2007). Cofilin is a constitutively active dephosphorylated protein, which regulates actin dynamics by increasing F-actin depolymerization and severing (Bamburg and Bernstein, 2010) in order to maintain a soluble pool of actin monomers. Phosphorylation leads to its inactivation facilitating actin filaments assembly (Gungabissoon and Bamburg, 2003). It has been described that LTP causes a rapid depolymerization of actin filaments correlated with the activation of Cofilin, followed by a transient phosphorylation - dependent inactivation of Cofilin (Chen et al., 2007) for promoting actin polymerization necessary for LTP maintenance and the structural modifications (Fukazawa et al., 2003). Conversely, LTD requires Cofilin activity to increase the depolymerization of actin filaments leading to shrinkage of spines (Zhou et al., 2004).
The cycle between active-unphosphorylated and inactive-phosphorylated Cofilin is regulated by Slingshot phosphatase (SHH) and LIM kinases (LIMK) which are the downstream effectors of the Rho GTPases, considered the main regulators of actin dynamics transducing the extracellular cues to the actin cytoskeleton (Fig. 1.4). The activation of RhoA and Rac/Cdc42 initiates an intracellular signalling cascade contributing to actin polymerization upon LTP. In particular, while the RhoA-ROCK pathway drives the initial actin polymerization for spine growth during LTP, the Rac/Cdc42-PAK signalling organizes and stabilizes the newly formed actin filament to make it resistant to depolymerization in order to maintain the structural modifications of the spines (Rex et al., 2009), (Murakoshi et al., 2011).

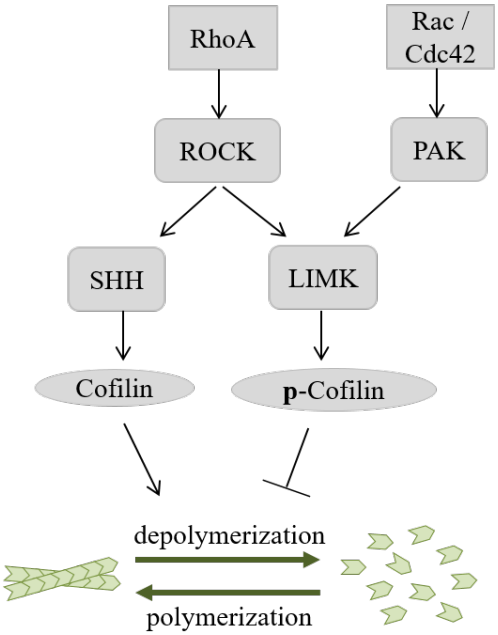

Figure 1.4: The RhoA-ROCK pathway regulates the phosphorylation of Cofilin through the Slingshot phosphatase (SHH) and the LIM kinases (LIMK). LIMK is also a downstream effector of the Rac/Cdc42-PAK pathway. Unphosphorylated Cofilin is active promoting the depolymerization of F-actin into G-actin. The phosphorylated Cofilin is inactive inhibiting the depolymerization, thus promoting the polymerization of G-actin into F-actin.

1.4 Nogo-A negatively regulates activity - dependent synaptic plasticity

In the mature neuronal network, some extracellular cues positively regulate the activity - dependent synaptic plasticity, while others prevent these plastic changes promoting the stability of synaptic configurations (Abel et al., 1998). In this context, Nogo-A protein has been characterized as a negative regulator of experience - dependent neuronal remodelling.

Nogo-A, also known as Reticulon-4A (Chen et al., 2000), is a transmembrane protein encoded by the reticulon gene 4 (RTN-4) (GrandPré et al., 2000) which also encode Nogo-B and Nogo-C by alternative promoter or splicing (Fig. 1.5A). While all the three proteins share the same Nogo-66 domain, the Nogo-A-Δ20 is the specific domain for Nogo-A (Fig. 1.5A,B). Over the years, the Nogo-66 receptor 1 (NgR1) and the paired immunoglobulin-like receptor B (PirB) have been identified as receptors for the Nogo-66 domain. Interestingly, NgR1 is anchored to the plasma membrane by the GPI anchor and lacks an intracellular signalling domain. For this reason, the p75 neurotrophin receptor ($p75^{NTR}$) and the leucine-rich repeat and immunoglobulin domain-containing 1 (Lingo1) have been proposed to form a heterotrimeric complex with NgR1 (Fig. 1.5B) activating an intracellular signalling cascade (Wang et al., 2002a), (Mi et al., 2004). Regarding the Nogo-A-Δ20 domain, it has been recently discovered to specifically bind to the G-protein-coupled sphingosine 1-phosphate receptor 2 (S1PR2) (Fig. 1.5B). Being a reticulon protein, 90% of Nogo-A is located within the endoplasmatic reticulum (ER) with small amount at the cell surface of oligodendrocytes and neurons. Indeed, Nogo-A is expressed during development by many neurons, and in the adult brain both by myelin-forming oligodendrocytes and by neurons of area associated with plasticity, i.e. in the olfactory bulb, in dorsal root ganglia, in the cortex and in the hippocampus (Huber et al., 2002).

The first function attributed to Nogo-A in the adult CNS was related to its expression in the myelin-forming oligodendrocytes, thus inhibiting axonal regeneration after injury of spinal cord (Schwab and Caroni, 1988). Subsequently, also neuronal Nogo-A was characterized to restrict neurite outgrowth of uninjured neurons (Bareyre et al., 2002). This function is mediated both by the Nogo-66 (Fournier et al., 2001) and the Nogo-A-Δ20 (Oertle et al., 2003) domains. Indeed, both domains activate the RhoA-ROCK pathway (Niederöst et al., 2002), (Nash et al., 2009) to regulate the actin cytoskeleton at the growth cone (Hsieh et al., 2006), (Montani et al., 2009).

In addition to its role in restricting anatomical plasticity of neurites, Nogo-A limits the activity - dependent synaptic plasticity in several regions of the adult CNS (Mironova and Giger, 2013), (Schwab and Strittmatter, 2014), (Zagrebelsky and Korte, 2014). Indeed, Nogo-A has been demonstrated to restrict the ocular dominance plasticity in the visual cortex (McGee et al., 2005). Interestingly, not only in nogo-a ko mice but also in ngr ko and pirb ko mice the ocular dominance plasticity continue beyond the critical period (McGee et al., 2005), (Syken, 2006). Nogo-A as well as NgR1 have been detected at synapses in the adult CNS (Wang et al., 2002b) and expressed at pre- and post-synaptic sites (Lee et al., 2008) in pyramidal neurons (Huber et al., 2002), (Zagrebelsky et al., 2010), and their expression is regulated by neuronal activity (Josephson et al., 2003), (Bandtlow et al., 2004). Nogo-A has been demonstrated to stabilize the axonal and dendritic architecture of mature pyramidal neurons (Craveiro

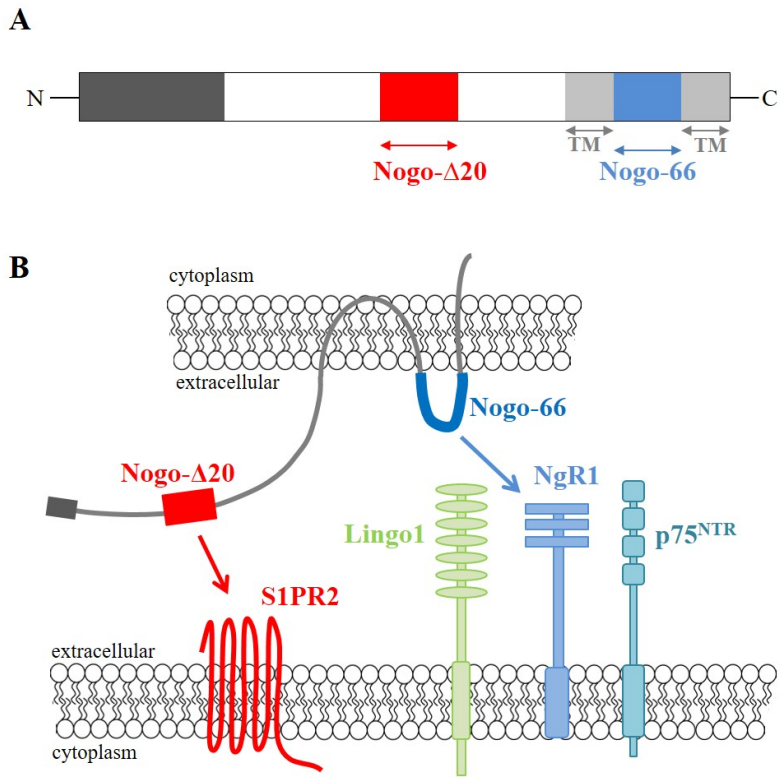

Figure 1.5: **(A)** Schematic structure of Nogo-A gene, with the Nogo-A-Δ20 domain and the Nogo-66 domain located between the transmembrane domains (TM). **(B)** The transmembrane Nogo-A protein. The Nogo-A-Δ20 domain signals via S1PR2, the Nogo-66 domain signals via NgR1 which forms a heterotrimeric complex with Lingo1 and $p75^{NTR}$.

et al., 2008), (Zagrebelsky et al., 2010), and its neutralization leads to increase the amount of stubby-immature spines (Zagrebelsky et al., 2010). Accordingly, NgR1 was shown to be required for the proper maintenance of mature spines (Lee et al., 2008), and genetic deletion of ngr1/2/3 negatively regulates synaptogenesis by restricting excitatory synapse formation (Wills et al., 2012). Nogo-A has been shown to restrict functional plasticity at the Schaffer collateral-CA1 pathway. Indeed, the magnitude of LTP is increased in the hippocampus of a microRNA-mediated Nogo-A knockdown rats (Tews et al., 2013) as well as upon acute neutralization of Nogo-A signalling (Delekate et al., 2011), while LTD is not affected, indicating that Nogo-A is specifically involved in regulating the potentiation of synapses. Interestingly, in nogo-a ko mice LTP is only slightly increased, suggesting that mechanisms might exist to compensate for chronic loss of Nogo-A (Delekate et al., 2011). Also the acute neutralization of NgR1 increases the level of LTP (Delekate et al., 2011), and acute hippocampal slices from ngr1 ko mice have shown decreased LTD, indicating that NgR1 not only regulates synaptic potentiation like Nogo-A, but also synaptic depotentiation. Regarding the NgR1 co-receptors, only a role for $p75^{NTR}$ has been addressed in regulating synaptic plasticity. Indeed, it negatively modulates dendritic structural plasticity in mature pyramidal cells of the hippocampus (Zagrebelsky et al., 2005), (Michaelsen et al., 2010) and attenuates LTD without affecting LTP (Xu et al., 2000), (Rösch et al., 2005), (Woo et al., 2005), (Barrett et al., 2010). Recently, the S1PR2 has been identified to mediate the Nogo-A-Δ20 function in restricting LTP. Indeed, the acute neutralization of the Nogo-A-Δ20 / S1PR2 signalling leads to increase the level of LTP without affecting LTD (Kempf et al., 2014). Nogo-A restricts the structural and functional plasticity also in the cortex. Indeed, in the motor cortex the acute neutralization of Nogo-A has been shown to increase spine formation and LTP level (Zemmar et al., 2014), (Tews et al., 2013). In addition, chronic time lapse *in vivo* imaging reveals that the high turnover of dendritic spines and axonal varicosities in the superficial layers of somatosensory cortex still occur in 1-year old mice lacking either NgR1 or Nogo-A, thus stabilizing synaptic anatomy (Akbik et al., 2013).

1.5 Aim of the study

Activity - dependent synaptic plasticity is thought to be an essential component of learning and memory processes. The adult brain has the ability of maintaining and recalling long-lasting memories while at the same time allowing the acquisition of new information and the formation of new memories. This observation indicates the clear need for maintaining the weight of synaptic transmission throughout the memory network coupled with a capacity for further plasticity of synaptic configurations to integrate old with new knowledge (Abraham and Robins, 2005). The molecular mechanisms regulating the tight balance between stability and plasticity of synapses within the mature CNS network are still largely unexplored. In this molecular context, memory suppressor genes (Abel et al., 1998) come into play, in particular molecules like Nogo-A.

Nogo-A protein limits functional plasticity at the Schaffer collateral-CA1 pathway of the adult hippocampus, especially by restricting the magnitude of LTP (Delekate et al., 2011), (Tews et al., 2013). However, the molecular mechanism mediating this role of Nogo-A is largely unknown. In this context, recent publications suggest a surface-receptor mediated function of Nogo-A via its two receptors: S1PR2 specifically binding the Nogo-A-Δ20 domain (Kempf et al., 2014), and NgR1 mediating the signalling of the Nogo-66 domain (Raiker et al., 2010), (Delekate et al., 2011). Interestingly, NgR1 lacking a cytoplasmatic domain (Venkatesh et al., 2005), signals via a heterotrimeric receptor complex including the $p75^{NTR}$ (Wang et al., 2002a) and Lingo1 (Mi et al., 2004). While a role for $p75^{NTR}$ has been described in regulating structural (Zagrebelsky et al., 2005), (Michaelsen et al., 2010) and functional plasticity (Rösch et al., 2005), (Woo et al., 2005), a possible activity of Lingo1 in regulating synaptic plasticity has not been addressed. Moreover, whether and how $p75^{NTR}$ and Lingo1 mediate the Nogo-66 / NgR1 signalling in restricting LTP is still unknown. In this work I addressed which is the contribution of NgR1 co-receptors in mediating the Nogo-66 / NgR1 signalling in restricting LTP. Furthermore, activity - dependent changes in synaptic transmission have been shown to require modifications in the polymeric status of actin within dendritic spines (Rudy, 2014), critical for LTP maintenance (Kim and Lisman, 1999), (Krucker et al., 2000), (Kramár et al., 2006) and the formation of long-term memory (Motanis and Maroun, 2012). Interestingly, what is the downstream intracellular pathway mediating the role of the Nogo-A signalling in restricting LTP is still unexplored. Here, I investigated whether Nogo-A might control the actin cytoskeleton dynamics in order to restrict LTP.

Synaptic plasticity requires both postsynaptic remodelling and concomitant reorganization of presynaptic structures. In addition to the role of Nogo-A in negatively regulating functional plasticity, it has been shown to limits structural changes of postsynaptic dendritic spines (Zagrebelsky et al., 2010), (Kellner et al., 2016), leaving unresolved the issue of whether Nogo-A is involved in regulating structural plasticity also at the presynaptic compartments. The mossy fibers synapses, projecting to the CA3 pyramidal neurons, are huge presynaptic structures regulating both synaptic excitation and inhibition of signal transduction to the CA3 circuitry of the hippocampus, and rearranging their morphological structure and functional connectivity in response to experience. Although the knowledge about the properties of the mossy fiber synapses is growing, the molecules involved in the regulation of the activity - dependent synaptic plasticity remain to be fully determined. Moreover, the mossy fibers are unmyelinated, thus providing an interesting model to discriminate the role of neuronal *versus* myelin Nogo-A. Hence, in the second part of my work I addressed the question of whether Nogo-A regulates the structural plasticity of mossy fiber synapses.

In conclusion, this work increases the knowledge of how Nogo-A regulates the balance between stability and plasticity processes within the mature network in the hippocampus.

2 | Materials and Methods

> Look deep into nature, and then you will understand everything better.
>
> *Albert Einstein*

2.1 Electrophysiology experiments at Schaffer collateral - CA1 pathway

2.1.1 The Artificial Cerebral Spinal Fluid (ACSF)

The Artificial Cerebral Spinal Fluid (ACSF) resembles the physiological composition of the cerebral spinal fluid maintaining the viability and neural activity of the acute hippocampal slices. The ACSF is equilibrated with carbogen (95% O_2 and 5% CO_2) in order to ensure a constant supply of oxygen and adjust the pH to a physiological value of 7.3. In this study, I used the high magnesium (Mg^{2+}) ACSF for the preparation of the acute hippocampal slices, and the low Mg^{2+} ACSF and the LTD-ACSF for LTP and LTD electrophysiological recording, respectively (Table 2.1).

2.1.2 Acute hippocampal slices preparation

The hippocampus is characterized by a lamellar structure making it suitable for studying synaptic transmission. Indeed the intrahippocampal connections are organized into parallel lamellae perpendicular to the longitudinal axis of the hippocampus, allowing

Table 2.1: Composition of ACSFs. Summary of the final concentration [mM] of the components (formula and molecular weight (MW [g/mol])) used for the preparation of the indicated ACSFs. All the chemicals were purchased from Applichem.

Component (MW)	high Mg^{2+} ACSF [mM]	low Mg^{2+} ACSF [mM]	LTD-ACSF [mM]
NaCl (58.44)	125	125	124
KCl (74.56)	2.5	2.5	3
NaH_2PO_4 (137.99)	1.25	1.25	-
KH_2PO_4 (136.09)	-	-	1.25
$MgCl_2$ * $6H_2O$ (203.3)	2	1	-
$MgSO_4$ * $7H_2O$ (246.48)	-	-	2
$NaHCO_3$ (84.01)	26	26	26
$CaCl_2$ (147.02)	2	2	2.5
D (+) Glucose (180.16)	25	25	10

the preparation of transversal acute hippocampal slices keeping intact the intrahippocampal network to be used for intracellular as well extracellular recording (Fig. 2.1C).

In this study, the acute hippocampal slices were prepared from wild-type C57BL/6 mice or $p75^{NTR}$ knock-out mice (von Schack et al., 2001) of either sex. Adult mice (P40-P60) were used for all LTP experiments and for mGlu receptor - dependent LTD recording, while juvenile mice (P14-P20) were used for the NMDA receptor - dependent LTD experiments. All procedures concerning mouse usage were approved by the animal welfare representative of the TU Braunschweig and the LAVES (Oldenburg, Germany, Az. §4 (02.05) TSchB TU BS). For preparing the acute hippocampal slices, mice were euthanized with CO_2 and decapitated. All the preparation steps were performed at $4°C$ to minimize cellular metabolism and oxidative stress, and avoid irreversible ischaemic damage. The brain was dissected from the skull and quickly transferred for 3 minutes into $4°C$ carbogenated high Mg^{2+} ACSF. The cerebellum and the prefrontal cortex were removed, and the two hemispheres were separated. The striatum was removed from the hemisphere and the hippocampus was finally separated from the cortex by cutting the subiculum. Once both hippocampi were dissected, they were glued onto the specimen plate leaning upright against an agar block with the dentate gyrus facing the agar (Fig. 2.1B). 400 µm thick transversal slices were cut using a vibratome (VT 1000S, Leica, Nussloch, Germany). Subsequently, the slices were transferred in a submerged-type storage chamber filled with carbogenated high Mg^{2+} ACSF and maintained at room temperature for at least 90 minutes in order to allow the metabolic stability before recording.

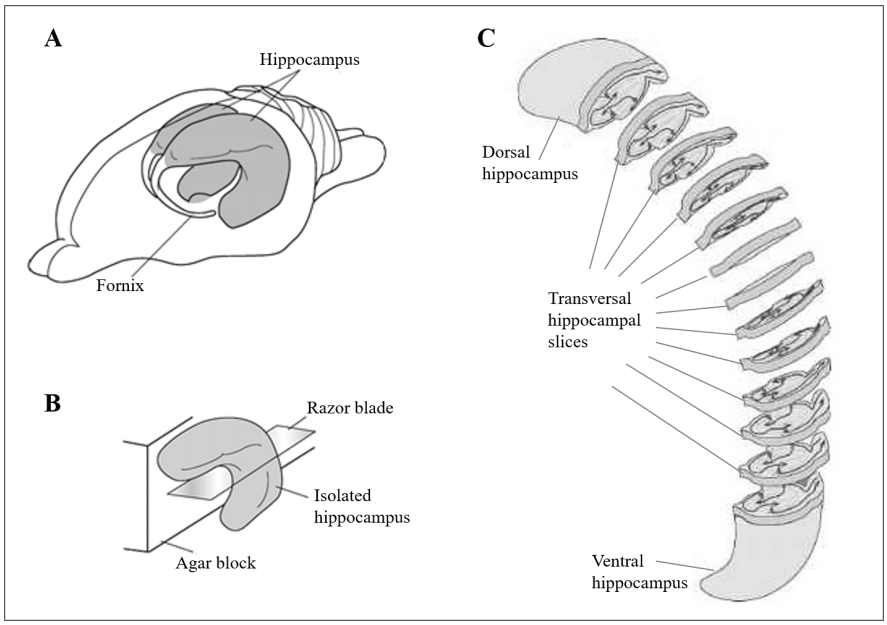

Figure 2.1: Acute hippocampal slices preparation. **(A)** Localization of both hippocampi in the mouse brain. **(B)** The dissected hippocampus is glued upright against an agar block and cut into 400 µm thick transversal slices by a vibratome. **(C)** The transversal acute hippocampal slices ranging from the dorsal to the ventral hippocampus conserve the intrahippocampal projections intact.

2.1.3 Extracellular recording

Extracellular recording allows to monitor the electrical activity of a population of cells. In this study I performed this measurement by using a submerged-type recording chamber (RC-22, Warner Instruments, USA, Fig. 2.2) where the acute hippocampal slices were continuously perfused with carbogenated ACSF at a rate of 1.5 ml/min. The electrical stimulation of the Schaffer collaterals elicits three electrical responses in the CA1 region of the hippocampus:

- the presynaptic fiber volley (FV), indicating the number of the presynaptic action potentials (Fig. 2.3);
- the field excitatory postsynaptic potential (fEPSP), reflecting changes in the excitatory postsynaptic membrane potential (Fig. 2.3);
- the population spike, representing the action potentials within the somata of neighbouring pyramidal neurons.

To record evoked fEPSPs, a borosilicate glass micropipette with low-resistance (2-10 MΩ) was filled with 3M NaCl and positioned at a depth of ∼ 150-200 µm in the stratum radiatum of CA1 region of the hippocampus. A monopolar tungsten electrode (WPI, Cat. # TM33B01, 0.1MΩ) was placed in the stratum radiatum of CA3 region of the

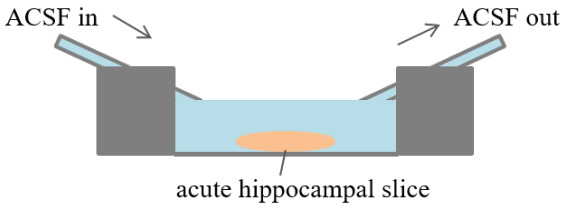

Figure 2.2: Acute hippocampal slice in a submerged-type recording chamber. This type of chamber is suitable for pharmacological experiments because the perfused drugs can be rapidly washed on and washed off.

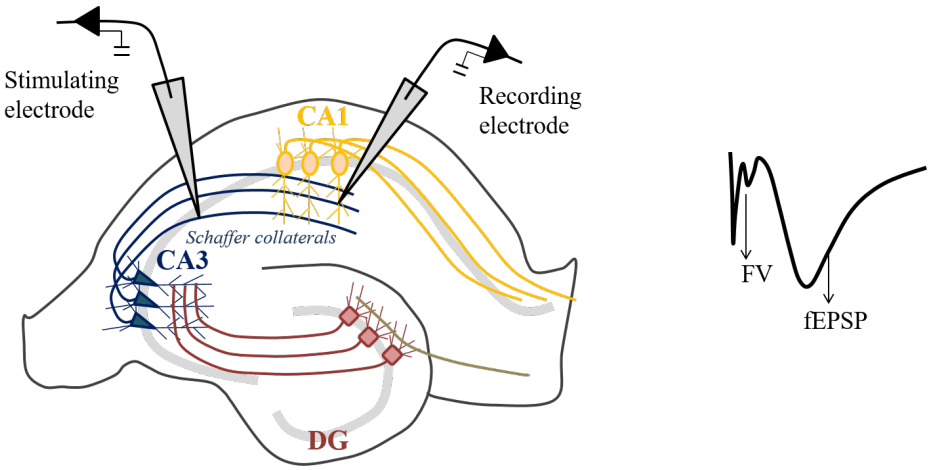

Figure 2.3: Left panel: positioning of the electrodes in the transversal acute hippocampal slice. The stimulating electrode stimulates the Schaffer collaterals. The recording electrode is placed in the stratum radiatum of CA1 region (apical dendritic layer). Right panel: trace of fEPSP showing also FV signal.

hippocampus to stimulate the Schaffer collaterals (Fig. 2.3). A silver/silver chloride (Ag/AgCl) extracellular reference electrode (A-M systems, Cat. # 550015) was used to provide a stable and well-defined electrochemical potential. A stimulus isolator (WPI, A360 or A365) was used to trigger the stimulation protocols programmed in the master pulse generator Master 8 (A.M.P.I.).

Protocols

The measurement of the input-output curves was performed by applying defined, progressively growing currents to reach the maximum slope. The 40% and the 60% of the maximum fEPSP slope was set for baseline stimulation before the induction of LTP and LTD, respectively.
The baseline recording was started by stimulating the axons with pulses of 0.2 ms duration at a frequency of 0.1 Hz, and the slope of fEPSP was monitored over time. After 20 minutes of stable baseline stimulation, LTP or LTD protocol was applied.
LTP was induced by a theta-burst stimulation (TBS) protocol consisting of three time repetition (10 seconds intertrain interval) of four bursts given at 100 Hz repeated ten times in a 200 milliseconds interval (5Hz), (Fig. 2.4A). This protocol induces NMDAR - dependent LTP. TBS is a physiological protocol used to induce LTP in comparison to other high frequency stimulation protocols, resembling the natural theta rhythms occurring in the hippocampus during memory processes. Indeed, theta rhythm within the physiological range of natural neuronal activity (4 to 12 Hz range) represents wave oscillation of hippocampal network observed in electroencephalographic (EEG) recordings of moving animals during hippocampal - dependent learning tasks. Moreover, it has been shown that the theta oscillations recorded from hippocampal slices *in vitro* correlate with those observed *in vivo* (Kowalczyk et al., 2013).
LTD in slices from juvenile mice was induced by using a low-frequency stimulation (LFS) protocol consisting of 900 pulses given at 1 Hz (Fig. 2.4B), while in slices from adult mice was induced with a paired-pulse low-frequency stimulation (PP-LFS) protocol based on 900 paired pulses given at 1 Hz with a 50 ms inter-stimulus interval (Fig. 2.4C). Indeed, it has been shown that NMDAR - dependent form of LTD induced by LFS is more efficiently inducible in juvenile that in adult hippocampus, while the mGluR - dependent LTD induced by a PP-LFS is inducible in both juvenile and adult hippocampus (Kemp et al., 2000). For LTP and LTD recording, the slices were maintained at $32°C \pm 0.2$.
To investigate the basal synaptic transmission, FV analysis was performed at room temperature by analysing the change in fEPSP slope size at different FV amplitude ranging from 0.1 to 0.8 mV.
To investigate short-term plasticity, paired-pulse facilitation (PPF) was analysed by stimulating the axons with two consecutive stimuli at increasing inter-stimulus intervals (ISI) as 10, 20, 40, 80 and 160 ms. The postsynaptic response is expected to be larger for the second than for the first pulse, due to the rise in the presynaptic calcium concentration leading to increase the probability release of neurotransmitter from synaptic vesicles.

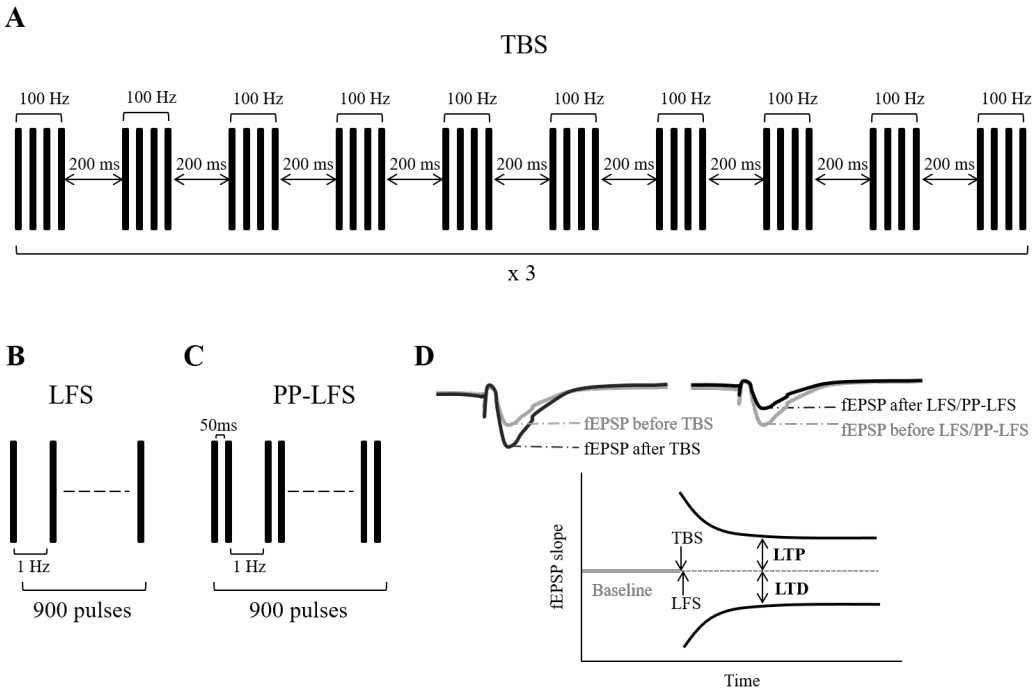

Figure 2.4: Protocols for LTP and LTD induction. **(A)** TBS protocol. **(B)** LFS protocol. **(C)** PP-LFS protocol. **(D)** Upper pane: fEPSP before and after TBS or LFS/PP-LFS. Lower panel: typical LTP and LTD curves.

2.1.4 Electrophysiological data acquisition and analysis

The recorded fEPSP signal was amplified by the Axoclamp2B differential amplifier (Axon Instruments-Molecular Devices, USA), band-pass filtered within a range of 1-1700 Hz (LHBF-48x-4HL, NPI, Germany), and the analog signal was digitized via a multi-IO card (National Instruments-Molecular Devices, USA).

Raw data from FV measurement and LTP/LTD recording were collected, stored and analysed with a custom-made program (ANA-DAP) written by Korte and Staiger in Lab View software (National Instruments, Austin, TX). Data from PPF measurement were analysed by the program ANA-PPF.

The change in the slope size after the induction of LTP/LTD (Fig. 2.4D) was normalized to the average size of the fEPSP slope recorded during the baseline stimulation and set at 100% as shown in Eq. (2.1):

$$\frac{fEPSP_{min}}{mean(fEPSP_{base})} \times 100 \tag{2.1}$$

where $fEPSP_{min}$ is the value of fEPSP slope per minute, $mean(fEPSP_{base})$ is the average of the values of fEPSP slopes recorded during baseline stimulation.

PPF data were analysed dividing the slope of the second fEPSP ($fEPSP_2$) by the slope of the first fEPSP ($fEPSP_1$) at different ISI and set at 100% as shown in Eq. (2.2).

$$\left(\frac{fEPSP_2}{fEPSP_1}\right)_{ISI} \times 100 \tag{2.2}$$

FV data were plotted as fEPSP slope against FV amplitude.
The statistical analysis was performed by using GraphPad Prism with a two-tailed unpaired Student's t-test for the comparison of two independent means, or with a one-way ANOVA and Tukey's post hoc test for multiple comparisons. Values of $p < 0.05$ were considered significant and plotted as follows: *$p < 0.05$, **$p < 0.01$, ***$p < 0.001$. All data are shown as mean ± SEM (Standard Error of the Mean). All graphs were generated using GraphPad Prism.

2.1.5 Pharmacology for electrophysiological recording

The specific drugs or antibodies listed in Table 2.2 were freshly prepared and dissolved in 20 ml of carbogenated ACSF.

Antibodies

The slices were pretreated at room temperature for 1 hour before the recording with different function blocking antibodies dissolved at a final concentration of 5 µg/ml in ACSF containing 0.1 mg/ml bovine serum albumin (BSA) to reduce the probability of their unspecific binding to the slices. To prevent sticking of the antibodies to the tubing or chamber, all the experiments were performed by using PharMed Ismaprene tubing (Ismatec). The following antibodies were used: a rabbit polyclonal anti-Lingo1 antibody (ab23631, Abcam), a mouse polyclonal Nogo Receptor/NgR antibody (Cat. # AF1440, R&D Systems), a Nogo-A-specific blocking antibody (11C7, mIgG1), a control antibody (anti BrdU, mIgG1).

Peptide and inhibitors

The rat Nogo inhibitory peptide Nogo-P4 (Cat. # Nogo-P4, Alpha Diagnostic international) is a 25-aa peptide corresponding to the 66-aa hydrophilic and inhibitory region of Nogo-A. The peptide was dissolved in PBS and used at a final concentration of 4 µM (Yamashita and Tohyama, 2003).
The cell-permeable $p75^{NTR}$ signalling inhibitor TAT-Pep5 (Cat. # 506181, Calbiochem), shown to inhibit the association of $p75^{NTR}$ with Rho-GDI, was dissolved in DMSO according to the manufacturer's instructions and used at a final concentration of 0.1 µM (Yamashita and Tohyama, 2003).
The selective p160ROCK inhibitor Y-27632 (Cat. # 1254, TOCRIS), that inhibits ROCK activity by competitive binding with ATP to the catalytic domain (Narumiya et al., 2000), was dissolved in distilled water and used at a final concentration of 100 µM (Ishizaki et al., 2000).
Jasplakinolide (Cat. # 2792, TOCRIS), that stabilizes pre-formed actin filaments inhibiting their depolymerization (Bubb et al., 1994), was dissolved in DMSO and used at a final concentration of 0.2 µM (Rex et al., 2009).
The specific blocker for the sphingosine-1-phosphate (S1P) receptor JTE-013 (Cat # 2392, TOCRIS) was dissolved in DMSO according to the manufacturer's instructions and used at a final concentration of 5 µM.

Table 2.2: Summary of the antibodies, peptide and inhibitors for electrophysiological recording

Substance	Concentration	Source
Nogo inhibitory peptide Nogo-P4	4 µM	Alpha Diagnostic International (# Nogo-P4)
$p75^{NTR}$ inhibitor TAT-Pep5	0.1 µM	Calbiochem (# 506181)
p160ROCK inhibitor Y-27632	100 µM	Tocris (# 1254)
Jasplakinolide	0.2 µM	Tocris (# 2792)
S1PR antagonist JTE-013	5 µM	Tocris (# 2392)
anti-Lingo1 antibody	5 µg/ml	Abcam (# ab23631)
anti-NgR antibody	5 µg/ml	R&D Systems (# AF1440)
anti-Nogo-A antibody 11c7	5 µg/ml	Schwab lab
anti-BrdU antibody	5 µg/ml	Schwab lab

The equivalent amounts of solvents were used as control for each treatment.

2.2 Western blot experiment

Each group was composed of 6-8 acute hippocampal slices treated by bath application with the appropriate drugs or antibodies (Table 2.2: Nogo-P4 peptide, p160ROCK inhibitor Y-27632, 11C7 antibody, NgR antibody, control conditions) for different duration of time. In one experiment, 10-12 isolated CA1 regions per group were dissected 10 minutes after TBS from acute hippocampal slices used in electrophysiology experiments, and subsequently pooled.
Slices were homogenized in 1% Chaps based lysis buffer (30 mM Tris-Cl at pH 7,5, 150 mM NaCl, 1% Chaps) containing Protease Inhibitor (Complete protease inhibitor cocktail tablets, Roche) and Phosphatase Inhibitor (PhosSTOP phosphatase inhibitor cocktail tablets, Roche), and the debris were pelleted by centrifugation (15000 x g for 15 minutes at $4°C$). Protein concentration was measured via Bradford assay. All samples were diluted with loading buffer, 100 µg of proteins per lane were loaded and separated onto 4%-12% NuPAGE Bis-Tris Mini Gels (Invitrogen), and then transferred onto a polyvinylidene difluoride (PVDF) membrane using a semidry blot. The membrane was blocked with 5% BSA in tris-buffered saline (TBS)-Tween for 1 hour at room temperature and incubated at 4°C over night with the following primary antibodies diluted in 3% BSA in TBS-T (Table 2.3): anti-Cofilin (1:10000), anti-phospho-Cofilin (1:500), and anti-α-Tubulin (1:10000). The membrane was washed in TBS-T and incubated for 1 hour at room temperature with the anti-mouse (1:20000) or anti-rabbit (1:10000) secondary antibodies (Table 2.3) conjugated with horseradish peroxidase (HRP). Immunoreactivity was detected on a X-ray film by chemiluminescence (Luminata Crescendo Western HRP substrate, Millipore). After detection of phospho-Cofilin the blot was stripped and re-probed for total Cofilin. The relative optical density of the immunoreactive bands was analysed with ImageJ software and α-Tubulin was used as loading control. The control treatment was set to 1, and the ratio phospho-protein

Table 2.3: Summary of the antibodies for western blot experiment and F/G-actin ratio assay

Antibody	Dilution	Source
anti-Cofilin	1:10000	Abcam (# ab11062)
anti-phospho-Cofilin	1:500	Abcam (# ab12866)
anti-alpha-Tubulin	1:10000	Sigma-Aldrich (# 9026)
anti-Actin	1:500	Cytoskeleton (# AAN01)
anti-rabbit IgG peroxidase	1:10000/5000	Sigma-Aldrich (# A0545)
anti-mouse IgG peroxidase	1:20000	Sigma-Aldrich (# A9044)

to total-protein was normalized to the control.

The statistical analysis was performed by using GraphPad Prism with a two-tailed unpaired Student's t-test for the comparison of two independent means, or with a one-way ANOVA and Tukey's post hoc test for multiple comparisons. Values of $p < 0.05$ were considered significant and plotted as follows: *$p < 0.05$, **$p < 0.01$, ***$p < 0.001$. All data are shown as mean ± SEM. All graphs were generated using GraphPad Prism.

2.3 F/G-actin ratio assay

The assay was performed according to the manufacturer's instructions (Cytoskeleton, CO, USA). Briefly, 6-8 acute hippocampal slices were pooled in each group and treated by bath application with the appropriate drugs (Table 2.2: Nogo-P4 peptide; p160ROCK inhibitor Y-27632; Jasplakinolide; control conditions). The samples were homogenized in lysis and F-actin stabilization buffer (Cytoskeleton) containing 100 mM ATP and a protease inhibitor cocktail (Cytoskeleton). Tissue lysates were incubated at $37°C$ for 10 minutes and centrifuged for 1 hour at 100000 x g to separate the F-actin (pellet) from the G-actin fractions (supernatant). The G-actin supernatant was gently removed and the F-actin pellet was re-suspended in a F-actin depolymerization buffer (Cytoskeleton). All samples were diluted with loading buffer and 10 µl of pellet and supernatant samples were loaded into each lane and separated onto 4%-12% NuPAGE Bis-Tris Mini Gels (Invitrogen). After the transfer, the PVDF membrane was blocked with 5% not-fat milk for 30 minutes at room temperature and incubated at $4°C$ over night with the anti-actin primary antibody (1:500) diluted in 0.1% not-fat milk in TBS-T (Table 2.3). The membrane was washed in TBS-T and incubated for 1 hour at room temperature with the anti-rabbit (1:5000) secondary antibody HRP (Table 2.3). Immunoreactivity was detected on a X-ray film by chemiluminescence and the F/G-actin ratio was quantified by using ImageJ software. For each condition, the assay was performed in duplicate for at least three independent samples.

The statistical analysis was performed by using GraphPad Prism with a Student's t test. Values of $p < 0.05$ were considered significant and plotted as *$p < 0.05$. All data are shown as mean ± SEM. All graphs were generated using GraphPad Prism.

2.4 Imaging of mossy fiber synapses

2.4.1 Preparation of organotypic hippocampal slice cultures

Organotypic hippocampal slice cultures (OHCs) were prepared as described by Stoppini and colleagues (Stoppini et al., 1991). Postnatal day 5 (P5) transgenic mice of either sex expressing a membrane targeted form of eGFP in a subpopulation of neurons through the brain (Thy-1 mGFP transgenic mice) were used. After decapitation, the brain was removed and cut horizontally from caudal to rostral direction. The hemispheres were separated along the midline, and the exposed hippocampi were rolled out and separated from the cortex. The hippocampi were dissected in ice-cold sterile Gey's balanced salt solution (GBSS, Table 2.4) and sliced transversally at a thickness of 400 µm using a tissue chopper. The slices were incubated at $4°C$ for 30 minutes, subsequently placed on Millicells CM membrane inserts (Millipore) in a proper medium (Table 2.4), and cultivated at $37°C$, 5% CO_2, 99% humidity environment. Three days after preparation a mixture of antimitotic drugs (cytosine arabinoside, uridine, and fluorodeoxyuridine; 10^{-6} - 10^{-7} M each; Sigma-Aldrich) was applied for 24 hours and 50% of medium was changed once a week. After 7 days in vitro (DIV) the medium was supplemented with 1.25 µg/ml of Fungizone, 100 U of Penicillin and 100 µg/ml of Streptomycin.

2.4.2 Imaging and antibody treatment

Time-lapse imaging and acute treatment

The 21 DIV OHCs were transferred to an open imaging chamber at $32°C$ and continuously perfused with high Mg^{2+} ACSF (Table 2.1) at a rate of 0.8 ml/min. Before starting imaging the slices were let adapt for 20 minutes. Confocal image stacks of eGFP labelled mossy fiber synapses located in the stratum lucidum of CA3 area of

Table 2.4: Recipes of solutions for the organotypic hippocampal slice cultures. Left panel: summary of the final concentration [mM] of the components used for the preparation of the GBSS. Right panel: receipt of the medium used for the cultivation of the organotypic slice cultures.

Gey's Balanced Salt Solution (GBSS)	
Component	Molarity [mM]
NaCl	1.37
KCl	5.0
NaH_2PO_4	0.86
KH_2PO_4	0.22
$MgCl_2$ * 6 H_2O	1.0
$MgSO_4$ * 7 H_2O	0.28
$NaHCO_3$	2.7
$CaCl_2$ * 2 H_2O	1.5
D (+) Glucose	5.5

Medium	
Component	Amount (ml)
BME	100
HBSS	50
Equine donor serum	50
L-Glutamine (200 mM)	1
Glucose (50%)	2

the hippocampus were acquired with a laser scanning confocal microscope (Olympus, BX61WI FluoView 1000) using a 60x water objective (1.0 NA). The eGFP was excited with an excitation wavelength of 488 nm and the power of the excitation laser was maintained low (1-2%). Stacks of 15/20 optical sections (512 x 256 pixel, final pixel size 65 nm, z-step size 0.35 µm) were collected.
The Nogo-A antibody 11C7 or control antibody (Table 2.2) was dissolved at a final concentration of 5 µg/ml in 20 ml of high Mg^{2+} ACSF containing 0.1 mg/ml BSA to prevent the unspecific binding of the antibodies. To prevent sticking of the antibodies to the tubing or chamber, the experiment was performed by using PharMed Ismaprene tubing (Ismatec). Stacks, collected every 5 minutes for 20 minutes, were acquired one time before (t0) and three times after the treatment (t1, t2, t3) at intervals of 1 hour (Fig. 2.5).

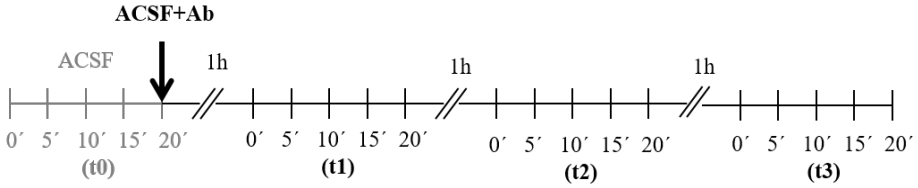

Figure 2.5: Time-lapse confocal imaging protocol.

Chronic treatment and imaging

The Nogo-A antibody 11C7 or control antibody (Table 2.2) was applied directly into the medium at a final concentration of 5 µg/ml, and the treatment was replaced and repeated twice during the four days of application. At the end of the treatment, the cultures were fixed with ice-cold 4% paraformaldehyde (PFA) and mounted using an anti-fading aqueous mounting medium (Fluoro-Gel Emsdiasum).
The eGFP expressing mossy synapses located in the stratum lucidum of CA3 area of the hippocampus and presenting any sign of degeneration were selected and imaged with an ApoTome imaging system (Zeiss) using a 63 x objective (1.32 NA), and z-sectioned at 0.475 µm.

2.4.3 Data analysis

Confocal images were deconvolved using AutoQuantX2 (Media cybernetics, Inc.) and analysed with ImageJ software. For each frame a maximum intensity projection was obtained, and two-dimensional morphometric analysis of mossy fiber synapsess was done using the segmented line tool of ImageJ to measure the area of the core of the terminals and the length of their filopodial extensions.
To analyse the short-term structural reorganization of mossy fiber synapses, the motility index (MI) was quantified (Chierzi et al., 2012). The area (A) of terminals and the length (L) of filopodia were measured for each frame (at 0, 5, 10, 15 and 20 minutes, Fig. 2.5). MI was calculated for all time points (t0, t1, t2 and t3, Fig. 2.5) according to the Eq. (2.3) and Eq. (2.4) for terminals and filopodia MI, respectively.

$$\frac{|A_2 - A_1| + |A_3 - A_2| + |A_4 - A_3| + |A_5 - A_4|}{(A_1 + A_2 + A_3 + A_4 + A_5)/5} \tag{2.3}$$

$$\frac{|L_2 - L_1| + |L_3 - L_2| + |L_4 - L_3| + |L_5 - L_4|}{(L_1 + L_2 + L_3 + L_4 + L_5)/5} \tag{2.4}$$

To asses the long-term structural reorganization of mossy fiber synapses, I analysed three-dimensional Apotome images. For all the synapses in the stack, I traced and measured the area of all the terminals and the length of their filopodial extensions by using Neurolucida software (MicroBrightField).

Statistical analysis was performed using GraphPad Prism with a two-tailed unpaired Student's t-test for the comparison of two independent means, or with a one-way ANOVA repeated measurement test and Dunnett's post hoc test for multiple comparisons. Values of $p < 0.05$ were considered significant and plotted as follows: *$p < 0.05$, **$p < 0.01$, ***$p < 0.001$. All data are shown as mean ± SEM. All graphs were generated using GraphPad Prism.

3 | Results

> Above all, don't fear difficult moments.
> The best comes from them.
>
> *Rita Levi Montalcini*

Morphological and functional changes at synapses are believed to be the cellular correlate of learning and memory processes. These alterations in large part depend on the remodelling of the actin cytoskeleton. Interestingly, Nogo-A protein has been shown to limits functional plasticity in the mature mouse hippocampus via two inhibitory domain, Nogo-A-Δ20 and Nogo-66. In particular, the Nogo-66 domain of Nogo-A restricts LTP at the Schaffer collateral-CA1 pathway signalling via its receptor NgR1. However, the question of which is the molecular mechanisms mediating this role of Nogo-A is unresolved. Moreover, although Nogo-A has been shown to restricts morphological changes at dendritic spines, its involvement in mediating remodelling at presynaptic compartment is still open. In the first part of my work, I addressed the molecular mechanism mediating the role of Nogo-A in limiting functional plasticity in the adult mouse hippocampus. In particular, in section 3.1 (3.1.1 - 3.1.4) I questioned whether and how the NgR1 co-receptors, $p75^{NTR}$ and Lingo1, mediate the Nogo-66 / NgR1 signalling in restricting LTP. In section 3.1 (3.1.5 - 3.1.7) I investigated whether Nogo-66 / NgR1 and Nogo-A-Δ20 / S1PR2 signalling might modulate actin dynamics to negatively regulate LTP. In the second part of my work, I addressed the question of whether Nogo-A is involved in regulating the structural reorganization at presynaptic compartment (section 3.2). For this purpose, I analyses whether Nogo-A affect the morphological remodelling of the mossy fiber synapses.

3.1 The molecular mechanism mediating the role of Nogo-A in negatively regulating LTP

3.1.1 Nogo-66 is a negative regulator of LTP but not of LTD

The Nogo-66 inhibitory domain of Nogo-A restricts LTP in the mature mouse hippocampus. In particular, it has been shown that a local application of a Nogo-66 peptide suppresses LTP (Raiker et al., 2010). Here, I assessed the role of Nogo-66 in regulating short- and long-term plasticity at the Schaffer collateral-CA1 pathway using a different approach. Indeed, for achieving this issue I treated the acute hippocampal slices from wild-type mice with the 25 amino acid peptide Nogo-P4, shown to mimic the Nogo-66 inhibitory activity on axonal regeneration (GrandPré et al., 2000) and to inhibit the neurite outgrowth *in vitro* (Yamashita and Tohyama, 2003), (Hasegawa et al., 2004), (Fujitani et al., 2005).

In order to investigate whether Nogo-66 regulate long-term plasticity, I applied the Nogo-P4 peptide and I analysed whether it affects LTP induced by a theta-burst stimulation (TBS) protocol. After 20 minutes of stable baseline stimulation, the induction of LTP by TBS led to increase the synaptic strength in control condition, resulting in a stable potentiation until the end of recordings (Fig. 3.1A, black diamonds). The application of Nogo-P4 peptide for 10 minutes around LTP induction resulted in a significantly lower LTP magnitude when compared to the control treatment (Fig. 3.1A, black diamonds *versus* white circles). The average potentiation at 55-60 minutes after TBS was 161.1 ± 12.1 for control / black bar ($n = 8$ slices / 5 animals) and 128.9 ± 5.3 for Nogo-P4 treatment / white bar ($n = 9$ slices / 5 animals), (Fig. 3.1A', $p < 0.05$).

To investigate whether Nogo-66 modulates LTD, I analysed both the NMDA receptor - dependent (Fig. 3.2) and independent form of LTD (Fig. 3.3). Indeed, the NMDAR - dependent LTD is more efficiently inducible in acute hippocampal slices from juvenile than adult mice. On the contrary, a NMDAR - independent form of LTD, the mGluR - dependent LTD, is inducible also in acute slices from adult hippocampus. First, I analysed NMDA receptor - dependent LTD induced by a low frequency stimulation (LFS) protocol to acute hippocampal slices from juvenile (P14-P20) wild-type mice. After 20 minutes of stable baseline stimulation, the induction of LTD by LFS led to decrease the synaptic strength in control condition, resulting in a stable depotentiation until the end of recordings (Fig. 3.2A, black diamonds). The application of Nogo-P4 peptide for the whole duration of recording did not influence the magnitude of this form of LTD (Fig. 3.2A, black diamonds *versus* white circles). Indeed, the average depression at 55-60 minutes after LFS was 71.8 ± 2.8 for control / black bar ($n = 8$

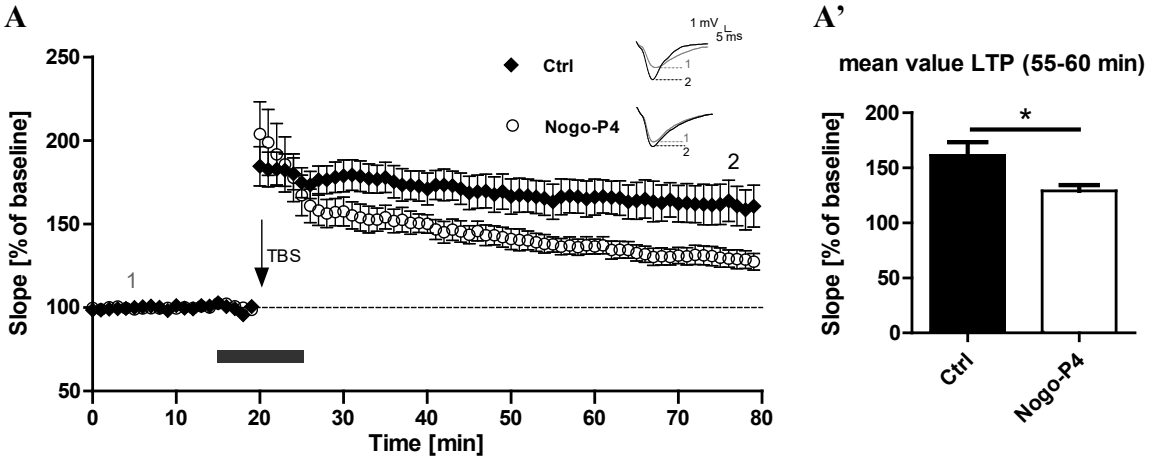

Figure 3.1: Nogo-66 decreases the magnitude of LTP. **(A)** LTP recordings after TBS (arrow), **(A')** mean fEPSP at 55-60 minutes post TBS upon application of Nogo-P4 peptide (white circles / bar 128.9 ± 5.3, $n = 9$ slices / 5 animals) or control (black diamonds / bar 161.1 ± 12.1, $n = 8$ slices / 5 animals) for 10 minutes around LTP induction (horizontal bar). *Insets* show original traces from representative individual experiments (1 is for fEPSP 5 minutes before TBS, 2 for fEPSP 55 minutes after TBS; vertical scale bar 1 mV, horizontal scale bar 5 ms). *p<0.05. *Error bars* SEM.

slices / 3 animals) and 73.7 ± 2.6 for Nogo-P4 treatment / white bar (n = 8 slices / 3 animals), (Fig. 3.2A'). Similarly, the application of the peptide only around LTD induction did not affect NMDA receptor - dependent LTD (Fig. 3.2B, black diamonds *versus* white circles). Indeed, the average depression at 55-60 minutes after LFS was 80.1 ± 6.1 for control / black bar (n = 8 slices / 4 animals) and 84.4 ± 2.3 for Nogo-P4 treatment / white bar (n = 7 slices / 4 animals), (Fig. 3.2B'). Next, I tested whether a NMDA receptor - independent form of LTD is modulated by the application of Nogo-P4 peptide. For this purpose, I applied a paired-pulse low frequency stimulation (PP-LFS) protocol to acute slices from adult (P40-P60) wild-type mice resulting in a mGlu receptor - dependent form of LTD (Kemp et al., 2000), (Huber, 2000). The application of Nogo-P4 peptide for the whole duration of recording did not influence

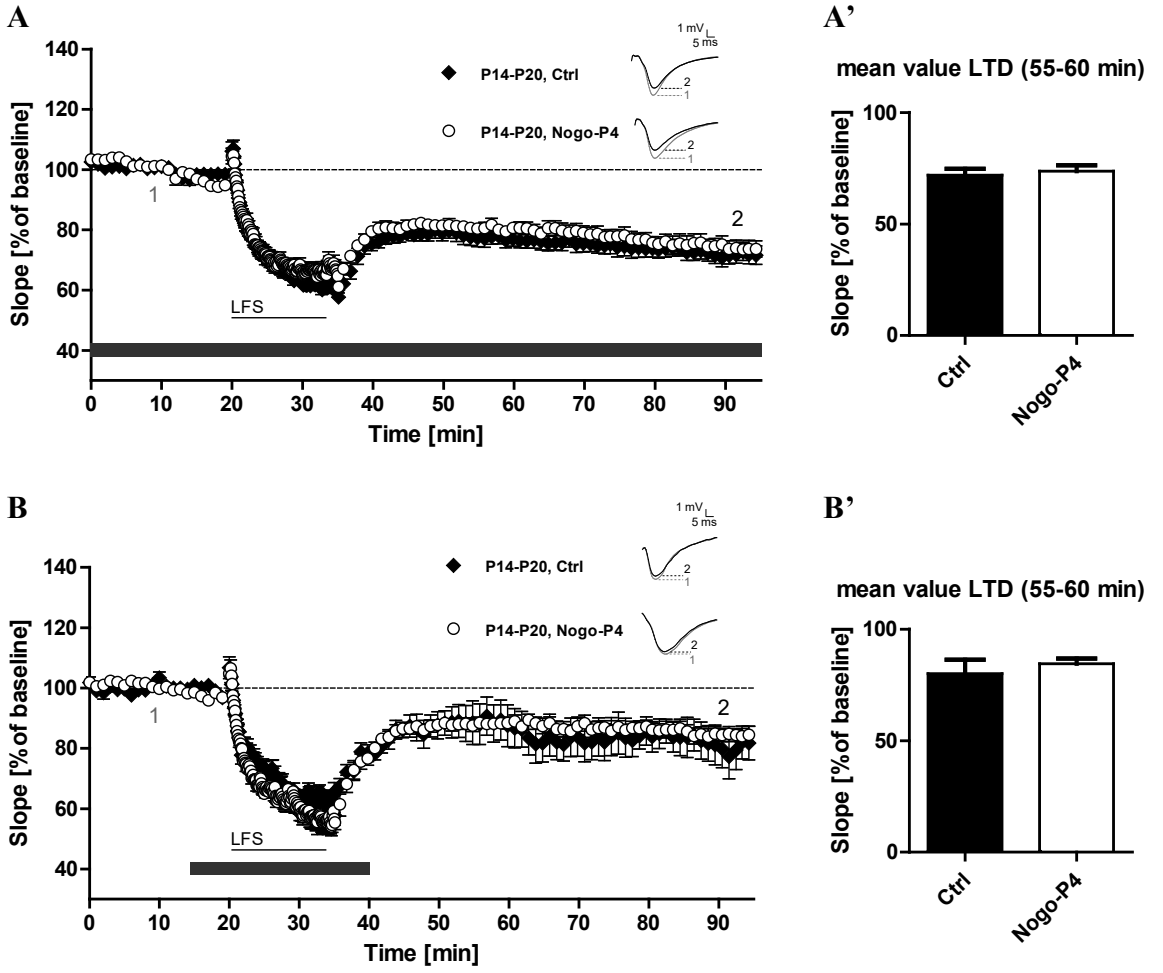

Figure 3.2: Nogo-66 does not alter NMDA receptor - dependent LTD. **(A)**, **(B)** LTD recordings in the CA1 region of acute hippocampal slices from juvenile mice (P14-P20) after LFS (line), **(A')** mean fEPSP at 55-60 minutes post LFS upon Nogo-P4 peptide application (white circles / bar, 73.7 ± 2.6, n = 8 slices / 3 animals) or control (black diamonds / bar 71.8 ± 2.8, n = 8 slices / 3 animals) for the whole experiment (horizontal bar), **(B')** mean fEPSP at 55-60 minutes post LFS upon Nogo-P4 peptide application (white circles / bar 84.4 ± 2.3, n = 7 slices / 4 animals) or control (black diamonds / bar 80.0 ± 6.1, n = 8 slices / 4 animals) for 25 minutes around LTD induction (horizontal bar). *Insets* show original traces from representative individual experiments (1 is for fEPSP 5 minutes before LFS, 2 for fEPSP 55 minutes after LFS; vertical scale bar 1 mV, horizontal scale bar 5 ms). *Error bars* SEM.

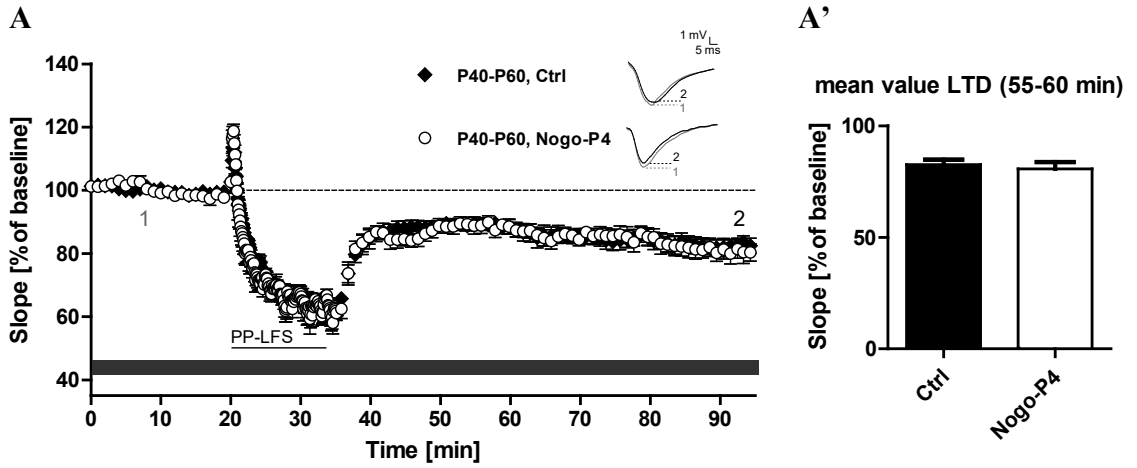

Figure 3.3: Nogo-66 does not alter mGlu receptor - dependent LTD. **(A)** LTD recordings in the CA1 region of acute hippocampal slices adult mice (P40-P60) after PP-LFS (line), **(A')** mean fEPSP at 55-60 minutes post PP-LFS upon Nogo-P4 peptide application (white circles / bar 80.7 ± 3.0, $n = 6$ slices / 4 animals) or control (black diamonds / bar 82.6 ± 2.2, $n = 9$ slices / 6 animals) for the whole duration of the experiments (horizontal bar). *Insets* show original traces from representative individual experiments (1 is for fEPSP 5 minutes before PP-LFS, 2 for fEPSP 55 minutes after PP-LFS; vertical scale bar 1 mV, horizontal scale bar 5 ms). *Error bars* SEM.

the level of mGlu receptor - dependent LTD in comparison to the control (Fig. 3.3A, black diamonds *versus* white circles; 3.3A' the average depression at 55-60 minutes after PP-LFS was 82.6 ± 2.2 for control / black bar ($n = 9$ slices / 6 animals) and 80.7 ± 3.0 for Nogo-P4 treatment / white bar ($n = 6$ slices / 4 animals)).
In order to analyse the influence of the application of Nogo-P4 peptide on short-term plasticity, I tested paired-pulse facilitation (PPF; Fig. 3.4A), as an indicator of a presynaptic calcium - dependent increase in neurotransmitter release. For this purpose, PPF was measured by dividing the slope of the second fEPSP by the slope of the first fEPSP elicited by two electrical pulses at different inter-stimulus intervals (ISI).

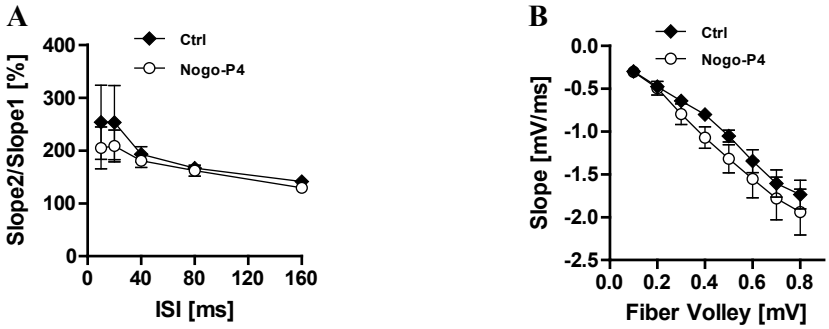

Figure 3.4: Nogo-66 does not influence short-term plasticity or basal synaptic transmission. PPF analysis (**A**, $n = 8$ slices / 4 animals for control treatment; $n = 6$ slices / 3 animals for Nogo-P4 treatment) performed by applying two stimuli separated by different ISI (10, 20, 40, 80, and 160 ms) and FV measurement (**B**, $n = 7$ slices / 3 animals for control treatment; $n = 8$ slices / 3 animals for Nogo-P4 treatment) upon application of Nogo-P4 peptide or control for 20 minutes. *Error bars* SEM.

The bath application of Nogo-P4 peptide did not result in any difference at any ISI analysed in comparison to the control (Fig. 3.4A). Additionally, I tested whether the LTP defect observed after application of Nogo-P4 peptide might be due to altered basal synaptic transmission. For this purpose, I compared the fiber volley (FV) amplitude, as an indicator of the number of presynaptic action potential, with the fEPSP slope. The average fEPSP slope was reduced at given increasing FV amplitudes in control condition. Bath application of Nogo-P4 peptide did not affect the FV amplitude to fEPSP slope ratio in comparison to the control (Fig. 3.4B).
Taken together, these data show a selective role for the Nogo-66 inhibitory domain in limiting LTP magnitude, without affecting basal synaptic transmission as well as other forms of activity - dependent functional plasticity as LTD or short-term plasticity.

3.1.2 Lingo1 mediates the activity of Nogo-66 in regulating LTP

Nogo-66 signals via the Nogo Receptor 1 (NgR1) to regulate synaptic function (Raiker et al., 2010). NgR1 lacks a cytosolic domain (Venkatesh et al., 2005), and forms a receptor complex to activate an intracellular signalling cascade (Wang et al., 2002a), (Mi et al., 2004). The transmembrane protein Lingo1 has been shown to be one co-receptor mediating NgR1 signalling in axonal regeneration. Here, I investigated whether Lingo1 might be involved in mediating the signalling activated by Nogo-66 domain in regulating LTP in the adult mouse hippocampus
First, I analysed the role of Lingo1 in regulating LTP at the Schaffer collateral-CA1 pathway by treating acute hippocampal slices with a specific Lingo1 function blocking antibody. The neutralization of Lingo1 1 hour before and during the entire recording resulted in a significant increase of LTP magnitude when compared to the control

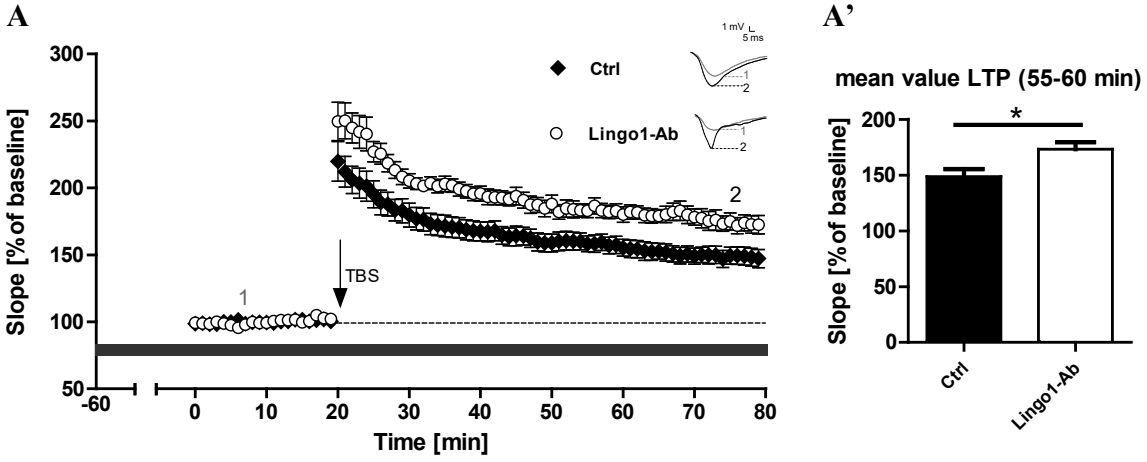

Figure 3.5: The neutralization of Lingo1 receptor increases LTP. **(A)** LTP recordings after TBS (arrow), **(A')** mean fEPSP at 55-60 minutes post TBS upon the neutralization of Lingo1 (white circles / bar 173.2 ± 6.2, $n = 8$ slices / 5 animals) or control (black diamonds / bar 148.7 ± 6.6, $n = 12$ slices / 7 animals) 1 hour before and during the whole recordings (horizontal bar). *Insets* show original traces from representative individual experiments (1 is for fEPSP 5 minutes before TBS, 2 for fEPSP 55 minutes after TBS; vertical scale bar 1 mV, horizontal scale bar 5 ms). *p<0.05. *Error bars* SEM.

treatment (Fig. 3.5A, black diamonds *versus* white circles). Indeed, the average potentiation at 55-60 minutes after TBS was 148.7 ± 6.6 for control / black bar ($n = 12$ slices / 7 animals) and 173.2 ± 6.2 for Lingo1 antibody treatment / white bar ($n = 8$ slices / 5 animals), (Fig. 3.5A', $p < 0.05$).

In order to analyse the influence of the neutralization of Lingo1 on short-term plasticity, I performed PPF measurement. The analysis of presynaptic function upon neutralization of Lingo1 for 1 hour revealed no alteration in PPF at any ISI analysed in comparison to the control treatment (Fig. 3.6A). Moreover, to test whether the LTP phenotype observed after neutralization of Lingo1 might be due to altered basal synaptic transmission, I performed FV measurements. The neutralization of Lingo1 did not affect the FV amplitude to fEPSP slope ratio in comparison to the control treatment (Fig. 3.6B).

To assess whether Lingo1 mediates the effect of Nogo-P4 application on LTP, I applied the peptide at the beginning of recording to slices pre-treated for 1 hour with the anti-Lingo1 antibody. Upon Lingo1 neutralization, the Nogo-P4-induced decrease in LTP was completely prevented (Fig. 3.7A, white circles *versus* grey squares). Indeed, in the Lingo1 antibody plus Nogo-P4 treated slices the LTP level was comparable to the one in control treatment (Fig. 3.7A, white circles *versus* black diamonds), revealing that blocking Lingo1 rescues the effect of a Nogo-P4 peptide application on LTP. The average of potentiation at 55-60 minutes after TBS for the single Nogo-P4 treatment / grey bar was 119.2 ± 6.5 ($n = 7$ slices / 5 animals) while the potentiation for the combined Lingo1 antibody plus Nogo-P4 treatment / white bar was 150.9 ± 4.2 ($n = 9$ slices /4 animals), (Fig. 3.7A', $p <= 0.01$), comparable with that of the control / black bar that was 148.7 ± 6.6 ($n = 12$ slices / 7 animals), (Fig. 3.7A'). The difference in potentiation between Lingo1 antibody plus Nogo-P4 co-treatment and for the control treatment was not significantly different.

Taken together, these data show that the NgR1 co-receptor Lingo1 regulates LTP without affecting short-term plasticity or basal synaptic transmission. Moreover, neutralization of Lingo1 rescues the effect of the Nogo-66 inhibitory domain on LTP, sug-

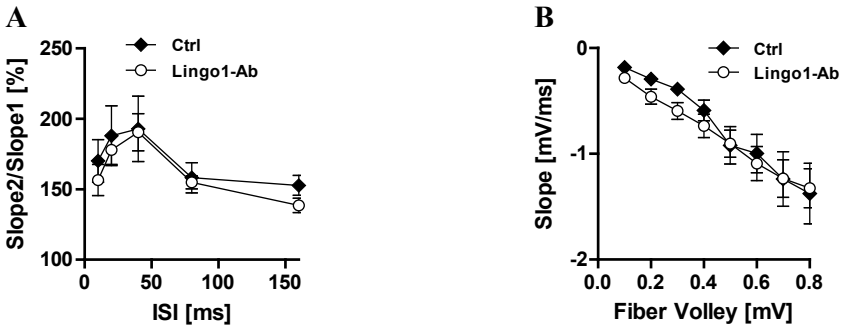

Figure 3.6: The neutralization of Lingo1 receptor does not influence short-term plasticity or basal synaptic transmission. PPF analysis (**A**, $n = 6$ slices / 3 animals for control treatment; $n = 8$ slices / 3 animals for Lingo1 antibody treatment) and FV measurements (**B**, $n = 6$ slices / 3 animals for control treatment; $n = 8$ slices / 3 animals for Lingo1 antibody) upon neutralization of Lingo1 or control treatment for 1 hour. *Error bars* SEM.

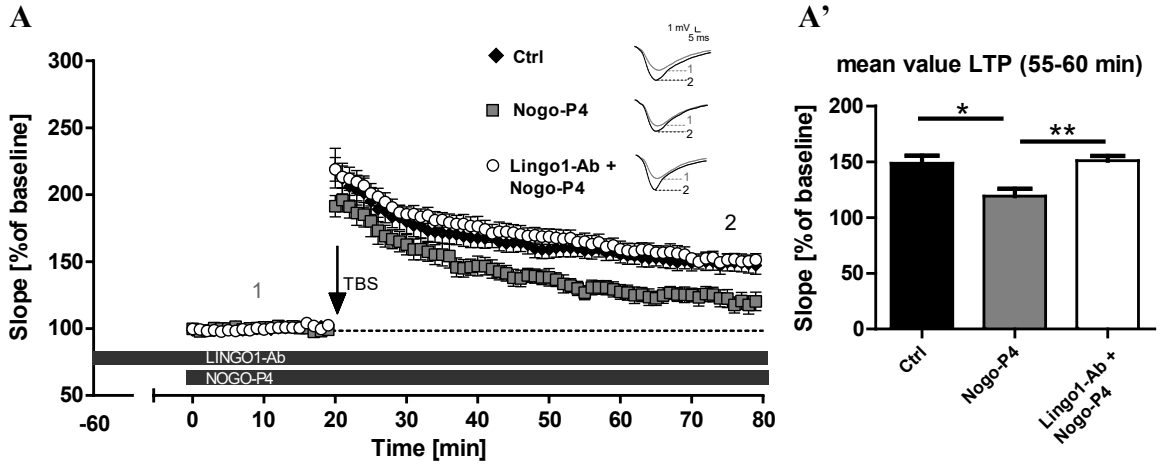

Figure 3.7: The neutralization of Lingo1 receptor rescues the Nogo-66 domain - dependent restriction of LTP. **(A)** LTP recordings after TBS (arrow), **(A')** mean fEPSP at 55-60 minutes post TBS upon application of Nogo-P4 peptide (grey squares / bar 119.2 ± 6.5, $n = 7$ slices / 5 animals) or application of Nogo-P4 peptide from the beginning of recordings (in lower horizontal bar) to slices pre-treated for 1 hour with Lingo1 antibody (white circles / bar 150.9 ± 4.2, $n = 9$ slices /4 animals) or control treatment (black diamonds / bar 148.7 ± 6.6, $n =$ 12 slices / 7 animals). *Insets* show original traces from representative individual experiments (1 is for fEPSP 5 minutes before TBS, 2 for fEPSP 55 minutes after TBS; vertical scale bar 1 mV, horizontal scale bar 5 ms). *p<0.05, **p<0.01). *Error bars* SEM.

gesting that Lingo1 might be the signalling partner of NgR1 mediating the Nogo-66 - dependent effect on LTP.

3.1.3 p75^{NTR} does not mediate the Nogo-66 - dependent effect on LTP

The p75 neurotrophin receptor p75^{NTR} has been shown to act as a co-receptor mediating NgR1 signalling in regulating axonal regeneration in the mature CNS (Wang et al., 2002a). Indeed, the receptor complex formed by NgR1 / Lingo1 / p75^{NTR} is needed to transduce the signalling pathway activated by Nogo-A to prevent neurite outgrowth (Mi et al., 2004). In the context of activity - dependent synaptic plasticity, it has been shown that p75^{NTR} knockout mice do not show any impairment of LTP (Rösch et al., 2005), (Woo et al., 2005). However, the questions of whether acutely blocking p75^{NTR} results in LTP defect and whether p75^{NTR} might be involved in the transduction of the Nogo-66 signalling in negatively regulating LTP have not yet been analysed. Here, I addressed these questions.

I analysed the role of p75^{NTR} in regulating LTP at the Schaffer collateral-CA1 pathway by treating the acute hippocampal slices from wild-type mice with the cell-permeable peptide TAT-Pep5 shown to be a specific inhibitor of p75^{NTR} (Yamashita and Tohyama, 2003). Blocking p75^{NTR} signalling 1 hour before and until the end of recording did not significantly change the magnitude of LTP in comparison to the control treatment (Fig. 3.8A, black diamonds *versus* white circles). Indeed, the average potentiation at 55-60 minutes after TBS was 158.0 ± 5.8 for control / black bar ($n = 6$ slices / 4 animals) and 149.8 ± 6.0 for TAT-Pep5 treatment / white bar ($n = 7$ slices / 4 animals), (Fig.

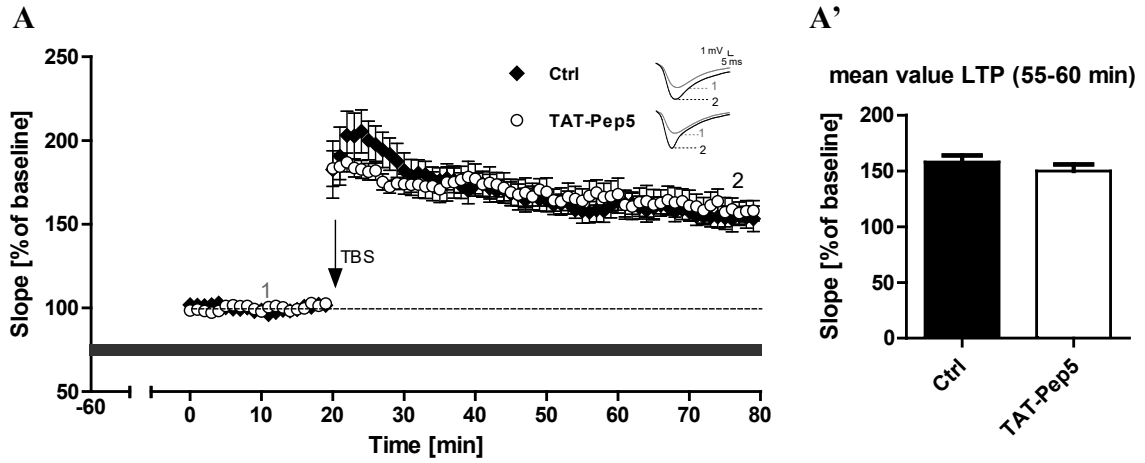

Figure 3.8: The neutralization of p75^{NTR} does not affect LTP. **(A)** LTP recordings after TBS (arrow), **(A')** mean fEPSP at 55-60 minutes post TBS upon inhibition of p75^{NTR} with the cell-permeable TAT-Pep5 inhibitor (white circles / bar 149.8 ± 6.0, n = 7 slices / 4 animals) or control (black diamonds / bar 158.0 ± 5.8, n = 6 slices / 4 animals) 1 hour before and during the whole experiments (horizontal bar). *Insets* show original traces from representative individual experiments (1 is for fEPSP 5 minutes before TBS, 2 for fEPSP 55 minutes after TBS; vertical scale bar 1 mV, horizontal scale bar 5 ms). *Error bars* SEM.

3.8A'). This finding confirms previous studies using genetic deletion of p75^{NTR} and showing that it is not necessary for the induction or expression of LTP (Rösch et al., 2005), (Woo et al., 2005).

I analysed whether the presynaptic function and basal synaptic transmission are affected upon blocking p75^{NTR}. The neutralization of p75^{NTR} for 1 hour with the TAT-Pep5 inhibitor did not influence PPF (Fig. 3.9A) or FV amplitude to fEPSP slope ratio (Fig. 3.9B) in comparison to the controls.

To test whether blocking p75^{NTR} might still rescue the negative effect of Nogo-P4 application on LTP, the peptide was applied to acute hippocampal slices derived from p75^{NTR} knock-out mice (Fig. 3.10). The application of Nogo-P4 peptide for the whole

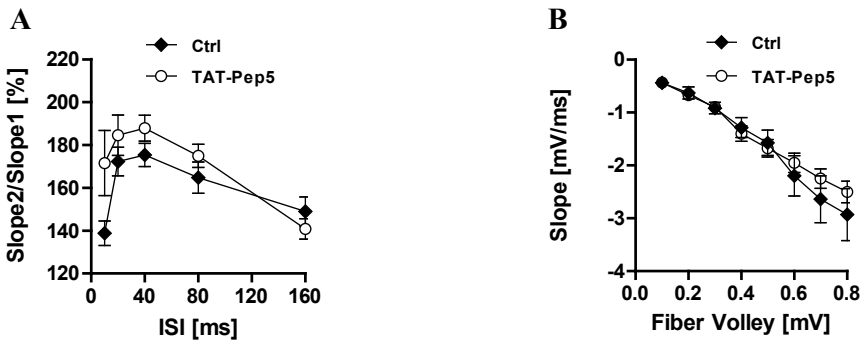

Figure 3.9: The neutralization of p75^{NTR} does not influence short-term plasticity or basal synaptic transmission. PPF analysis (**A**, n = 7 slices / 3 animals for control treatment; n = 8 slices / 3 animals for TAT-Pep5 treatment) and FV measurement (**B**, n = 9 slices / 3 animals for control treatment; n = 9 slices / 3 animals for TAT-Pep5 treatment) upon inhibition of p75^{NTR} or control treatment for 1 hour. *Error bars* SEM.

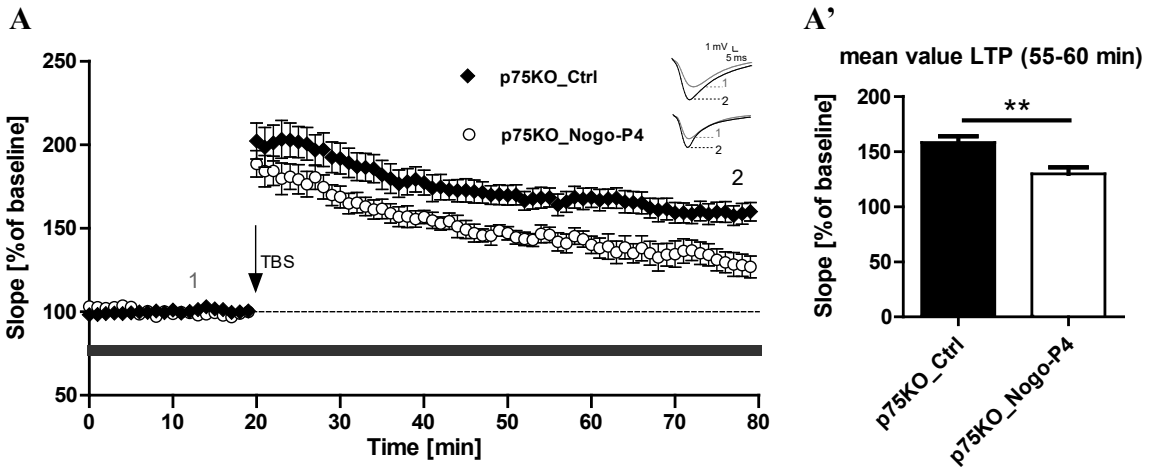

Figure 3.10: The deletion of $p75^{NTR}$ does not rescue the Nogo-66 domain - dependent restriction of LTP. **(A)** LTP recordings in the CA1 region of acute hippocampal slices from $p75^{NTR}$ KO mice after TBS (arrow), **(A')** mean fEPSP at 55-60 minutes post TBS upon application of Nogo-P4 peptide (white bar / circles 129.7 ± 5.9, n = 6 slices / 3 animals) or control (black diamonds / bar 158.2 ± 5.6, n = 9 slices / 3 animals) from the beginning of recording. *Insets* show original traces from representative individual experiments (1 is for fEPSP 5 minutes before TBS, 2 for fEPSP 55 minutes after TBS; vertical scale bar 1 mV, horizontal scale bar 5 ms). **p<0.01. *Error bars* SEM.

duration of recording significantly decreased the level of LTP in comparison to the control treatment (Fig. 3.10A, black diamonds *versus* white circles), reproducing the effect of the Nogo-P4 peptide observed for LTP in wild-type slices (Fig. 3.1A-A'). The average potentiation at 55-60 minutes after TBS was 158.2 ± 5.6 for control / black bar (n = 9 slices / 3 animals) and 129.7 ± 5.9 for Nogo-P4 treatment / white bar (n = 6 slices / 3 animals), (Fig. 3.10A', $p < 0.01$).

Taken together, these data show that the neurotrophin receptor $p75^{NTR}$ does not have a role in regulating LTP as well as short-term plasticity or basal synaptic transmission. Because inhibition of $p75^{NTR}$ does not rescue the effect of Nogo-66 inhibitory domain on LTP, one can conclude that $p75^{NTR}$ is not the signalling partner of NgR1 mediating the transduction of the signalling pathway activated by Nogo-66 domain to restrict LTP.

3.1.4 Loss-of-function for NgR1 and $p75^{NTR}$, but not for Lingo1, attenuates LTD

While a gain-of-function approach for Nogo-66 did not affect both NMDAR- and mGluR - dependent LTD (Fig. 3.2A-A'), in NgR1 KO mice NMDA receptor - dependent LTD was shown to be attenuated (Lee et al., 2008), suggesting that this activity of NgR1 might be independent of Nogo-66. Thus, I first confirmed the role of NgR1 in regulating LTD at the Schaffer collateral-CA1 pathway by acutely blocking its function. Indeed, the treatment of acute hippocampal slices with a NgR function blocking antibody 1 hour before and during the whole experiment significantly attenuated NMDA receptor - dependent LTD induced by a low frequency stimulation (LFS)

protocol in comparison to the control treatment (Fig. 3.11A, black diamonds *versus* white circles). The average depression at 55-60 minutes after LFS was 80.2 ± 2.9 for control / black bar (n = 7 slices / 3 animals) and 93.8 ± 3.7 for NgR antibody treatment / white bar (n = 6 slices / 3 animals), (Fig. 3.11A', $p < 0.01$).
To examine whether the NgR1 co-receptors $p75^{NTR}$ might be involved in modulating LTD at the Schaffer collateral-CA1 pathway, I induced the NMDA receptor - dependent form of LTD using LFS protocol to acute hippocampal slices after treatment for 1 hour with the inhibitor of $p75^{NTR}$ TAT-Pep5. As expected from previous publications (Rösch et al., 2005), (Woo et al., 2005), inhibition of $p75^{NTR}$ signalling resulted in a significant attenuated LTD (Fig. 3.12A, black diamonds *versus* white circles), mimicking the effect observed after the neutralization of NgR1 (Fig. 3.11). The average depression was 68.5 ± 2.7 for control / black bar (n = 5 slices / 3 animals) and 82.1 ± 2.8 for TAT-Pep5 treatment / white bar (n = 8 slices / 3 animals), (Fig. 3.12A', $p < 0.05$).
To examine whether the NgR1 co-receptors Lingo1 might be involved in modulating LTD, I induced NMDA receptor - dependent LTD using a LFS protocol to acute hippocampal slices after treatment for 1 hour with the Lingo1 function blocking antibody. The neutralization of Lingo1 did not affect LTD (Fig. 3.13A, black diamonds *versus* white circles), as the magnitude of LTD is comparable with that of the control treatment (Fig. 3.13A', the average depression was 81.3 ± 2.5 for control / black bar (n = 10 slices / 4 animals) and 84.0 ± 3.4 for Lingo1 antibody treatment / white bar (n = 11 slices / 4 animals)).
Taken together, these data show that NgR1 as well as $p75^{NTR}$ attenuate LTD, while Lingo1 does not play a role in regulating LTD, suggesting that NgR1 might attenuate LTD in a $p75^{NTR}$ - dependent manner but independently of Lingo1 signalling.

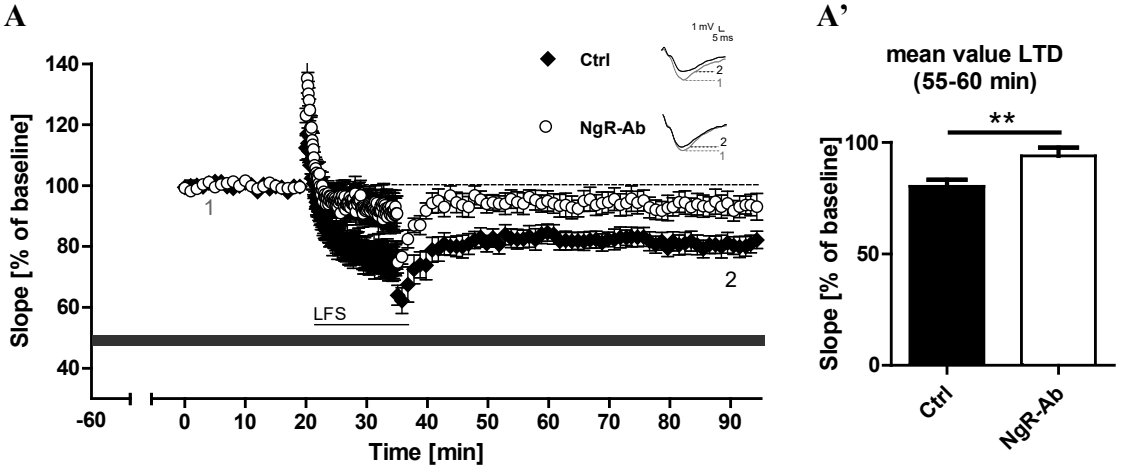

Figure 3.11: The neutralization of NgR1 attenuates LTD. **(A)** LTD recordings after LFS (line), **(A')** mean fEPSP at 55-60 minutes post LFS upon neutralization of NgR1 (white circles / bar 93.8 ± 3.7, n = 6 slices / 3 animals) or control treatment (black diamonds / bar 80.2 ± 2.9, n = 7 slices / 3 animals) 1 hour before and during the whole experiments (horizontal bar). *Insets* show original traces from representative individual experiments (1 is for fEPSP 5 minutes before LFS, 2 for fEPSP 55 minutes after LFS; vertical scale bar 1 mV, horizontal scale bar 5 ms). **p<0.01. *Error bars* SEM.

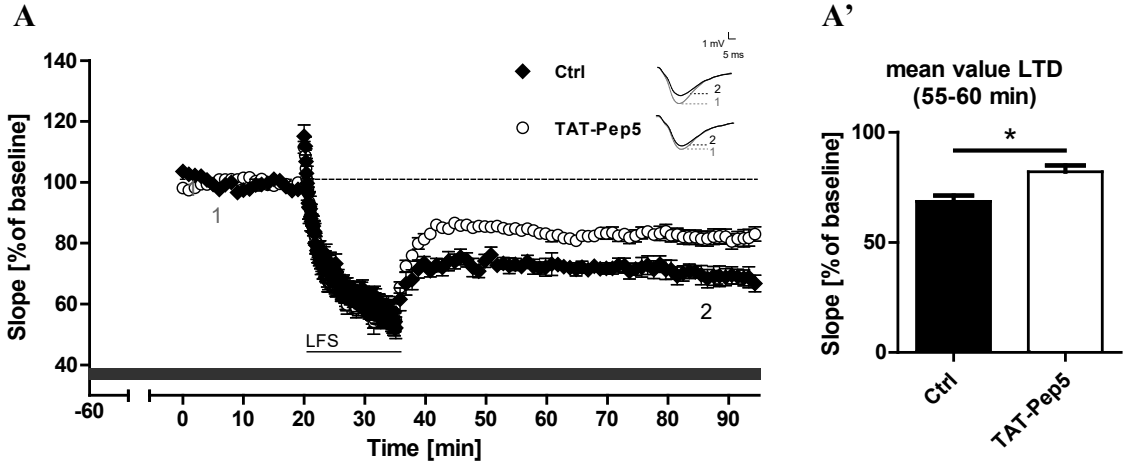

Figure 3.12: The neutralization of p75^{NTR} attenuates LTD. **(A)** LTD recordings after LFS (line), **(A')**mean fEPSP at 55-60 minutes post LFS upon inhibition of p75^{NTR} (white circles / bar 82.1 ± 2.8, $n = 8$ slices / 3 animals) or control treatment (black diamonds / bar 68.5 ± 2.7, $n = 5$ slices / 3 animals) 1 hour before and during the entire experiments (horizontal bar). *Insets* show original traces from representative individual experiments (1 is for fEPSP 5 minutes before LFS, 2 for fEPSP 55 minutes after LFS; vertical scale bar 1 mV, horizontal scale bar 5 ms). *p<0.05. *Error bars* SEM.

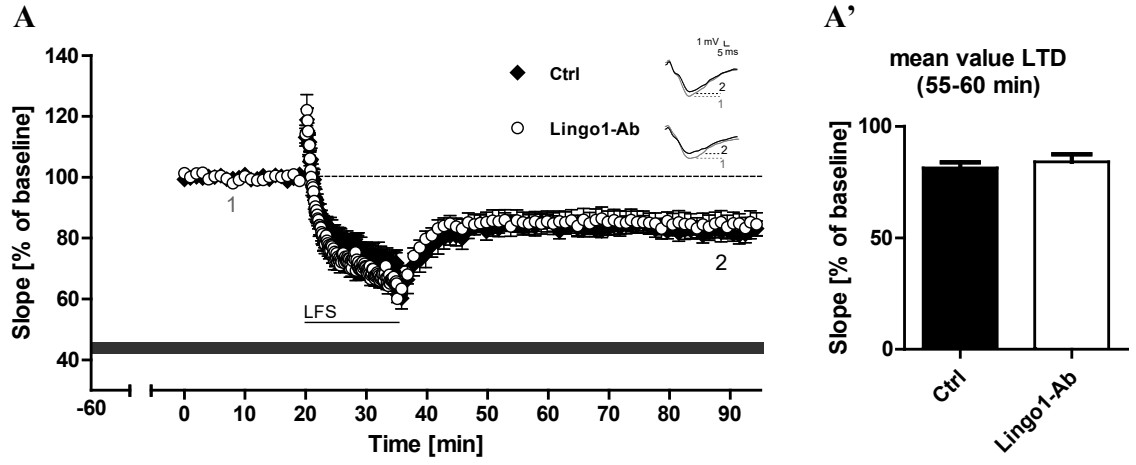

Figure 3.13: The neutralization of Lingo1 does not attenuate LTD. **(A)** LTD recordings after LFS (line), **(A')** mean fEPSP at 55-60 minutes post LFS upon neutralization of Lingo 1 (white circles / bar 84.0 ± 3.4, $n = 11$ slices / 4 animals) or control treatment (black diamonds / bar 81.3 ± 2.5, $n = 10$ slices / 4 animals) 1 hour before and for the entire experiments (horizontal bar). *Insets* show original traces from representative individual experiments (1 is for fEPSP 5 minutes before LFS, 2 for fEPSP 55 minutes after LFS; vertical scale bar 1 mV, horizontal scale bar 5 ms). *Error bars* SEM.

3.1.5 Nogo-66 signalling regulates actin dynamics and Cofilin activation via ROCK2

Changes in actin dynamics underlie the morphological and functional modifications occurring at dendritic spines during plasticity processes (Hotulainen and Hoogenraad, 2010). Due to the crucial role of actin dynamics in mediating processes of activity -

dependent plasticity, I assessed whether Nogo-66 signalling regulates actin dynamics within the adult hippocampus. For this purpose, I analysed the ratio of F / G-actin fractions upon Nogo-66 gain-of function treatment. Bath application of Nogo-P4 peptide to acute hippocampal slices for 20 minutes significantly decreased the ratio of F / G-actin by -62.7 ± 21.8% when compared to the control, resulting in a shift of the equilibrium between F- and G-actin toward G-actin (Fig. 3.14, $p < 0.05$ for black *versus* dark grey bar). Interestingly, the bath application of Nogo-P4 peptide along with the F-actin stabilizing drug Jasplakinolide for 20 minutes increased the ratio of F / G-actin by +32.9 ± 13.8% when compared to the treatment with the peptide alone, clearly indicating a role for Nogo-66 domain in promoting actin depolymerization (Fig. 3.14, $p < 0.05$ for dark grey *versus* light-grey bar). Moreover, the bath application of Nogo-P4 peptide along with the specific p160ROCK inhibitor Y27632 for 20 minutes resulted in an increase in the ratio of F / G-actin by +39.8 ± 18.4%, rescuing the actin depolymerizing effect of Nogo-P4 peptide (Fig. 3.14, $p < 0.05$ for dark grey *versus* white bar), and indicating that ROCK2 is downstream of Nogo-66 / NgR1 signalling in controlling actin dynamics.

Among the many actin binding proteins, modulation of the activity of the actin depolymerizing protein Cofilin, a downstream target of ROCK2, has been shown to be essential for the reorganization of the actin cytoskeleton (Bamburg and Bernstein, 2010). Therefore, I assessed whether Nogo-66 signalling might control actin dynamics within the adult hippocampus via the regulation of Cofilin activity. To this aim, I analysed the level of phosphorylated Cofilin upon a Nogo-66 gain-of-function approach. Bath application of Nogo-P4 peptide to acute hippocampal slices for 20 minutes significantly decreased the level of inactive phosphorylated Cofilin by -33.9 ± 5.1% when compared to the control treatment (Fig. 3.15A, $p < 0.05$ for black *versus* grey bar), without affecting total protein levels (Fig. 3.15A, upper panel). Interestingly, bath application of Nogo-P4 peptide along with the specific p160ROCK inhibitor Y27632 for 20 minutes

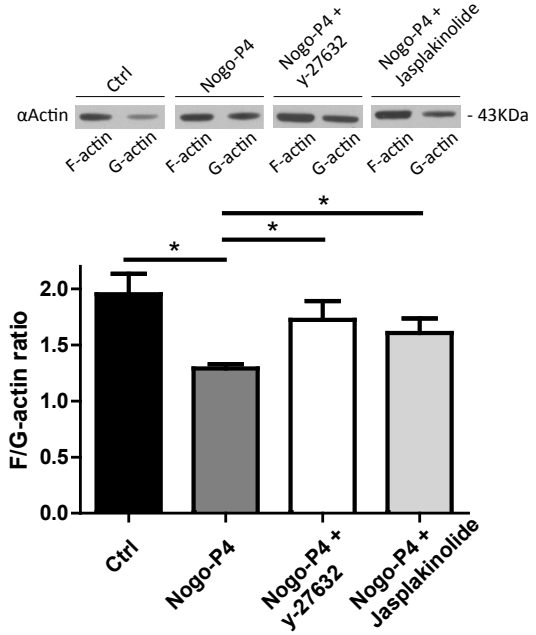

Figure 3.14: Nogo-66 affects the F/G-actin ratio. Analysis of F / G-actin ratio from acute hippocampal slices. Upper panel, representative blots; bottom panel, quantification of F / G-actin ratio upon application of Nogo-P4 peptide (dark grey bar, $n = 4$ independent experiments), or control treatment (black bar, $n = 4$ independent experiments), or combined application of Nogo-P4 peptide with Jasplakinolide (light grey bar, $n = 3$ independent experiments) or with p160ROCK inhibitor y-27632 (white bar, $n = 3$ independent experiments) for 20 minutes. *p<0.05. *Error bars* SEM.

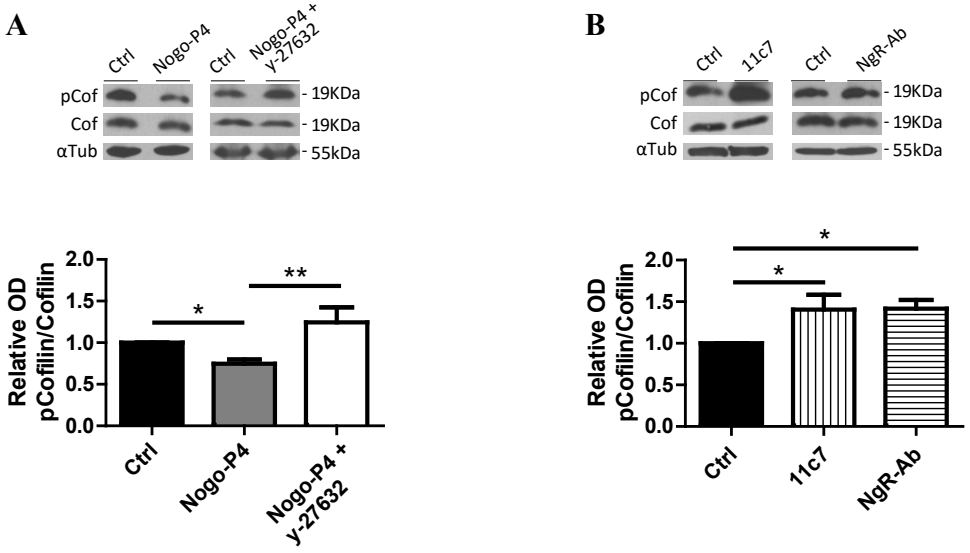

Figure 3.15: The application of Nogo-P4 peptide or the neutralization of Nogo-A-Δ20 domain or of NgR1 affect the phosphorylation of Cofilin. **(A)**, **(B)** Western blot detection of phospho-Cofilin to Cofilin ratio on acute hippocampal slices. Upper panel, representative blots; bottom panel, quantification of phospho-Cofilin to Cofilin ratio upon application of Nogo-P4 peptide (grey bar, $n = 5$ independent experiments) or combined application of Nogo-P4 peptide with the p160ROCK inhibitor y-27632 (white bar, $n = 4$ independent experiments) or control treatment (black bar, $n = 5$ independent experiments) for 20 minutes **(A)**, or upon neutralization of Nogo-A-Δ20 domain with the 11C7 antibody (white vertical-striped bar, $n = 5$ independent experiments) or neutralization of NgR1 with the specific function blocking antibody (white horizontal-striped bar, $n = 3$ independent experiments) or control treatment (black bar, $n = 5$ independent experiments) for 1 hour **(B)**. *$p < 0.05$, **$p < 0.01$. *Error bars* SEM.

significantly increased the ratio of phospho-Cofilin to Cofilin level by +58.4 ± 18.9% when compared to the treatment of the peptide alone, rescuing the effect of Nogo-P4 peptide on Cofilin phosphorylation to control levels (Fig. 3.15A, $p<0.01$ for grey *versus* white bar). To confirm the role of Nogo-A signalling in regulating Cofilin activity, I analysed Cofilin phosphorylation upon a loss-of-function approach. Both the neutralization of Nogo-A and of NgR1 with the specific function blocking antibodies to acute hippocampal slices for 1 hour significantly increased the level of active phosphorylated Cofilin by +50.5 ± 17.5% and by +41.6 ± 10.4%, respectively (Fig. 3.15B, $p < 0.05$ for control / black bar *versus* Nogo-A antibody treatment / white vertical-striped bar or NgR antibody treatment / white horizontal-striped bar), without affecting the total level of the protein (Fig. 3.15B, upper panel).
Taken together, these data show that under basal condition Nogo-66 signals via ROCK2 in order to increase the activity of Cofilin and by this means it shifts the F / G-actin ratio toward G-actin.

3.1.6 Nogo-66 regulates actin dynamics via the ROCK2-Cofilin pathway to restrict LTP

The expression and maintenance of LTP depends on modifications in the organization of the actin cytoskeleton within dendritic spines (Rudy, 2014). Indeed, LTP induction is

followed by the polymerization of actin filaments resulting in a transient increase in the ratio of F-actin to G-actin within dendritic spines (Okamoto et al., 2004). My previous results indicate a role of Nogo-66 signalling in destabilizing the actin cytoskeleton (Fig. 3.14) as well as in restricting LTP at the Schaffer collateral-CA1 pathway (Fig. 3.1). Thus, I tested whether Nogo-66 may restrict LTP by negatively regulating actin dynamics.

To this aim, I first analysed whether stabilizing the actin cytoskeleton, by application of Jasplakinolide, rescues the decrease in LTP magnitude induced by Nogo-P4 peptide. The combined application of Nogo-P4 peptide with Jasplakinolide around LTP induction completely rescued the decreased LTP observed after the application of the peptide alone (Fig. 3.16A, white circles *versus* grey squares) to the level of LTP of the control (Fig. 3.16A, black diamonds). Indeed, the average potentiation at 55-60 minutes after TBS was 128.8 ± 4.2 for the single Nogo-P4 treatment / grey bar (n = 9 slices / 4 animals), while for the combined Nogo-P4 plus Jasplakinolide treatment / white bar was 168.8 ± 13.3 (n = 7 slices / 3 animals, Fig. 3.16A', p < 0.01), comparable with that of the control treatment / black bar that was 155.6 ± 4.8 (n = 9 slices / 5 animals, Fig. 3.16A'). I also tested whether Jasplakinolide alone affects LTP. The application of Jasplakinolide around LTP induction did not change the magnitude of LTP when compared to the control (Fig. 3.17A, black diamonds *versus* white circles). Indeed, the average potentiation at 55-60 minutes after TBS was 155.6 ± 4.8 for control (n = 9 slices / 5 animals) and 145.3 ± 7.1 for Jasplakinolide treatment (n = 7 slices / 3 animals), (Fig. 3.17A').

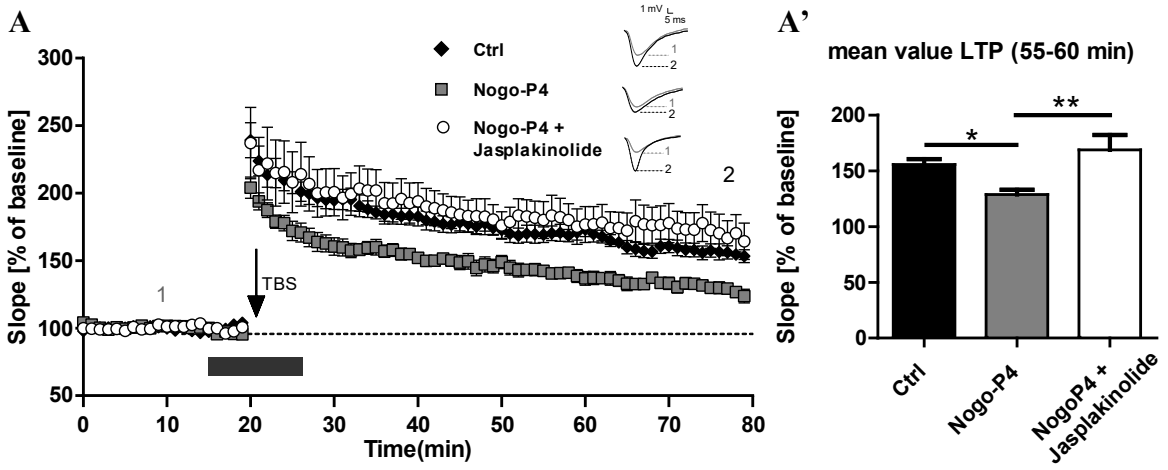

Figure 3.16: The application of Jasplakinolide rescues the Nogo-66 domain - dependent restriction of LTP. **(A)** LTP recordings after TBS (arrow), **(A')** mean fEPSP at 55-60 minutes post TBS upon combined application of Nogo-P4 peptide with Jasplakinolide (white circles / bar 168.79 ± 13.3, n = 7 slices / 3 animals), or application of the peptide alone (dark grey squares / bar 128.8 ± 4.2, n = 9 slices / 4 animals) or control treatment (black diamonds / bar 155.6 ± 4.8, n = 9 slices / 5 animals) for 10 minutes around LTP induction (horizontal bar). *Insets* show original traces from representative individual experiments (1 is for fEPSP 5 minutes before TBS, 2 for fEPSP 55 minutes after TBS; vertical scale bar 1 mV, horizontal scale bar 5 ms). *p<0.05, **p<0.01. *Error bars* SEM.

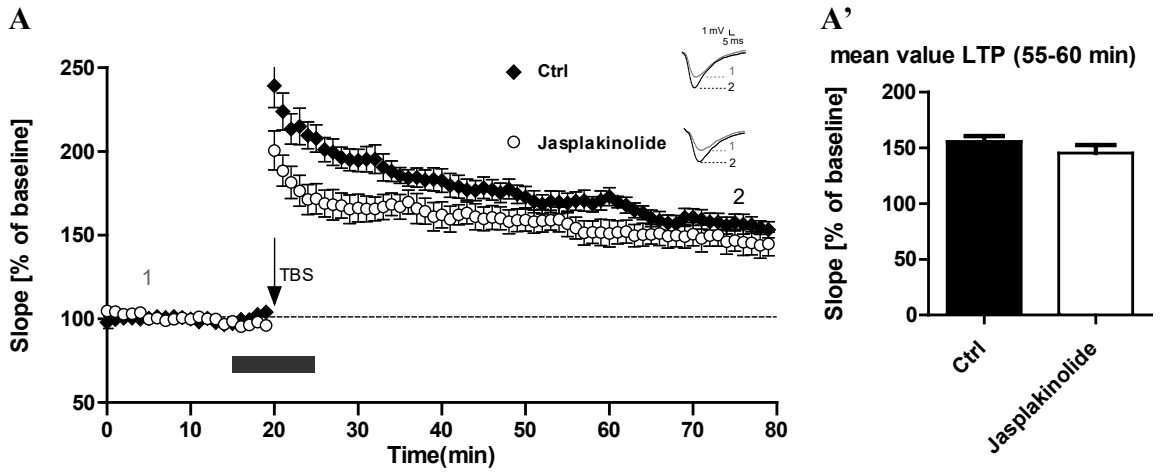

Figure 3.17: The application of Jasplakinolide does not affect LTP. **(A)** LTP recordings after TBS (arrow), **(A')** mean fEPSP at 55-60 minutes post TBS upon application of Jasplakinolide (white circles / bar 145.3 ± 7.1, $n = 7$ slices / 3 animals) or control treatment (black diamonds / bar 155.6 ± 4.8, $n = 9$ slices / 5 animals) 10 minutes around LTP induction (horizontal bar). *Insets* show original traces from representative individual experiments (1 is for fEPSP 5 minutes before TBS, 2 for fEPSP 55 minutes after TBS; vertical scale bar 1 mV, horizontal scale bar 5 ms). *Error bars* SEM.

My previous results indicate that Nogo-66 destabilizes the actin cytoskeleton via ROCK2 (Fig. 3.14). To elucidate the intracellular cascade mediating the activity of Nogo-66 on the actin cytoskeleton during LTP, I used a combined application of Nogo-P4 peptide with the specific p160ROCK inhibitor Y27632 around LTP induction. The co-application of Y27632 inhibitor and Nogo-P4 peptide completely rescued the decreased LTP observed after the application of the peptide alone (Fig. 3.18A, white circles *versus* grey squares). Indeed, the average potentiation at 55-60 minutes after TBS was 166.3 ± 3.9 for the combined Nogo-P4 plus y-27632 treatment / white bar ($n = 7$ slices / 3 animals), and 128.8 ± 4.2 for the single Nogo-P4 treatment / grey bar ($n = 9$ slices / 4 animals), (Fig. 3.18A', $p < 0.01$). I also tested whether ROCK2 alone affects LTP. The application of the p160ROCK inhibitor Y27632 around LTP induction did not affect the level of LTP when compared to the control (Fig. 3.19A, black diamonds *versus* white circles). Indeed, the average potentiation at 55-60 minutes after TBS was 155.6 ± 4.8 for control / black bar ($n = 9$ slices/5 animals) and 150.8 ± 6.9 for p160ROCK inhibitor Y27632 treatment / white bar ($n = 10$ slices / 5 animals), (Fig. 3.19A').

Changes in the activity of the actin depolymerizing protein Cofilin are necessary for the expression and maintenance of LTP. Indeed, LTP induction is associated with a transient increase in the phosphorylation - dependent inactivation of Cofilin (Fukazawa et al., 2003), (Chen et al., 2007), (Gu et al., 2010), (Rex et al., 2009). As my previous result shows a role of Nogo-66 in regulating Cofilin activity (Fig. 3.15A), I tested whether Nogo-66 regulates the activity - dependent phosphorylation of Cofilin upon LTP induction at the Shaffer collateral-CA1 pathway. For this purpose, I analysed Cofilin phosphorylation levels specifically within the CA1 region of control and Nogo-P4 treated acute hippocampal slices 10 minutes after TBS (Fig. 3.20B). In control

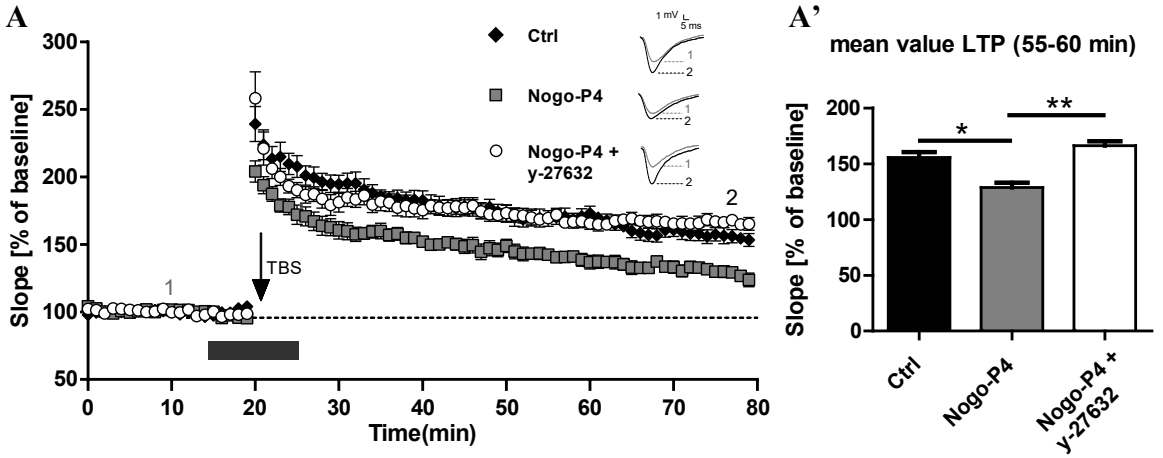

Figure 3.18: The application of p160ROCK inhibitor rescues the Nogo-66 domain - dependent restriction of LTP. **(A)** LTP recordings after TBS (arrow), **(A')** mean fEPSP at 55-60 minutes post TBS upon combined application of Nogo-P4 peptide with the p160ROCK inhibitor y-27632 (white circles / bar 166.3 ± 3.9, $n = 7$ slices / 3 animals) or application of the peptide alone (grey squares / bar 128.8 ± 4.2, $n = 9$ slices / 4 animals) or control treatment (black diamonds / bar 155.6 ± 4.8, $n = 9$ slices / 5 animals) for 10 minutes around LTP induction (horizontal bar). *Insets* show original traces from representative individual experiments (1 is for fEPSP 5 minutes before TBS, 2 for fEPSP 55 minutes after TBS; vertical scale bar 1 mV, horizontal scale bar 5 ms). *p<0.05, **p<0.01. *Error bars* SEM.

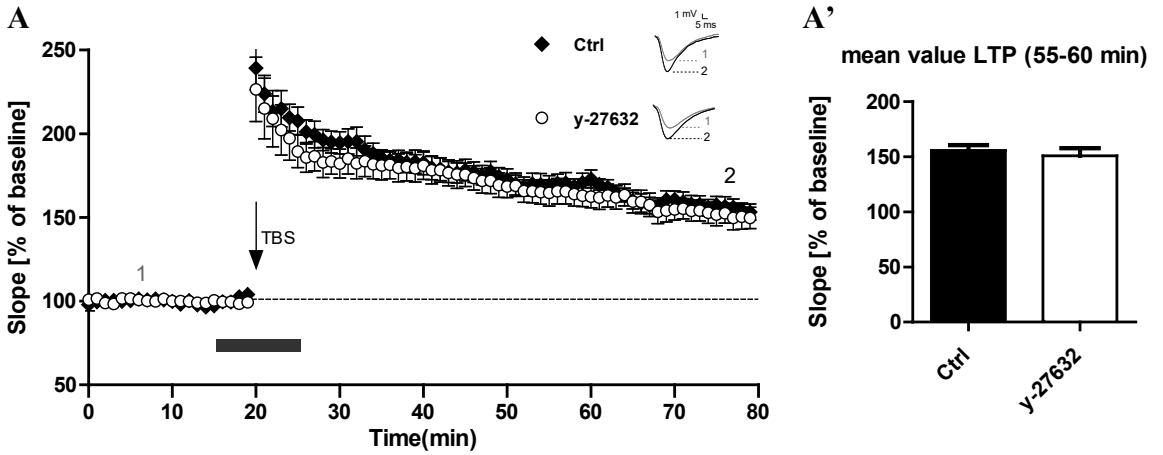

Figure 3.19: The application of p160ROCK inhibitor does not affect LTP. **(A)** LTP recordings after TBS (arrow), **(A')** mean fEPSP at 55-60 minutes post TBS upon application of p160ROCK inhibitor y-27632 (white circles / bar 150.8 ± 6.9, $n = 10$ slices / 5 animals) or control treatment (black diamonds / bar 155.6 ± 2.6, $n = 9$ slices/5 animals) around LTP induction (horizontal bar) . *Insets* show original traces from representative individual experiments (1 is for fEPSP 5 minutes before TBS, 2 for fEPSP 55 minutes after TBS; vertical scale bar 1 mV, horizontal scale bar 5 ms). *Error bars* SEM.

treated slices the level of inactive phosphorylated Cofilin is significantly increased 10 minutes after TBS by +52.7 ± 9.6% when compared to control treated slices which did not receive TBS (Fig. 3.20A, black *versus* light grey bar, $p < 0.001$), confirming previous reports (Chen et al., 2007), (Gu et al., 2010). Interestingly, the increase in phospho-Cofilin levels could not be observed in slices where the Nogo-P4 peptide was

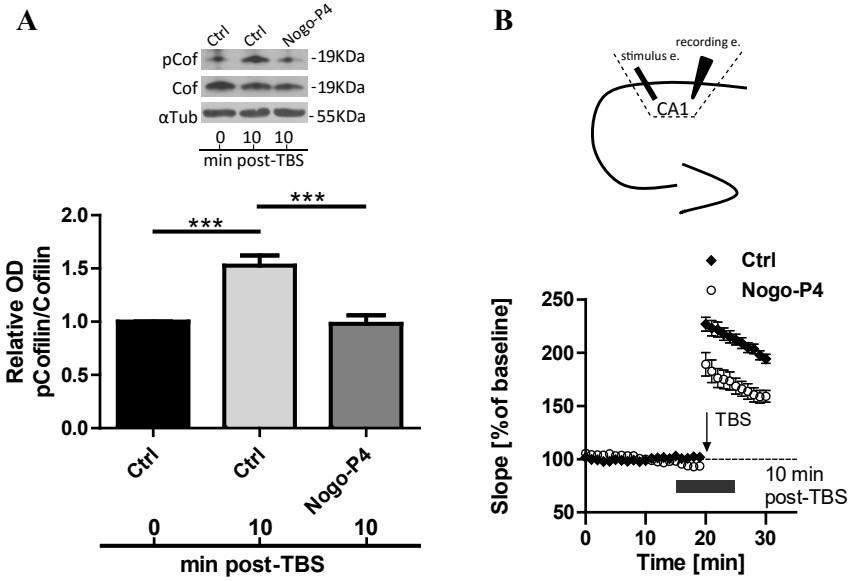

Figure 3.20: The application of Nogo-P4 peptide affects the activity - dependent phosphorylation of Cofilin. **(A)** Western blot detection of phospho-Cofilin to Cofilin ratio from CA1 regions of acute hippocampal slices. Upper panel, representative blots; bottom panel, quantification of phospho-Cofilin to Cofilin ratio upon delivery of a single TBS with application of Nogo-P4 peptide (dark grey bar, $n = 3$ independent experiments) or control (light-grey bar, $n = 3$ independent experiments) for 10 minutes around LTP induction. **(B)** Upper panel, dissection of the CA1 regions from acute hippocampal slices; bottom panel, representative LTP recordings after TBS (arrow) upon application of Nogo-P4 peptide ($n = 11$ slices / 1 animal) or control ($n = 10$ slices / 1 animal) for 10 minutes around LTP induction (horizontal bar). Recordings were stopped 10 minutes after TBS. ***p<0.001. *Error bars* SEM.

applied during TBS. Indeed, the level of phosphorylated Cofilin in Nogo-P4 treated slices significantly decreased by -54.7 ± 12.5% when compared to control treated slices 10 minutes after TBS (Fig. 3.20A, light *versus* dark grey bar, $p < 0.001$). In all the treatments, the total level of Cofilin protein was not altered (Fig. 3.20A, upper panel). Taken together, these data show that Nogo-66 signalling affects LTP maintenance by modulating the actin cytoskeleton dynamics during LTP induction. Moreover, because ROCK2 rescues the effect of Nogo-66 on LTP and on the other hand Nogo-66 prevents the activity - dependent phosphorylation of Cofilin, one can conclude that Nogo-66 signals via the activation of ROCK2-Cofilin pathway to restrict LTP.

3.1.7 Both Nogo-A receptors might activate the same intracellular signalling pathway

Both Nogo-A receptors have been shown to negatively regulate LTP. Indeed, the neutralization of the Nogo-66 receptor NgR1 with a function blocking antibody increases the level of LTP (Delekate et al., 2011). Similarly, the neutralization of the Nogo-A-Δ20 receptor S1PR2 with the specific inhibitor JTE-013 enhances the magnitude of LTP (Kempf et al., 2014). In this series of experiments, I questioned which is the outcome of the combined neutralization of both Nogo-A receptors in comparison to the blockage of either one. Indeed, an additive effect on potentiation upon neutralization

of both receptors would prompt the idea that they might regulate LTP by activating two different intracellular cascades.

First of all, I confirmed that S1PR2 restricts LTP. Indeed, the application of the S1PR2 inhibitor JTE-013 increased the level of LTP when compared to control (Fig. 3.21A grey triangles *versus* black diamonds). The average potentiation at 55-60 minutes after TBS was 174.0 ± 14.4 for the single JTE-013 treatment / grey bar (n = 8 slices / 4 animals) and 142.0 ± 8.4 for the control treatment / black bar (n = 7 slices / 4 animals), (Fig. 3.21A' p<0.01). Next, the application of the S1PR2 inhibitor JTE-013 at the beginning of recording to slices pre-treated for 1 hour with the anti-NgR antibody increased the level of LTP when compared to the control treatment (Fig. 3.21A white circles *versus* black diamonds). Indeed, the average of potentiation at 55-60 minutes after TBS was 142.0 ± 8.4 for control / black bar (n = 7 slices / 4 animals) and 172.5 ± 10.6 for the combined NgR antibody plus JTE-013 inhibitor treatment / white bar (n = 9 slices / 4 animals), (Fig. 3.21A' p<0.001). However, the difference in potentiation between NgR antibody plus JTE-013 co-treatment and the single JTE-013 treatment was not significantly different, as the level of LTP upon blocking both receptors was comparable with that upon the neutralization of only a single receptor.

Taken together, the data show that blocking both Nogo-A receptors led to a similar potentiation, suggesting that the Nogo-A-Δ20 / S1PR2 signalling might converge onto the same intracellular pathway activated by Nogo-66 / NgR1 signalling, most likely activating the same ROCK2-Cofilin pathway.

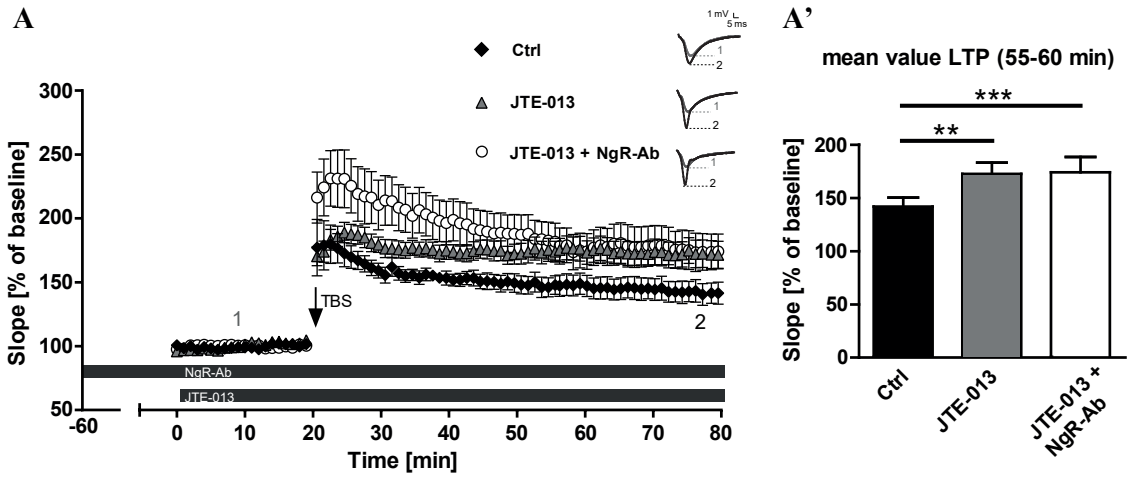

Figure 3.21: The neutralization of both Nogo-A receptors, NgR1 and S1PR2, has the same effect on LTP than the single neutralization of S1PR2. **(A)** LTP recordings after TBS (arrow), **(A')** mean fEPSP at 55-60 minutes post TBS upon application of JTE-013 to slices pretreated for 1 h with NgR antibody (white circles / bar 172.5 ± 10.6, n = 9 slices / 4 animals) or with control antibody (grey triangles / bar 174.0 ± 14.4, n = 8 slices / 4 animals), or control treatment (black diamonds / bar 142.0 ± 8.4, n = 7 slices / 4 animals). *Insets* show original traces from representative individual experiments (1 is for fEPSP 5 minutes before TBS, 2 for fEPSP 55 minutes after TBS; vertical scale bar 1 mV, horizontal scale bar 5 ms). **p<0.01, ***p<0.001. *Error bars* SEM.

3.2 The role of Nogo-A in regulating the structural dynamics of mossy fiber synapses

In the second part of this work, I questioned whether Nogo-A regulates the remodelling of presynaptic mossy fiber synapses.

At first, I addressed whether Nogo-A might acutely regulate the structural reorganization of these synapses. To achieve this purpose, I performed a time-lapse confocal imaging of 21 DIV organotypic hippocampal slice cultures derived from Thy-1 mGFP transgenic mice. In particular, after selection of a eGPF-positive terminal, I acquired one frame every 5 minutes for 20 minutes upon application of ACSF (Fig. 3.22). Then, in order to describe the extent of their remodelling over time I calculated the motility index (MI) of the main core of the terminals as well as of the filopodial extensions protruding from each terminal (to; Fig. 3.23A,B grey bars). I found that the core of the terminals was motile upon application of ACSF (Fig. 3.22) with an averaged MI value of 0.143 ± 0.020 (to; Fig. 3.23A, grey bars). Subsequently, for three times at intervals of 1 hour (t1, t2, t3) I repeated the time-lapse imaging during the incubation of the organotypic slices with the specific Nogo-A function blocking antibody 11C7 or control antibody. The MI value of the core of the terminals did not change over time upon application of the control antibody (t1,t2,t3; Fig. 3.23A, black bars). Indeed the MI at t1 was 0.158 ± 0.020, at t2 was 0.153 ± 0.020, and at t3 was 0.135 ± 0.010. However, the acute neutralization of Nogo-A with a function blocking antibody slightly but not statistically increased the MI of the core of the terminals when compared to the control treatment (t1,t2,t3; Fig. 3.23A, white bars). Indeed, the MI at t1 was 0.143 ± 0.020, at t2 was 0.167 ± 0.020, and at t3 was 0.190 ± 0.030. Regarding the filopodial extensions, they were motile upon application of the ACSF (Fig. 3.22) with an averaged MI value of 0.211 ± 0.021 (to; Fig. 3.23B, grey bars). They continued to be motile also upon application of the control antibody (t1,t2,t3; Fig. 3.23B, black bars). Indeed the MI at t1 was 0.204 ± 0.020, at t2 was 0.203 ± 0.020, and at t3 was 0.197 ± 0.023. The acute neutralization of Nogo-A with a function blocking antibody

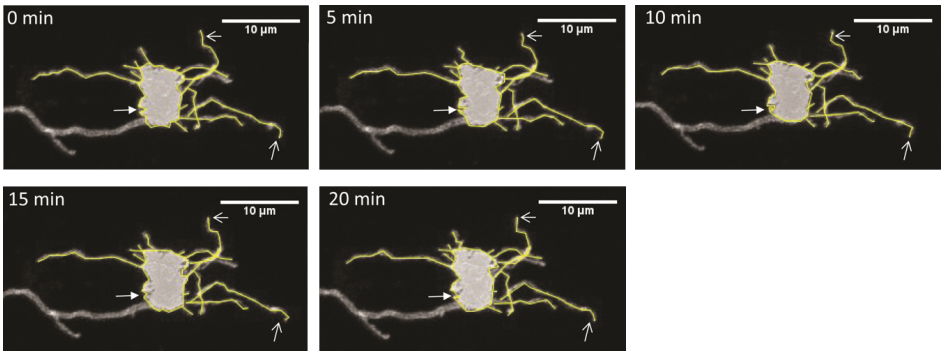

Figure 3.22: Maximum intensity projection of the Z-series stacks of a time-lapse confocal imaging of eGFP mossy fiber synapses upon application of ACSF. For each frame, the area of the core terminal and the length of its filopodial extensions were traced. The two thin arrows indicate the motility of two representative filopodia, the filled arrow indicates the motility of the core terminal.

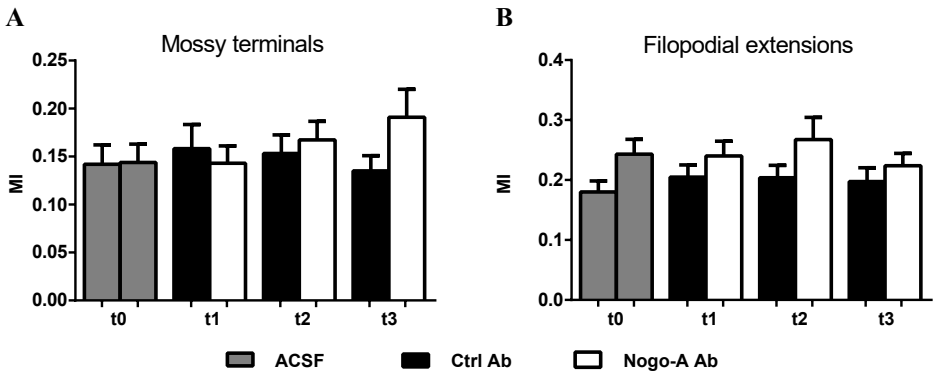

Figure 3.23: Repeated confocal imaging of eGFP mossy terminals. **(A)** Average of the terminals MI, **(B)** average of the filopodial extensions MI per terminal over the time points t0, t1, t2, t3 upon the ACSF perfusion (t0, grey bars $n = 15$ terminals and $n = 16$ terminals, respectively) or Nogo-A antibody treatment (t1, t2, t3, white bars) or control antibody treatment (t1, t2, t3, black bars). *Error bars* SEM.

did not change the MI value of the filopodial extensions in comparison to the control treatment (t1,t2,t3; Fig. 3.23B, white bars). Indeed, the MI at t1 was 0.240 ± 0.024, at t2 was 0.267 ± 0.036, and at t3 was 0.223 ± 0.020.

These data show that the acute neutralization of Nogo-A does not significantly change the motility index of the core terminals as well as of their filopodial extensions, indicating that Nogo-A did not alter the short-term structural remodelling of the mossy fiber synapses over time.

Then, I addressed whether Nogo-A might chronically regulate the structural reorganization of mossy fiber synapses. To achieve this purpose, I treated for four days 21 DIV organotypic hippocampal slice cultures derived from Thy-1 mGFP transgenic mice with a specific Nogo-A function blocking antibody or control antibody. I calculated the area of the core terminals (µm^2) as well as the length of their filopodial extensions (µm). The chronic neutralization of Nogo-A significantly decreased the area of the core terminals by -45.5 ± 14.2% in comparison to the control (Fig. 3.24A, black *versus*

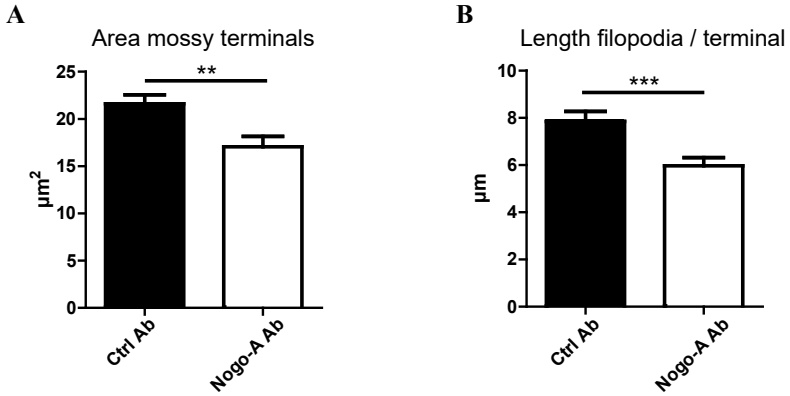

Figure 3.24: Apotome imaging of eGFP mossy terminals. **(A)** Average area of the terminals, **(B)** average length of filopodial extensions per terminal upon 4 days of treatment with the Nogo-A antibody (white bars, $n = 62$ terminals) or control antibody (black bars, $n = 69$ terminals). **p<0.01, ***p<0.001. *Error bars* SEM.

white bar). Indeed, the averaged area of the terminals was 17.06 ± 1.08 µm^2 for the Nogo-A antibody treatment and 21.61 ± 0.93 µm^2 for the control treatment. Similarly, the chronic neutralization of Nogo-A significantly decreased the length of the filopodial extensions *per* each terminal by -18.8 ± 5.5% in comparison to the control (Fig. 3.24B, black *versus* white bar). Indeed, the averaged length of the filopodial extensions *per* each terminal was 5.96 ± 0.34 µm for the Nogo-A antibody treatment and 7.85 ± 0.42 µm for the control treatment.

These data show that the chronic neutralization of Nogo-A decrease the size of the mossy fiber synapses, indicating that Nogo-A alters the long-term structural reorganization of the mossy fiber synapses.

Taken together, these data suggest that Nogo-A regulates the structural dynamics of the mossy fiber synapses, depending on the time-scale.

4 | Discussion

> It is imperfection - not perfection - that is the end result of the program written into that formidably complex engine that is the human brain.
>
> *Rita Levi Montalcini*

Nogo-A has been shown to act as a negative regulator of activity - dependent synaptic plasticity, restricting the magnitude of LTP and the structural plasticity of dendritic spines in the adult mouse hippocampus. However, the molecular mechanism mediating the role of Nogo-A on LTP and a possible role of Nogo-A in regulating the remodelling of presynaptic structures are largely unknown.
In the first part of this study I investigated the signalling pathway mediating the effect of the Nogo-66 domain of Nogo-A on LTP in the CA1 region of the adult mouse hippocampus. The results described here indicate that, upon binding of the Nogo-66 domain, NgR1 cooperates with Lingo1 to negatively regulate LTP (Fig. 4.1). In addition, the data show that this activity of Nogo-66 depends on the modulation of the activity of the actin-binding protein Cofilin via the Rho-A downstream effector ROCK2 in order to destabilize actin filaments (Fig. 4.1). Finally, the results suggest a NgR1 / $p75^{NTR}$ mediated regulation of LTD independently of Nogo-A (Fig. 4.1).
In the second part of the work I addressed the role of neuronal Nogo-A in regulating structural plasticity at mossy fiber synapses in the CA3 region of the adult mouse hippocampus. The results suggest that Nogo-A is not involved in regulating the remodelling of the mossy fiber synapses in a fast time scale, while it regulates their structural reorganization in a long time scale.

4.1 Receptor signalling mediating the role of Nogo-66 on activity - dependent synaptic plasticity

In this study, I first addressed the role of Nogo-66 in acutely regulating long- and short-term plasticity by using a gain-of-function approach, and I found that the Nogo-66 domain selectively restricts LTP, without affecting LTD or paired-pulse facilitation. This is in line with a previous publication showing that a local application of a Nogo-66 peptide suppresses NMDA receptor - dependent LTP via NgR1 - dependent signalling (Raiker et al., 2010). Moreover, interfering with the Nogo-A / S1PR2 signalling has been shown to lead to higher LTP without influencing LTD (Delekate et al., 2011), (Kempf et al., 2014), suggesting a general role for Nogo-A signalling in specifically controlling LTP magnitude.

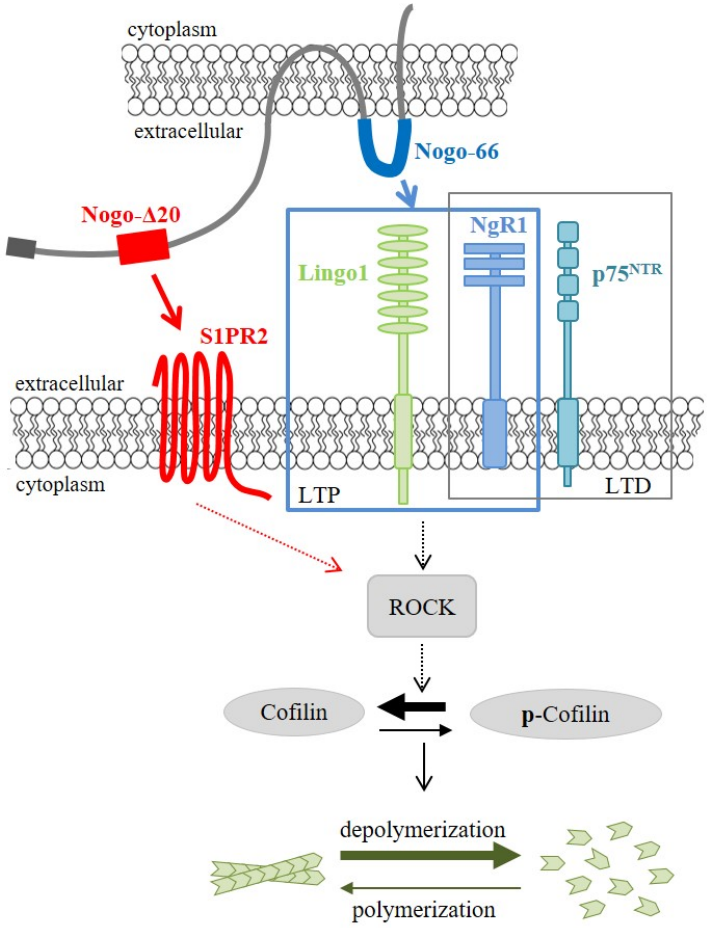

Figure 4.1: The molecular mechanism mediating the role of Nogo-A in restricting LTP. This summary cartoon depicts a possible molecular cascade activated by Nogo-66 in order to restrict LTP. Nogo-A has two inhibitory domains: Nogo-A-Δ20 signalling via S1PR2, and Nogo-66 signalling via NgR1. Nogo-66 activates a signalling cascade whereby NgR1 cooperates with Lingo1 to negatively regulate LTP (thick box). NgR1 cooperate with $p75^{NTR}$ to regulate LTD independently on Nogo-66 (thin box). Nogo-66 increases the activity of the actin-binding protein Cofilin via the Rho-A downstream effector ROCK2 in order to increase the depolymerization of the actin filaments within spines. By activating this molecular pathway Nogo-66 restricts LTP, hereby promoting the stability of the circuits in the mature hippocampus. The Nogo-A-Δ20/ S1PR2 signalling might converge onto the same intracellular cascade activated by Nogo-66 (dashed line). Abbreviations: NgR1, Nogo-receptor 1; S1PR2, sphingosine-1-phosphate receptor 2; Lingo1, leucine-rich repeat and immunoglobulin domain-containing 1; $p75^{NTR}$, low affinity nerve growth factor receptor p75; ROCK2, rho-associated coiled-coil kinase 2; pCofilin, phosphorylated Cofilin; F-actin, filamentous actin; G-actin, globular actin; LTP, long-term potentiation; LTD, long-term depression. Dashed lines indicate an indirect interaction.

The Nogo-66 receptor NgR1, lacking a cytosolic domain (Venkatesh et al., 2005), has been shown to signal via a heterotrimeric receptor complex composed of the transmembrane protein Lingo1 (Mi et al., 2004), and the pan-neurotrophin receptor $p75^{NTR}$ (Wang et al., 2002a). The receptor complex NgR1 / Lingo1 / $p75^{NTR}$ mediates the Nogo-A function in negatively regulating neurite outgrowth and axonal regeneration (Thallmair et al., 1998), (Mi et al., 2004), (Schwab, 2010). Indeed, the neutralization of Nogo-A with a specific function blocking antibody promotes the regeneration of lesioned axons, and the sprouting of injured and uninjured collaterals in the spinal cord

(Zörner and Schwab, 2010) (Bareyre et al., 2002), as well as in the cerebellum (Buffo et al., 2000) of adult rats. Comparable results have been observed upon blockage of NgR1 (Fournier et al., 2002) and Lingo-1 (Ji et al., 2006). Taken together, these data show that the interaction of $p75^{NTR}$ and Lingo-1 with NgR1 is essential for transducing the NgR1 - dependent signalling in response to myelin-associated inhibitors and for preventing the axonal regeneration and neurite outgrowth (Wang et al., 2002a), (Mi et al., 2004).

My experiments show that in the context of activity - dependent synaptic plasticity in the adult mouse hippocampus Lingo1, and not $p75^{NTR}$ is involved in transducing the specific effect of Nogo-66 / NgR1 signalling in restricting LTP. Similarly, the oligodendrocyte-myelin glycoprotein (OMgp), another member of the myelin-associated inhibitors and ligand for NgR1, has been shown to restrict LTP independently of $p75^{NTR}$ (Raiker et al., 2010). Indeed, while $p75^{NTR}$ signalling *perse* does not modulate LTP (our results), (Rösch et al., 2005), (Woo et al., 2005), my data show that neutralization of Lingo1 function results in higher LTP, supporting its specific role in transducing the Nogo-66 / NgR1 signalling in restricting functional plasticity. Interestingly, a recent study describes that in neurons endogenous Lingo-1 is localized intracellularly, associated to membranes of the endocytic pathway (Meabon et al., 2015). This notion suggests that Lingo-1 might transiently be inserted at the plasma membrane to form a ternary cell-surface complex for mediating the myelin-associated inhibitor - dependent signalling. Moreover, this observation prompts for the possibility that Lingo1 exposure at the plasma membrane might be specifically regulated in an activity - dependent manner. It is interesting to note that an internalization into signalling endosomes has been described also for the S1PR2 upon binding of its ligand Nogo-A-Δ20 (Kempf et al., 2014). Hence, these observations indicate that the receptor composition at the plasma membrane is dynamically regulated, and might vary between different physiological conditions or activity patterns. It remains unresolved whether Nogo-A and its receptors plus co-receptors are found within the same or in different membrane microdomains (e.g. lipid raft) and cellular compartment (e.g. endosomes), and whether and how they are regulated by activity.

In my experiments, the acute neutralization of NgR1 leads to an attenuated LTD, confirming previous studies showing that LTD is decreased in ngr1 KO mice (Lee et al., 2008). Regarding the NgR1 co-receptors, while neutralization of Lingo1 does not impair LTD, blocking $p75^{NTR}$ signalling reproduces the effect observed upon NgR1 neutralization. Indeed, I could confirm the observations that $p75^{NTR}$ is specifically involved in modulating LTD (Rösch et al., 2005). Moreover, $p75^{NTR}$ *perse* has been shown to mediate the proBDNF effect in facilitating LTD (Woo et al., 2005). My findings here open an interesting scenario whereby NgR1 cooperates with Lingo1 for mediating the role of Nogo-66 domain in restricting LTP, while it cooperates with $p75^{NTR}$ to regulate LTD (Fig. 4.1). It is important to note that the induction of LTP and LTD in the hippocampus are age - dependent processes, with NMDAR - dependent LTD being more inducible in the juvenile than in the adult hippocampus (Kemp et al., 2000). Accordingly, while $p75^{NTR}$ expression decreases during development, Lingo1 ex-

pression remains constant in the mature CNS (Llorens et al., 2008). This observation suggests the existence of different NgR1 / co-receptors complexes in the hippocampus depending on the developmental stage, thus possibly mediating different activity of NgR1. On the other hand, because Nogo-66 does not affect LTD, the NgR1 / $p75^{NTR}$ - dependent effect in this context is likely to be mediated by a different ligand than Nogo-A. Possible candidates for this effect might be the chondroitin sulfate proteoglycans (CSPGs) which have been shown to bind NgR1 at a distinct binding site than Nogo-A (Dickendesher et al., 2012) and whose enzymatic digestion leads to impaired LTD (Bukalo et al., 2001). Thus, the binding of different ligands might result in specific conformational changes of NgR1 promoting its interaction with either one or the other co-receptor. This notion is well known for the G protein-coupled receptors (GPCR). For instance, it has been shown that different ligands induce various conformational changes of the GPCR beta 2 adrenergic receptor, that in turn interact with specific intracellular downstream effectors leading to distinct signalling outcomes (Deupi et al., 2012). In another example, also the estrogen receptors change their conformations upon binding of different ligands, and this trigger the recruitment of specific coregulators, subsequently modulating different intracellular signalling pathways (Moggs and Orphanides, 2001).

4.2 Intracellular pathway mediating the role of Nogo-A signalling on LTP

4.2.1 The regulation of the actin cytoskeleton dynamics by Nogo-A

It is well established that long-term plasticity is associated with a rapid and persistent reorganization of actin within spines (Rudy, 2014). Indeed, LTP induction is followed by a brief decrease in phosphorylation - dependent inactivation of Cofilin associated with an increase in actin depolymerization allowing trafficking of AMPAR (Gu et al., 2010) and other plasticity promoting molecules e.g. CamKII (Ouyang et al., 2005) into activated synapses. Moreover, F-actin has been shown to be highly dynamic and to undergo a fast and transient re-organization upon LTP induction (Chen et al., 2015). This early phase is followed by a transient increase in phosphorylated-inactive Cofilin allowing for actin polymerization and leading to an increase in the ratio of F-actin to G-actin into spines (Okamoto et al., 2004), (Fukazawa et al., 2003), critical for LTP maintenance and for activity - dependent structural changes. On the other hand, LTD causes a decrease in the ratio between F-actin and G-actin (Okamoto et al., 2004) due to the activation of Cofilin (Zhou et al., 2004).

The data described here show that within the adult hippocampus Nogo-66 modulates actin dynamics decreasing the ratio of F- to G-actin, and increases the amount of activated-unphosphorylated Cofilin via ROCK2 signalling, possibly via the activation of the ROCK2 downstream target Slingshot phosphatase (SHH). Indeed, it has been shown that Nogo-66 inhibits neuronal outgrowth by first decreasing and then increasing Cofilin activation levels via a ROCK - dependent sequential activation of LIM kinase

(LIMK) and SSH phosphatase (Hsieh et al., 2006). In addition, my data show that the neutralization of Nogo-A or NgR1 signalling results in an increase in the level of inactive phosphorylated-Cofilin. This is in line with the observation that in Nogo-A KO mice inactivated Cofilin is increased leading to actin polymerization within the growth cone supporting neurite formation and extension (Montani et al., 2009). The actin remodelling observed upon Nogo-A signalling under basal conditions suggests that it might regulate the anatomical plasticity of spines. Indeed, the acute neutralization of Nogo-A transiently increases the amount of stable F-actin within dendritic spines of CA3 hippocampal neurons associated with an increase in their number and length, while a gain-of-function approach for Nogo-A results in a destabilization of the actin cytoskeleton (Kellner et al., 2016). Accordingly, NgR1 restricts the formation of excitatory synapses in developing hippocampal neurons via a RhoA - dependent pathway (Wills et al., 2012), implicating the regulation of the ROCK-Cofilin pathway by NgR1 signalling also at synapses. Hence, a similar pathway as observed in growth cones might also mediate the Nogo-66 signalling at dendritic spines. Indeed, both the neuronal growth cone and the dendritic spines are enriched in actin filaments. Particularly, in the growth cone bundles of actin filaments extend from the central to the periphery region forming filopodia-like protrusions, and branched actin filaments are in the periphery forming lamellipodia-like structures. In the dendritic spines bundles of parallel actin filaments are in the neck, and lattice-twisted filaments in the head (Korobova and Tatyana, 2010). However, while at the growth cone the F-actin polymerized rearward at the tip of the membrane, in spines the actin flow is slow and not rearward polarized (Chazeau et al., 2014), (Honkura et al., 2008). Interestingly, actin filaments are highly dynamics within both structures, supporting neurites outgrowth and spine remodelling respectively. Indeed, a more dynamic and less dense actin cytoskeleton at the growth cone support neurite outgrowth (Dent et al., 2011). Similarly, changes in actin cytoskeleton dynamics in spines allow their morphological modifications and sustain their motility during synaptic development and synaptic plasticity (Rudy, 2014). Nevertheless, being the neuronal growth cone a protrusive structure, nucleation and elongation of either bundles or branched F-actin are co-localized, promoting a pushing force on the plasma membrane (Chazeau et al., 2014). On the contrary, elongation and nucleation are spatially separated events in spines (Chazeau et al., 2014), possibly to allow rapid F-actin remodelling following changes in synaptic activity.

The results of this thesis indicate that Nogo-66 regulates actin dynamics and the Cofilin activation *status* also in the context of activity - dependent synaptic plasticity. A short application of Nogo-66 around LTP induction results in impaired LTP maintenance preventing the expected increase in Cofilin phosphorylation and the activity - dependent actin polymerization resulting in the instability of the actin cytoskeleton. Indeed, applying the actin stabilizing agent Jasplakinolide completely rescues the impairment of LTP maintenance observed upon Nogo-66 treatment. Accordingly, treatments that inhibit the polymerization of actin filaments before or shortly after LTP induction have been shown to generate but to fail to maintain it over time (Rudy, 2014), (Kim and Lisman, 1999), (Krucker et al., 2000), (Kramár et al., 2006), suggesting that actin

polymerization and reorganization upon LTP induction does not affect the generation of LTP but is crucial for its maintenance.
It has been shown that the magnitude of LTP is increased upon acute neutralization of NgR1 (Delekate et al., 2011) and S1PR2 (Kempf et al., 2014). Interestingly, my data show that while the single neutralization of NgR1 and of S1PR2 increases the magnitude of LTP, their combined blockade does not show an additive effect on LTP potentiation (Kempf and Schwab, 2013), suggesting that the signalling of the two Nogo-A receptors might converge onto the same ROCK2 - dependent intracellular pathway in order to restrict LTP. This is in line with the data showing that both Nogo-66 and Nogo-A-Δ20 domains, via their respective receptors, trigger the activation of the small GTPase RhoA and its effector ROCK to promote growth cone collapse and axonal repulsion (Kempf and Schwab, 2013), (Niederöst et al., 2002), (Yiu and He, 2006). It remains unresolved how the receptor complex NgR1 / Lingo1 and S1PR2 might interact to activate the same intracellular cascade. Indeed, they may directly trigger the same signalling pathway independently of each other. Another possibility is that they may act through a transactivation - dependent mechanism. Transactivation is considered to be an important way of communication to integrate different signalling systems, as it has been shown for the epidermal growth factor receptor (EGFR) (Gschwind et al., 2001) and for the brain-derived neurotrophic factor (BDNF) receptor TrkB (Rajagopal, 2004), (Puehringer et al., 2013). For instance, Nogo-A acting through S1PR2, may transactivate neighbouring NgR1 which would then activate the RhoA - dependent signalling pathway. Finally, in another scenario, both direct and transactivation processes may exist, e.g. with weak activation of RhoA via downstream S1PR2 - dependent signalling being reinforced by signalling from transactivated NgR1.
It is interesting to note that in the hippocampus Nogo-A and NgR1 have been shown to localize at both pre- and post-synapses, while Lingo-1 is associated with the presynaptic fraction (Raiker et al., 2010), (Lee et al., 2008). This notion leaves unresolved the possibility for a cis (where the receptor binds the ligand expressed in an other cell) and/or trans (where the receptor binds the ligand expressed onto the same cell) Nogo-A / receptor complex signalling (Held and Mariuzza, 2011). However, in line with previous observations, the analysis of PPF reveals that the presynaptic function is not affected by the Nogo-66 / NgR1 signalling (Raiker et al., 2010), (Lee et al., 2008), (Delekate et al., 2011), by Lingo-1 (my data), or by the Nogo-A-Δ20 / S1PR2 signalling (Kempf et al., 2014), indicating a Nogo-A / receptor complex postsynaptic mechanism of action.

4.2.2 Other intracellular pathway mediating the role of Nogo-A

While my data clearly implicate the ROCK2-Cofilin pathway in mediating the Nogo-66 / NgR1 effect on LTP, this is most likely not the only intracellular cascade activated by Nogo-A signalling in this context. Indeed, although activation of NMDARs is necessary for induction of LTP in the CA1 region of the hippocampus, calcium-induced calcium release (CICR) from ER is crucial for the induction of NMDA receptor - dependent LTP (Fitzjohn and Collingridge, 2002), promoting the resulting insertion of new AMPARs

and the changes in the status of actin filaments within spines (Oertner and Matus, 2005). Moreover, the ER is specifically localized in larger and mature spines associated with higher postsynaptic calcium release events (Holbro et al., 2009). Interestingly, beside its localization at synapses, Nogo-A is a reticulon protein shown to be localized at the endoplasmatic reticulum (ER) in high amount (Teng and Bor, 2008), (Oertle and Schwab, 2003), suggesting a function of Nogo-A associated to this subcellular compartment localization. The only evidence for this notion regards the finding that Nogo-A modulates the shape of the ER (Voeltz et al., 2006), and direct proofs are missing for correlating the Nogo-A localization at the ER and its role in regulating synaptic plasticity. Interestingly, another member of the reticulon family, the reticulon protein RTN1A, has been associated at the ER with the ryanodine receptor RyR2 (Kaya et al., 2013), a member of the ryanodine receptor Ca^{2+}-release channels (RyRs) implicated in the regulation of the CICR (Tully, 2004). Moreover, Nogo-A signalling has been shown to increase the intracellular calcium concentration leading to growth cone collapse (Bandtlow et al., 1993). These observations suggest the possibility that in the context of activity - dependent functional plasticity Nogo-A might modulate the calcium-influx from the ER. However, this hypothesis remains to be investigated.
Upon LTP induction, the increased insertion of new AMPARs is a crucial event for LTP expression and maintenance. Interestingly, it has been shown that a shRNA mediated downregulation of Nogo-A increases the expression of NMDAR and AMPAR subunits in hippocampal neurons (Peng et al., 2011). In addition, data from the lab show that the acute neutralization of Nogo-A increases the amplitude of miniature excitatory synaptic current (mEPSC) recorded from CA3 hippocampal neurons as well as promotes the insertion of AMPA receptors at synapses under basal conditions and upon chemical induction of LTP (Kellner et al., 2016), indicating a role of Nogo-A in regulating the strength of excitatory synaptic transmission at hippocampal synapses. Moreover, the trafficking of AMPAR upon LTP has been shown to be regulated by the biphasic modulation of actin dynamics via Cofilin (Gu et al., 2010) and by NgR1 signalling (Jitsuki et al., 2015). These observations suggest that the Nogo-66 / NgR1 signalling might restrict LTP by influencing the ROCK-Cofilin pathway to negatively regulate the insertion of AMPAR at post-synaptic sites.

4.2.3 Nogo-A receptor complex

Although the ligand-receptor interaction is usually a two-player event, the Nogo-A signalling represents one example of a multi-site / multi ligand receptor complex. First of all, Nogo-A ligand binds more than one receptor, i.e. Nogo-66 domain binds to NgR1 and the paired immunoglobulin-like receptor B (PirB) (Atwal et al., 2008). Although it has been well clarified the role of Nogo-66 / NgR1 signalling in regulating LTP (my data) (Delekate et al., 2011) (Raiker et al., 2010), pirb-ko mice show normal LTP in acute hippocampal slices (Raiker et al., 2010). Whether acutely blocking PirB modulate LTP and a possible role of Nogo-66 / PirB signalling in regulating LTP remains to be addressed. Second, multiple ligands bind the same Nogo-A receptors. Indeed, the Nogo-66 domain of Nogo-A, OMgp, the myelin-associated glycoprotein (MAG),

the CSPGs bind to NgR1 (Yiu and He, 2006), (Dickendesher et al., 2012), and the sphingosine-1-phosphate S1P and the Nogo-A-Δ20 domain bind to S1PR2 (Spiegel and Milstien, 2002), (Kempf et al., 2014). Interestingly, although they are unrelated ligands binding the same receptor, all have been shown to mediate the same function, i.e. the inhibition of neurite outgrowth. Thus, the multi-site / multi ligand receptor complex mediating the role of Nogo-A might represent a way to increase the signalling specificity and dynamics, and to amplify the ligand effects. This model of multisubunit receptor complex has been shown also for other molecules, e.g. the neurotrophins (Huang and Reichardt, 2003). Indeed, one single neurotrophin can bind more than one receptor, and more neurotrophins can bind the same TrK receptor. For instance, neurotrophin-3 (NT-3) has been shown to activate not only its receptor TrkC but also TrKB, the known receptor for BDNF, representing an example of redundant functionality (Fariñas et al., 1998). Moreover, all neurotrophins have been demonstrated to bind to $p75^{NTR}$, which mediate the activation of distinct signalling pathways by regulating the affinity and the specificity of Trk receptor activation (Huang and Reichardt, 2003). Here, it is interesting to note that although Trk and NgR1 mediate unrelated signalling pathways, they share the same co-receptor $p75^{NTR}$. This observation raises the possibility of a cross-talk occurring between the pro-plasticity (by neurotrophins) and the anti-plasticity (by Nogo-A) signalling pathways. In this work I could show that $p75^{NTR}$ is not involved in mediating the Nogo-66 signalling, while it might regulate the NgR1 effect in regulating LTD. This leaves open the question of how $p75^{NTR}$ is modulated to regulate the NgR1- and Trk - dependent signalling. Interestingly, the existence of a possible cross-talk between neurotrophins and Nogo-A comes from other findings showing that BDNF counteracts the injury related upregulation of Nogo-A in the hippocampus (Chytrova et al., 2008), and that Nogo-66 attenuates BDNF - dependent activation of both the AKT-p70S6K and ERK1/2 pathways in hippocampal neurons (Raiker et al., 2010). Moreover, BDNF / TrkB signalling positively regulates LTP maintenance in the hippocampus by promoting actin polymerization within dendritic spines (Rex et al., 2007), while Nogo-66 / NgR1 signalling restricts LTP by activating the ROCK2-Cofilin pathway to prevent activity - dependent actin polymerization (Fig. 4.1). It remains to investigate whether BDNF counteracts the Nogo-66 signalling at actin cytoskeleton, or vice versa.

4.3 The role of Nogo-A in regulating the mossy fiber synapses remodelling

Plastic changes in the brain range from the large-scale reorganization at axons and dendrites, to the nanometer changes occurring at presynaptic terminals and postsynaptic dendritic spines. These rearrangements are prominent in the juvenile brain during development, and diminish with maturation. Indeed, in the mature brain the organization of neurons connection is remarkably stable (Holtmaat and Svoboda, 2009). While structural alterations still occur in the mature CNS, they are limited to changes at synapses (De Paola et al., 2006), and are induced by experience and activity as well

as by aging and disease. Rearrangement of synaptic connections affects the number and size of dendritic spines as well as of presynaptic terminals, although at a different rate. Indeed, the turnover of axonal varicosities have been shown to be lower than that of dendritic spines (De Paola et al., 2006).

Nogo-A / NgR1 signalling has been demonstrated to play an important role in controlling the anatomical plasticity in the adult brain (Akbik et al., 2013). In particular, Nogo-A and NgR1 has been shown to restrict the rearrangement of synaptic connections in the somatosensory cortex of adult mice. Indeed, the dendritic spines and axonal varicosities turnover *in vivo* is increased in adult nogo-a/b ko mice as well as adult ngr1 ko mice (Akbik et al., 2013). On the other hand, another publication reveals that the turnover of both pre- and post-synaptic compartments is indistinguishable in the somatosensory cortex between adult wild type and ngr1 ko mice (Park et al., 2014), leaving the issue still open. Moreover, Nogo-A and NgR1 have been identified as essential proteins for closing the critical period in the visual cortex (McGee et al., 2005). Indeed, adult mice lacking a functional ngr1 or nogo-a gene show a greater ocular dominance plasticity that is typical of the developmental phase. However, the turnover of axonal varicosities in visual cortex is similar between wild type and ngr1 ko mice, suggesting that axonal boutons are stable during changes in cortical circuit function (Frantz et al., 2015).

In the hippocampus, Nogo-A / NgR1 signalling stabilizes the architecture of axons and dendrites of mature pyramidal neurons (Zagrebelsky et al., 2010), and the dendritic complexity of hippocampal neurons is increased in ngr-triple ko mice (Wills et al., 2012). Moreover, the acute blockage of Nogo-A in organotypic hippocampal slice cultures has been shown to increase the density of dendritic spines of mature CA3 hippocampal neurons in a fast time scale (Kellner et al., 2016), while its prolonged neutralisation or its genetic deletion does not change the spine density (Zagrebelsky et al., 2010). These observations suggest that the spines that are gained on a short-time scale might not be maintained over a long-time scale. Furthermore, the acute neutralization of Nogo-A increases the length of spines, while its chronic neutralization leads to immature stubby-like spines (Zagrebelsky et al., 2010), suggesting that a chronic neutralisation of Nogo-A might be compensated by the signalling of other molecules binding the NgR1 receptor. Interestingly, despite the acute neutralization of Nogo-A has been associated with increased axonal regeneration as well as higher LTP levels, the genetic deletion of the gene in different nogo-a ko mice show milder phenotypes, possibly due to differences in Nogo deletion mutants, mouse strain genetic background effects, or compensatory mechanisms by other reticulon proteins or Nogo-A isoforms, e.g. Nogo-B (Dimou et al., 2006), (Delekate et al., 2011), (Schwab, 2004), (Tews et al., 2013). Hence, these findings suggest that Nogo-A acutely plays a role in regulating the structural remodelling of dendritic spines, while its signalling might get compensated on a long-time scale. However, it remains unresolved whether Nogo-A might change the reorganization of the presynaptic structures in the hippocampus.

In this context, the mossy fiber synapses onto CA3 pyramidal cells show several unique features in comparison to the presynaptic structures in the other regions of the hip-

pocampus, representing an interesting system to study presynaptic rearrangement. First of all, the mossy fibers are unmyelinated, thus providing a model to discriminate the role of neuronal *versus* myelin Nogo-A. Indeed, in the mature hippocampus Nogo-A is expressed in myelin-forming oligodendrocytes as well as in pyramidal neurons (Huber et al., 2002). Then, the mossy fiber synapses regulate both the excitation and the inhibition of signal transduction to the CA3 circuitry of the hippocampus, as the terminals form excitatory synapses on thorny excrescences of CA3 pyramidal cells while the filopodial extensions protruding from each terminal form inhibitory synapses with inhibitory interneurons. Moreover, the mossy fiber synapses have been previously shown to undergo short-term structural remodelling. Indeed, they have been shown to be motile structure in organotypic hippocampal slice cultures (Chierzi et al., 2012), and short-term activity suppression leads to reduced motility of the terminal, but not that of their filopodia. Furthermore, the mossy fiber synapses undergo long-term structural remodelling, increasing their volume during development *in vitro* as well as *in vivo* in the adult hippocampus following exposure of the mice to enriched environment (Galimberti et al., 2006). On the contrary, long-term activity suppression leads to reduced terminals size without changing that of their filopodial extension, suggesting that both structures might remodel independently of each other (Chierzi et al., 2012).

Here, I addressed whether Nogo-A signalling regulates the structural reorganization of mossy fiber synapses upon a specific loss-of-function approach. I found that the acute neutralization of Nogo-A did not significantly change the motility of the core region of the mossy fiber terminals, while the chronic treatment with a Nogo-A blocking antibody leads to a reduction in their size, indicating that Nogo-A plays a positive role in maintaining the size of the terminals on a long-time scale. These data suggest that Nogo-A might modify local connectivity between individual terminals and CA3 pyramidal cells, thereby reducing synaptic activation of CA3 neurons by possibly altering the number of neurotransmitter release sites. Indeed, it has been shown that the increase in the size of mossy fiber terminals positively correlates with an increase in the number of active zone, leading to a stronger excitatory postsynaptic response as well as to increased size of thorny excrescences, the postsynaptic target of mossy fiber terminals on CA3 neurons (Galimberti et al., 2006). However, it has been demonstrated that the changes in the size of the terminal and the number of synapses formed by the terminal are regulated through distinct signalling mechanisms. Indeed, the synaptic vesicles protein Rab3A has been shown to specifically affects only the size of individual mossy fiber terminals, whereas the Wnt - dependent signalling leads to a global increase in synapse numbers, regulating the connectivity of the mossy fiber synapses (Gogolla et al., 2009). In addition, my data show that the acute neutralization of Nogo-A did not affect the motility of the filopodial extensions protruding from each terminal. On the contrary, the chronic Nogo-A neutralization leads to reduced filopodial extensions length, indicating that Nogo-A plays a positive role in maintaining the structure not only of the terminals but also of their filopodial extensions. Although the functional significance of filopodial extensions remodelling is less clear, they have been shown to contact inhibitory interneurons (Acsády et al., 1998) to mediate feedforward inhibi-

tion of CA3 pyramidal cells (Ruediger et al., 2011). Hence, Nogo-A might play a role in modifying the local connectivity of CA3 pyramidal cells potentially regulating the balance between excitation and inhibition.

4.4 The role of Nogo-A in regulating synaptic plasticity and its physiological relevance

Connectivity remodelling and synapse stabilization are correlated with learning and memory processes (Caroni et al., 2012). Indeed, morphological and functional changes of synaptic connections are associated with learning of new tasks, and the stabilization of selective subpopulations of spines with memory storage. Moreover, the formation of new spines is believed to carry a new memory trace (Caroni et al., 2012).
Nogo-A / NgR1 signalling has been described to negatively regulate synaptic plasticity and motor learning (Zemmar et al., 2014). Indeed, their acute neutralization with a function blocking antibodies leads to increased LTP as well as the spine density of pyramidal neurons in layer II/III of the motor cortex. Interestingly, this is correlated with an improvement in learning a new motor task in mice receiving a Nogo-A function blocking antibody.
In the hippocampus, Nogo-A restricts functional and structural plasticity by controlling the stability of actin cytoskeleton within spines (Iobbi et al., 2016), (Kellner et al., 2016). Moreover, in the context of functional plasticity, Nogo-A exerts its function via the activation of the ROCK2-Cofilin signalling pathway (Iobbi et al., 2016). Hence, Nogo-A represents an upstream modulator that stabilizes the functionality and morphology of dendritic spines within the hippocampus controlling the actin cytoskeleton dynamics. Interestingly, several studies have been demonstrated that interfering with polymerization of actin filaments impairs LTP formation (Fukazawa et al., 2003) (Kramár et al., 2006) (Krucker et al., 2000) (Kim and Lisman, 1999) and affects the spine enlargement associated with LTP (Huber and Menzel, 2004), indicating that actin rearrangement is needed for synaptic plasticity. Moreover, interfering with actin polymerization has been shown to affect different types of memories formation and in different regions of the brain (Lamprecht, 2014). It remains to understand which is the behavioural consequences of the activity of Nogo-A in the adult mouse hippocampus. Indeed, its role in negatively regulating synaptic plasticity might lead to change neuronal circuits affecting hippocampal - dependent memory formation. Unpublished data from the lab show that nogo-a ko mice are facilitated in spatial learning and memory reference formation during the water maze task, indicating that Nogo-A negatively regulates spatial learning and memory formation. Interestingly, over the years hippocampal computational models and lesions on the distinct areas of the hippocampus have revealed that each region of the hippocampus plays a different role in the acquisition and consolidation of memories. For instance, the CA3 region has been shown to be involved in the formation and temporary storage of episodic, spatial and contextual memories (Daumas et al., 2005). Particularly, the mossy fiber projections have been described to make strong but sparse number of synaptic contacts onto CA3

pyramidal neurons, resulting in a sparse firing activity in CA3. This enables sparse and decorrelated representations of distinct events (pattern separation), so that different or similar memories do not interfere with each other (Rolls, 2013). In addition, the synaptic contacts between filopodial extension emerging from the terminals and the interneurons trigger feedforward inhibition in CA3, increasing the precision of memory encoding in the hippocampus (Ruediger et al., 2011) and contributing to form sparse representations. On the contrary, the recurrent collaterals in CA3 promote an auto-associative memory network for the rapid elaboration of a unified representation of the context (pattern completion), enabling associations between any spatial location and an object, e.g. external cues to recall the position of a hidden platform in water maze task (Rolls, 2013). The CA1 region is required for consolidation of contextual memory (Daumas et al., 2005), and is a critical output structure (Ji and Maren, 2008). Indeed, the Schaffer collateral input to CA1 allows that the information in CA3 are retrieved in CA1. In turn, the CA1 neurons project back to the cortical structures, i.e. the entorhinal cortex. Thus, it would be an important goal to understand how Nogo-A regulates different types of learning and memories in the hippocampus, and what is its role in memory acquisition and consolidation.

5 | Conclusion and Outlook

Learning never exhausts the mind.

Leonardo da Vinci

The data described in the first part of this work identify the cellular mechanism mediating the signalling of one of the extracellular cues involved in limiting activity - dependent functional plasticity processes. Indeed, in the context of brain plasticity, it is now clear that specific molecules come into play in order to maintain the tight balance between plasticity and stability for promoting the correct functioning of the neuronal network in many regions of the brain, e.g. the mature hippocampus. Here, I could show that the Nogo-66 domain of Nogo-A restricts LTP. It exerts its function via a receptor complex formed by NgR1 and its co-receptor Lingo-1 rather than $p75^{NTR}$, the other NgR1 co-receptor needed for mediating the signalling of NgR1 and Lingo1 in other context. Moreover, Nogo-66 prevents the actin polymerization crucial for LTP maintenance increasing the activity of Cofilin via ROCK2. Thus, Nogo-66 restricts synaptic strengthening via Lingo1 and the ROCK2-Cofilin pathway by counteracting activity - dependent actin polymerization (Iobbi et al., 2016).
Regarding the other inhibitory domain of Nogo-A, my data suggest that also the Nogo-A-Δ20 domain might restricts LTP via the same signalling pathway activated by Nogo-66. Indeed, it has been shown that Nogo-A-Δ20 / S1PR2 signalling activates the G protein G_{13}, the Rho GEF LARG, and RhoA to inhibit neurite outgrowth (Kempf et al., 2014). Hence, it would be interesting to prove whether Nogo-A-Δ20 signalling via S1PR2 activate the ROCK2-Cofilin pathway to modulate actin dynamics. This can be achieved by analysing the F- to G- actin ratio in order to assess changes in actin dynamics, and by analysing the level of phosphorylated Cofilin upon a loss-of function approach for Nogo-A-Δ20 / S1PR2 signalling.
Moreover, the evidence of how Nogo-A and its receptors modulate actin dynamics is still missing. A way to achieve this purpose would be to use STED microscopy, a single-molecule super resolution method. This imaging technique would allow the analysis of the subspine distribution of dye-tagged F-actin at the nanoscale resolution upon a gain- or loss- of function approach for Nogo-A in acute as well as organotypic hippocampal slices.
Although my data support a role of Nogo-A in regulating the actin dynamics to restrict LTP, they leave open the possibility that it exerts its function also by regulating other signalling pathways within spines. Given the importance of calcium influx for the induction of LTP, future experiments should address whether Nogo-66 / NgR1 plus Lingo1 as well as Nogo-A-Δ20 / S1PR2 signalling pathways play a role in regulating the ER - dependent calcium influx upon LTP induction. For this purpose,

electrophysiology measurements or calcium imaging could be performed on acute hippocampal slices upon a loss- or gain-of function approach for Nogo-A and its receptors along with the inhibition or the activation of the ER - dependent calcium receptors, respectively. Besides calcium involvement in LTP, a crucial step for LTP expression and maintenance is insertion of new AMPARs at the spine membrane. For this reason it would be interesting to address whether Nogo-A signalling regulates the insertion of the AMPARs. To achieve this purpose, the influx of current through NMDARs and AMPARs upon Nogo-A loss- or gain-of function approaches could be measured in pact-clamp experiments. In addition, whether Nogo-A regulate the expression of specific subunits of NMDARs and AMPARs could be assessed using biochemical experiments.

A still open question is how the localization of Nogo-A and its receptors is regulated by activity. Indeed, an activity - dependent insertion or internalization of them at the plasma membrane might be temporally achieved to mediate their function. For this issue, STED microscopy would allow to trace in live samples the movement of fluorescently tagged Nogo-A or receptors upon changes of neuronal activity.

Functional changes are tightly correlated with structural modifications at synapses. Although Nogo-A negatively regulates LTP and spine morphology, proofs for a direct correlation between the two events are still missing. A nice way to achieve this purpose it would be performing electrophysiological recordings combined with two-photon imaging in acute hippocampal slices in order to assess the functional and structural changes occurring within the same cell and at the same time upon modulating Nogo-A signalling.

Moreover, Nogo-A has been described to restrict morphological changes at dendritic spines, leaving unresolved the issue of whether it plays a role also at presynaptic compartments. In the second part of the work, I focused on the presynaptic mossy fiber synapses, and my data indicate a role of Nogo-A in regulating the remodelling of these synapses. Indeed, while the acute neutralization of Nogo-A does not significantly affect their motility, its chronic neutralization leads to a reduction of the size of the main terminal and of the length of the filopodial extensions. What is the functional significance of this role of Nogo-A is not yet known. Electrophysiological measurements could provide a way to analyse the role of Nogo-A in regulating the magnitude of LTP at the mossy fiber-CA3 pathway in acute hippocampal slices upon a loss of function approach for Nogo-A. Furthermore, given the notion that the mossy fiber synapses control both excitation and inhibition of signal transduction on CA3, Nogo-A might play a role in regulating the balance between excitation and inhibition. For this reason, the inhibitory postsynaptic potentials (IPSPs) derived by interneurons and the excitatory postsynaptic potentials (EPSPs) derived by excitatory pyramidal cells could be measured onto CA3 upon a loss of function for Nogo-A to discriminate whether it might play specific roles in regulating excitation and inhibition. Moreover, it has been shown that activity is crucial for mossy fiber synapses structural changes (Galimberti et al., 2006). Hence, Nogo-A neutralization might affect the remodelling of the mossy fiber synapses and become visible in an activity - dependent manner, e.g. upon silencing as well as inducing activity. Future experiments could be aimed at addressing the role of

Nogo-A in regulating activity - dependent structural reorganization of the mossy fiber synapses. For this purpose, organotypic hippocampal slice cultures should be treated with drugs for silencing or inducing activity, and analyse whether the motility and the size of the terminals and filopodia change upon an acute or chronic loss-of-function approach for Nogo-A. Finally, it is interesting to note that the same molecule can play different roles in regulating structural plasticity at presynaptic structures, depending on the region of the brain. For instance, in rab3a-ko mice the size of the mossy fiber terminals is reduced, while the size of the hippocampal Schaffer collateral boutons as well as of cerebellar parallel fiber boutons is not affected (Gogolla et al., 2009). It remains to address whether and how Nogo-A affect the structural remodelling in other regions of the hippocampus, e.g. the size and number of the presynaptic varicosities on the CA3 pyramidal neurons axons.

Functional and structural changes are believed to be the cellular correlates of learning and memory processes. In order to understand whether the role of Nogo-A in negatively regulating synaptic plasticity correlates with behavioural consequences, specific behavioural tests could be performed to assess the involvement of Nogo-A in regulating different types of hippocampus - dependent memories, e.g. by comparing the results of the contextual fear conditioning, in which a rodent has to associate a context with a stimulus, with the water maze, a task used to assess spatial learning. Moreover, given the notion that different areas of the hippocampus have been shown to play distinct function in acquisition and consolidation of a memory, future experiments could be aimed at addressing which is the role of Nogo-A in memory acquisition and consolidation. Here, transgenic mouse lines carrying inducible Cre enzyme driven by subregion-specific promoters could be used to delete nogo-a gene in specific areas of the hippocampus, or viruses for Nogo-A siRNA-mediated knockdown could be injected into distinct hippocampal subregions, for testing whether different cognitive impairment occur upon behavioural tasks. Alternatively, in another approach it would be possible to use a knock-in mouse expressing GFP-Nogo-A under promoter of immediate early genes (IEGs), which are upregulated by LTP as well as by behavioural tasks (Kubik et al., 2007), to activate Nogo-A specifically in circuits that are involved in particular behaviour, and analyse the cognitive performance upon behavioural tasks.

In conclusion, this work deepens the knowledge on how Nogo-A protein limits the experience - dependent plasticity to stabilize neural circuits in the adult hippocampus, a structure known to remain plastic throughout life. Indeed, a tightly regulated balance between plasticity and stability of neural circuits in the mature brain ensures the spatial and temporal specificity necessary for learning memory storage processes. For instance, signalling from myelin-associate neurite growth inhibitors has been shown to be upregulated in a model of cognitive impaired aged rats (Vanguilder et al., 2012), suggesting that an excessive stabilization of synaptic networks might prevent the acquisition and consolidation of new memories. In parallel, in a microRNA-mediated Nogo-A knockdown rat, the depletion of Nogo-A is associated with symptoms correlated to schizophrenia (Tews et al., 2013), suggesting that a reduction of the mechanisms that control stability of neuronal network might be detrimental for cognitive functions.

Bibliography

Abel, T., Martin, K. C., Bartsch, D., and Kandel, E. R. (1998). Memory suppressor genes: inhibitory constraints on the storage of long-term memory. *Science*, 279:338–341.

Abraham, W. C. and Robins, A. (2005). Memory retention-the synaptic stability versus plasticity dilemma. *Trends Neurosci.*, 28:73–78.

Acsády, L., Kamondi, A., Sík, A., Freund, T., and Buzsáki, G. (1998). GABAergic Cells Are the Major Postsynaptic Targets of Mossy Fibers in the Rat Hippocampus. *J. Neurosci.*, 18:3386–3403.

Akbik, F. V., Bhagat, S. M., Patel, P. R., Cafferty, W. B. J., and Strittmatter, S. M. (2013). Anatomical plasticity of adult brain is titrated by Nogo Receptor 1. *Neuron*, 77:859–66.

Atwal, J. K., Pinkston-Gosse, J., Syken, J., Stawicki, S., Wu, Y., Shatz, C., and Tessier-Lavigne, M. (2008). PirB is a functional receptor for myelin inhibitors of axonal regeneration. *Science*, 322:967–970.

Bailey, C. H., Giustetto, M., Huang, Y. Y., Hawkins, R. D., and Kandel, E. R. (2000). Is heterosynaptic modulation essential for stabilizing Hebbian plasticity and memory? *Nat. Rev. Neurosci.*, 1:11–20.

Bamburg, J. R. and Bernstein, B. W. (2010). Roles of ADF/cofilin in actin polymerization and beyond. *F1000 Biol. Rep.*, 2:62.

Bandtlow, C. E., Dlaska, M., Pirker, S., Czech, T., Baumgartner, C., and Sperk, G. (2004). Increased expression of Nogo-A in hippocampal neurons of patients with temporal lobe epilepsy. *Eur. J. Neurosci.*, 20:195–206.

Bandtlow, C. E., Schmidt, M. F., Hassinger, T. D., Schwab, M. E., and Kater, S. B. (1993). Role of intracellular calcium in NI-35-evoked collapse of neuronal growth cones. *Science*, 259:80–83.

Bareyre, F. M., Haudenschild, B., and Schwab, M. E. (2002). Long-lasting sprouting and gene expression changes induced by the monoclonal antibody IN-1 in the adult spinal cord. *J. Neurosci.*, 22:7097–7110.

Barrett, G. L., Reid, C. a., Tsafoulis, C., Zhu, W., Williams, D. a., Paolini, A. G., Trieu, J., and Murphy, M. (2010). Enhanced spatial memory and hippocampal long-term potentiation in p75 neurotrophin receptor knockout mice. *Hippocampus*, 20:145–152.

Becker, N., Wierenga, C. J., Fonseca, R., Bonhoeffer, T., and Nägerl, U. V. (2008). LTD induction causes morphological changes of presynaptic boutons and reduces their contacts with spines. *Neuron*, 60:590–7.

Bliss, T. V. and Lomo, T. (1973). Long-lasting potentiation of synaptic transmission in the dentate area of the unanaestetized rabbit following stimulation of the perforant path. *J. Physiol.*, 232:331–356.

Bosch, M., Castro, J., Saneyoshi, T., Matsuno, H., Sur, M., and Hayashi, Y. (2014). Structural and Molecular Remodeling of Dendritic Spine Substructures during Long-Term Potentiation. *Neuron*, 82:444–459.

Bourne, J. and Harris, K. M. (2007). Do thin spines learn to be mushroom spines that remember? *Curr. Opin. Neurobiol.*, 17:381–386.

Bubb, M. R., Senderowicz, A. M. J., Sausville, E. a., Duncan, K. L. K., and Korn, E. D. (1994). Jasplakinolide, a cytotoxic natural product, induces actin polymerization and competitively inhibits the binding of phalloidin to F-actin. *J. Biol. Chem.*, 269:14869–14871.

Buffo, A., Zagrebelsky, M., Huber, A. B., Skerra, A., Schwab, M. E., Strata, P., and Rossi, F. (2000). Application of Neutralizing Antibodies against NI-35/250 Myelin-Associated Neurite Growth Inhibitory Proteins to Purkinje Cell Axons. *J. Neurosci.*, 20:2275–2286.

Bukalo, O., Schachner, M., and Dityatev, A. (2001). Modification of extracellular matrix by enzymatic removal of chondroitin sulfate and by lack of tenascin-R differentially affects several forms of synaptic plasticity in the hippocampus. *Neuroscience*, 104:359–369.

Burgess, N., Maguire, E. A., and O'Keefe, J. (2002). The Human Hippocampus and Spatial and Episodic Memory. *Neuron*, 35:625–641.

Caroni, P., Donato, F., and Muller, D. (2012). Structural plasticity upon learning: regulation and functions. *Nat. Rev. Neurosci.*, 13:478–90.

Chazeau, A., Mehidi, A., Nair, D., Gautier, J. J., Leduc, C., Chamma, I., Kage, F., Kechkar, A., Thoumine, O., Rottner, K., Choquet, D., Gautreau, A., Sibarita, J.-B., and Giannone, G. (2014). Nanoscale segregation of actin nucleation and elongation factors determines dendritic spine protrusion. *EMBO J.*, 33:1–20.

Chen, J.-H., Kellner, Y., Zagrebelsky, M., Grunwald, M., Korte, M., and Walla, P. J. (2015). Two-Photon Correlation Spectroscopy in Single Dendritic Spines Reveals Fast Actin Filament Reorganization during Activity-Dependent Growth. *PLoS One*, 10:e0128241.

Chen, L. Y., Rex, C. S., Casale, M. S., Gall, C. M., and Lynch, G. (2007). Changes in synaptic morphology accompany actin signaling during LTP. *J. Neurosci.*, 27:5363–5372.

Chen, M. S., Huber, A. B., van der Haar, M. E., Frank, M., Schnell, L., Spillmann, A. A., Christ, F., and Schwab, M. E. (2000). Nogo-A is a myelin-associated neurite outgrowth inhibitor and an antigen for monoclonal antibody IN-1. *Nature*, 403:434–9.

Chierzi, S., Stachniak, T. J., Trudel, E., Bourque, C. W., and Murai, K. K. (2012). Activity maintains structural plasticity of mossy fiber terminals in the hippocampus. *Mol. Cell. Neurosci.*, 50:260–71.

Chytrova, G., Ying, Z., and Gomez-Pinilla, F. (2008). Exercise normalizes levels of MAG and Nogo-A growth inhibitors after brain trauma. *Eur. J. Neurosci.*, 27:1–11.

Craveiro, L. M., Hakkoum, D., Weinmann, O., Montani, L., Stoppini, L., and Schwab, M. E. (2008). Neutralization of the membrane protein Nogo-A enhances growth and reactive sprouting in established organotypic hippocampal slice cultures. *Eur. J. Neurosci.*, 28:1808–24.

Daumas, S., Halley, H., Francés, B., and Lassalle, J.-M. (2005). Encoding, consolidation, and retrieval of contextual memory: Differential involvement of dorsal CA3 and CA1 hippocampal subregions. *Learn. Mem.*, 12:375–382.

De Paola, V., Arber, S., and Caroni, P. (2003). AMPA receptors regulate dynamic equilibrium of presynaptic terminals in mature hippocampal networks. *Nat. Neurosci.*, 6:491–500.

De Paola, V., Holtmaat, A., Knott, G., Song, S., Wilbrecht, L., Caroni, P., and Svoboda, K. (2006). Cell Type-Specific Structural Plasticity of Axonal Branches and Boutons in the Adult Neocortex. *Neuron*, 49:861–875.

Delekate, A., Zagrebelsky, M., Kramer, S., Schwab, M. E., and Korte, M. (2011). NogoA restricts synaptic plasticity in the adult hippocampus on a fast time scale. *Proc. Natl. Acad. Sci. U. S. A.*, 108:2569–2574.

Dent, E. W., Gupton, S. L., and Gertler, F. B. (2011). The growth cone cytoskeleton in Axon outgrowth and guidance. *Cold Spring Harb. Perspect. Biol.*, 3:1–39.

Deupi, Li, and Schertler (2012). Ligands Stabilize Specific GPCR Conformations: But How? *Cell*, 20:1289–1290.

Dickendesher, T. L., Baldwin, K. T., Mironova, Y. a., Koriyama, Y., Raiker, S. J., Askew, K. L., Wood, A., Geoffroy, C. G., Zheng, B., Liepmann, C. D., Katagiri, Y., Benowitz, L. I., Geller, H. M., and Giger, R. J. (2012). NgR1 and NgR3 are receptors for chondroitin sulfate proteoglycans. *Nat. Neurosci.*, 15:703–712.

Dimou, L., Schnell, L., Montani, L., Duncan, C., Simonen, M., Schneider, R., Liebscher, T., Gullo, M., and Schwab, M. E. (2006). Nogo-A-deficient mice reveal strain-dependent differences in axonal regeneration. *J. Neurosci.*, 26:5591–603.

Dudek, S. M. and Bear, M. F. (1992). Homosynaptic long-term depression in area CA1 of hippocampus and effects of N-methyl-D-aspartate receptor blockade. *Proc. Natl. Acad. Sci. U. S. A.*, 89:4363–4367.

Eichenbaum, H. (2004). Hippocampus: Cognitive processes and neural representations that underlie declarative memory. *Neuron*, 44:109–120.

Eichenbaum, H. (2015). The Hippocampus as a Cognitive Map ... of Social Space. *Neuron*, 87:9–11.

Evstratova, A. and Tóth, K. (2014). Information processing and synaptic plasticity at hippocampal mossy fiber terminals. *Front. Cell. Neurosci.*, 8:1–12.

Fariñas, I., Wilkinson, G. A., Backus, C., Reichardt, L. F., and Patapoutian, A. (1998). Characterization of neurotrophin and Trk receptor functions in developing sensory ganglia: direct NT-3 activation of TrkB neurons in vivo. *Neuron*, 21:325–334.

Fischer, M., Kaech, S., Knutti, D., and Matus, A. (1998). Rapid Actin-Based Plasticity in Dendritic Spines. *Neuron*, 20:847–854.

Fitzjohn, S. M. and Collingridge, G. L. (2002). Calcium stores and synaptic plasticity. *Cell Calcium*, 32:405–11.

Fournier, A. E., Gould, G. C., Liu, B. P., and Strittmatter, S. M. (2002). Truncated soluble Nogo receptor binds Nogo-66 and blocks inhibition of axon growth by myelin. *J. Neurosci.*, 22:8876–8883.

Fournier, A. E., GrandPre, T., and Strittmatter, S. M. (2001). Identification of a receptor mediating Nogo-66 inhibition of axonal regeneration. *Nature*, 409:341–346.

Frantz, M. G., Kast, R. J., Dorton, H. M., Chapman, K. S., and McGee, a. W. (2015). Nogo Receptor 1 Limits Ocular Dominance Plasticity but not Turnover of Axonal Boutons in a Model of Amblyopia. *Cereb. Cortex*, (10.1093/cercor/bhv014):1–11.

Frisk, V. and Milner, B. (1990). The role of the left hippocampal region in the acquisition and retention of story content. *Neuropsychologia*, 28:349–359.

Fu, M. and Zuo, Y. (2011). Experience-dependent structural plasticity in the cortex. *Trends Neurosci.*, 34:177–87.

Fujitani, M., Kawai, H., Proia, R. L., Kashiwagi, A., Yasuda, H., and Yamashita, T. (2005). Binding of soluble myelin-associated glycoprotein to specific gangliosides induces the association of p75NTR to lipid rafts and signal transduction. *J. Neurochem.*, 94:15–21.

Fukazawa, Y., Saitoh, Y., Ozawa, F., Ohta, Y., Mizuno, K., and Inokuchi, K. (2003). Hippocampal LTP Is Accompanied by Enhanced F-Actin Content within the Dendritic Spine that Is Essential for Late LTP Maintenance In Vivo. *Neuron*, 38:447–460.

Galimberti, I., Gogolla, N., Alberi, S., Santos, A. F., Muller, D., and Caroni, P. (2006). Long-term rearrangements of hippocampal mossy fiber terminal connectivity in the adult regulated by experience. *Neuron*, 50:749–63.

Gogolla, N., Galimberti, I., Deguchi, Y., and Caroni, P. (2009). Wnt signaling mediates experience-related regulation of synapse numbers and mossy fiber connectivities in the adult hippocampus. *Neuron*, 62:510–25.

GrandPré, T., Nakamura, F., Vartanian, T., and Strittmatter, S. M. (2000). Identification of the Nogo inhibitor of axon regeneration as a Reticulon protein. *Nature*, 403:439–444.

Gschwind, a., Zwick, E., Prenzel, N., Leserer, M., and Ullrich, A. (2001). Cell communication networks: epidermal growth factor receptor transactivation as the paradigm for interreceptor signal transmission. *Oncogene*, 20:1594–1600.

Gu, J., Lee, C. W., Fan, Y., Komlos, D., Tang, X., Sun, C., Yu, K., Hartzell, H. C., Chen, G., Bamburg, J. R., and Zheng, J. Q. (2010). ADF/cofilin-mediated actin dynamics regulate AMPA receptor trafficking during synaptic plasticity. *Nat. Neurosci.*, 13:1208–1215.

Gungabissoon, R. A. and Bamburg, J. R. (2003). Regulation of Growth Cone Actin Dynamics by ADF/Cofilin 1. *Histochemistry*, 51:411–420.

Hasegawa, Y., Fujitani, M., Hata, K., Tohyama, M., Yamagishi, S., and Yamashita, T. (2004). Promotion of axon regeneration by myelin-associated glycoprotein and Nogo through divergent signals downstream of Gi/G. *J. Neurosci.*, 24:6826–6832.

Held, W. and Mariuzza, R. a. (2011). Cis-trans interactions of cell surface receptors: biological roles and structural basis. *Cell. Mol. Life Sci.*, 68:3469–78.

Hensch, T. K. (2005). Critical period plasticity in local cortical circuits. *Nat. Rev. Neurosci.*, 6:877–888.

Holbro, N., Grunditz, A., and Oertner, T. G. (2009). Differential distribution of endoplasmic reticulum controls metabotropic signaling and plasticity at hippocampal synapses. *Proc. Natl. Acad. Sci. U. S. A.*, 106:15055–60.

Holtmaat, A. and Svoboda, K. (2009). Experience-dependent structural synaptic plasticity in the mammalian brain. *Nat. Rev. Neurosci.*, 10:647–58.

Honkura, N., Matsuzaki, M., Noguchi, J., Ellis-Davies, G. C. R., and Kasai, H. (2008). The Subspine Organization of Actin Fibers Regulates the Structure and Plasticity of Dendritic Spines. *Neuron*, 57:719–729.

Hotulainen, P. and Hoogenraad, C. C. (2010). Actin in dendritic spines: connecting dynamics to function. *J. Cell Biol.*, 189:619–629.

Hsieh, S. H.-K., Ferraro, G. B., and Fournier, A. E. (2006). Myelin-associated inhibitors regulate cofilin phosphorylation and neuronal inhibition through LIM kinase and Slingshot phosphatase. *J. Neurosci.*, 26:1006–1015.

Huang, E. J. and Reichardt, L. F. (2003). TRK receptors: roles in neuronal signal transduction. *Annu. Rev. Biochem.*, 72:609–642.

Hübener, M. and Bonhoeffer, T. (2014). Neuronal Plasticity: Beyond the Critical Period. *Cell*, 159:727–737.

Huber, A. B., Weinmann, O., Brösamle, C., Oertle, T., and Schwab, M. E. (2002). Patterns of Nogo mRNA and protein expression in the developing and adult rat and after CNS lesions. *J. Neurosci.*, 22:3553–67.

Huber, K. M. (2000). Role for Rapid Dendritic Protein Synthesis in Hippocampal mGluR-Dependent Long-Term Depression. *Science*, 288:1254–1256.

Huber, L. and Menzel, R. (2004). Structural basis of long-term potentiation in single dendritic spines. *Nature*, 429:761–766.

Iobbi, C., Korte, M., and Zagrebelsky, M. (2016). Nogo-66 Restricts Synaptic Strengthening via Lingo1 and the ROCK2-Cofilin Pathway to Control Actin Dynamics. *Cereb. Cortex*, (10.1093/cercor/bhw122):1–14.

Ishizaki, T., Uehata, M., Tamechika, I., Keel, J., Nonomura, K., Maekawa, M., and Narumiya, S. (2000). Pharmacological properties of Y-27632, a specific inhibitor of rho-associated kinases. *Mol. Pharmacol.*, 57:976–983.

Ji, B., Li, M., Wu, W. T., Yick, L. W., Lee, X., Shao, Z., Wang, J., So, K. F., McCoy, J. M., Blake Pepinsky, R., Mi, S., and Relton, J. K. (2006). LINGO-1 antagonist promotes functional recovery and axonal sprouting after spinal cord injury. *Mol. Cell. Neurosci.*, 33:311–320.

Ji, J. and Maren, S. (2008). Differential roles for hippocampal areas CA1 and CA3 in the contextual encoding and retrieval of extinguished fear. *Learn. Mem.*, 15:244–51.

Jitsuki, S., Nakajima, W., Takemoto, K., Sano, A., Tada, H., Takahashi-Jitsuki, A., and Takahashi, T. (2015). Nogo Receptor Signaling Restricts Adult Neural Plasticity by Limiting Synaptic AMPA Receptor Delivery. *Cereb. Cortex*, 26:427–439.

Josephson, A., Trifunovski, A., Schéele, C., Widenfalk, J., Wahlestedt, C., Brené, S., Olson, L., and Spenger, C. (2003). Activity-induced and developmental downregulation of the Nogo receptor. *Cell Tissue Res.*, 311:333–42.

Kasai, H., Matsuzaki, M., Noguchi, J., Yasumatsu, N., and Nakahara, H. (2003). Structure-stability-function relationships of dendritic spines. *Trends Neurosci.*, 26:360–368.

Kaya, L., Meissner, B., Riedl, M. C., Muik, M., Schwarzer, C., Ferraguti, F., Sarg, B., Lindner, H., Schweigreiter, R., Knaus, H. G., Romanin, C., and Bandtlow, C. E. (2013). Direct association of the reticulon protein RTN1A with the ryanodine receptor 2 in neurons. *Biochim. Biophys. Acta - Mol. Cell Res.*, 1833:1421–1433.

Kellner, Y., Fricke, S., Kramer, S., Iobbi, C., Wierenga, C. J., Schwab, M. E., Korte, M., and Zagrebelsky, M. (2016). Nogo-A controls structural plasticity at dendritic spines by rapidly modulating actin dynamics. *Hippocampus*, (10.1002/hipo.22565):1–16.

Kemp, N., Mcqueen, J., Faulkes, S., and Bashir, Z. I. (2000). Different forms of LTD in the CA1 region of the hippocampus : role of age and stimulus protocol. *Eur. J. Neurosci.*, 12:360–366.

Kempf, A. and Schwab, M. E. (2013). Nogo-a represses anatomical and synaptic plasticity in the central nervous system. *Physiology*, 28:151–63.

Kempf, A., Tews, B., Arzt, M. E., Weinmann, O., Obermair, F. J., Pernet, V., Zagrebelsky, M., Delekate, A., Iobbi, C., Zemmar, A., Ristic, Z., Gullo, M., Spies, P., Dodd, D., Gygax, D., Korte, M., and Schwab, M. E. (2014). The Sphingolipid Receptor S1PR2 Is a Receptor for Nogo-A Repressing Synaptic Plasticity. *PLoS Biol.*, 12:1–16.

Kim, C. H. and Lisman, J. E. (1999). A role of actin filament in synaptic transmission and long-term potentiation. *J. Neurosci.*, 19:4314–4324.

Korobova, F. and Tatyana, S. (2010). Molecular architecture of synaptic actin cytoskeleton in hippocampal neurons reveals a mechanism of dendritic spine morphogenesis. *Mol. Biol. Cell*, 21:165–176.

Kowalczyk, T., Bocian, R., and Konopacki, J. (2013). The generation of theta rhythm in hippocampal formation maintained in vitro. *Eur. J. Neurosci.*, 37:679–699.

Kramár, E. a., Lin, B., Rex, C. S., Gall, C. M., and Lynch, G. (2006). Integrin-driven actin polymerization consolidates long-term potentiation. *Proc. Natl. Acad. Sci. U. S. A.*, 103:5579–5584.

Krucker, T., Siggins, G. R., and Halpain, S. (2000). Dynamic actin filaments are required for stable long-term potentiation (LTP) in area CA1 of the hippocampus. *Proc. Natl. Acad. Sci. U. S. A.*, 97:6856–6861.

Kubik, S., Miyashita, T., and Guzowski, J. F. (2007). Using immediate-early genes to map hippocampal subregional functions. *Learn. Mem.*, 14:758–770.

Kwon, H.-b. and Castillo, P. E. (2008). Long-Term Potentiation Selectively Expressed by NMDA Receptors at Hippocampal Mossy Fiber Synapses. *Cell*, 57:108–120.

Lamprecht, R. (2014). The actin cytoskeleton in memory formation. *Prog. Neurobiol.*, 117:1–19.

Lappalainen, P., Hotulainen, P., Llano, O., Smirnov, S., Tanhuanpää, K., Faix, J., Rivera, C., and Lappalainen, P. (2009). Defining mechanisms of actin polymerization and depolymerization during dendritic spine morphogenesis. *J. Cell Biol.*, 185:323–39.

Lee, H., Raiker, S. J., Venkatesh, K., Geary, R., Robak, L. a., Zhang, Y., Yeh, H. H., Shrager, P., and Giger, R. J. (2008). Synaptic function for the Nogo-66 receptor NgR1: regulation of dendritic spine morphology and activity-dependent synaptic strength. *J. Neurosci.*, 28:2753–2765.

Llorens, F., Gil, V., Iraola, S., Carim-Todd, L., Martí, E., Estivill, X., Soriano, E., del Rio, J. A., and Sumoy, L. (2008). Developmental analysis of Lingo-1/Lern1 protein expression in the mouse brain: Interaction of its intracellular domain with Myt1l. *Dev. Neurobiol.*, 68:521–541.

Malenka, R. C. and Kauer, J. A. (2007). Synaptic plasticity and addiction. *Nat. Rev. Neurosci.*, 8:844–58.

Martin, S. J., Grimwood, P. D., and Morris, R. G. M. (2000). Synaptic plasticity and memory: an evaluation of the hypothesis. *Annu. Rev. Neurosci.*, 23:649–711.

Matsuzaki, M., Honkura, N., Ellis-Davies, G. C. R., and Kasai, H. (2004). Structural basis of long-term potentiation in single dendritic spines. *Nature*, 429:761–6.

Matus, a. (2000). Actin-based plasticity in dendritic spines. *Science*, 290:754–758.

McGee, A. W., Yang, Y., Fischer, Q. S., Daw, N. W., and Strittmatter, S. M. (2005). Experience-driven plasticity of visual cortex limited by myelin and Nogo receptor. *Science*, 309:2222–2226.

Meabon, J. S., De Laat, R., Ieguchi, K., Wiley, J. C., Hudson, M. P., and Bothwell, M. (2015). LINGO-1 Interacts with the p75 Neurotrophin Receptor in Intracellular Membrane Compartments. *J. Biol. Chem.*, 290:9511–9520.

Meyer, D., Bonhoeffer, T., and Scheuss, V. (2014). Balance and Stability of Synaptic Structures during Synaptic Plasticity. *Neuron*, 82:430–443.

Mi, S., Lee, X., Shao, Z., Thill, G., Ji, B., Relton, J., Levesque, M., Allaire, N., Perrin, S., Sands, B., Crowell, T., Cate, R. L., McCoy, J. M., and Pepinsky, R. B. (2004). LINGO-1 is a component of the Nogo-66 receptor/p75 signaling complex. *Nat. Neurosci.*, 7:221–228.

Michaelsen, K., Zagrebelsky, M., Berndt-Huch, J., Polack, M., Buschler, A., Sendtner, M., and Korte, M. (2010). Neurotrophin receptors TrkB.T1 and p75NTR cooperate in modulating both functional and structural plasticity in mature hippocampal neurons. *Eur. J. Neurosci.*, 32:1854–1865.

Mironova, Y. a. and Giger, R. J. (2013). Where no synapses go: gatekeepers of circuit remodeling and synaptic strength. *Trends Neurosci.*, 36:363–373.

Moggs, J. G. and Orphanides, G. (2001). Estrogen receptors: orchestrators of pleiotropic cellular responses. *EMBO Rep.*, 2:775–781.

Montani, L., Gerrits, B., Gehrig, P., Kempf, A., Dimou, L., Wollscheid, B., and Schwab, M. E. (2009). Neuronal Nogo-A modulates growth cone motility via Rho-GTP/LIMK1/cofilin in the unlesioned adult nervous system. *J. Biol. Chem.*, 284:10793–10807.

Morris, R., Anderson, E., Lynch, G. S., and Baudry, M. (1986). Selective impairment of learning and blockade of long-term potentiation by an N-methyl-D-aspartate receptor antagonist, AP5. *Nature*, 319:774–776.

Motanis, H. and Maroun, M. (2012). Differential involvement of protein synthesis and actin rearrangement in the reacquisition of contextual fear conditioning. *Hippocampus*, 22:494–500.

Murakoshi, H., Wang, H., and Yasuda, R. (2011). Local, persistent activation of Rho GTPases during plasticity of single dendritic spines. *Nature*, 472:100–4.

Nabavi, S., Fox, R., Proulx, C. D., Lin, J. Y., Tsien, R. Y., and Malinow, R. (2014). Engineering a memory with LTD and LTP. *Nature*, 511:348–352.

Narumiya, S., Ishizaki, T., and Ufhata, M. (2000). Regulators and Effectors of Small GTPases - Part D: Rho Family. *Methods Enzymol.*, 325:273–284.

Nash, M., Pribiag, H., Fournier, A. E., and Jacobson, C. (2009). Central nervous system regeneration inhibitors and their intracellular substrates. *Mol. Neurobiol.*, 40:224–235.

Nicoll, R. a. and Schmitz, D. (2005). Synaptic plasticity at hippocampal mossy fibre synapses. *Nat. Rev. Neurosci.*, 6:863–76.

Niederöst, B., Oertle, T., Fritsche, J., McKinney, R. A., and Bandtlow, C. E. (2002). Nogo-A and myelin-associated glycoprotein mediate neurite growth inhibition by antagonistic regulation of RhoA and Rac1. *J. Neurosci.*, 22:10368–10376.

Nishiyama, J. and Yasuda, R. (2015). Biochemical Computation for Spine Structural Plasticity. *Neuron*, 87:63–75.

Oertle, T. and Schwab, M. E. (2003). Nogo and its paRTNers. *Trends Cell Biol.*, 13:187–194.

Oertle, T., van der Haar, M. E., Bandtlow, C. E., Robeva, A., Burfeind, P., Buss, A., Huber, A. B., Simonen, M., Schnell, L., Brösamle, C., Kaupmann, K., Vallon, R., and Schwab, M. E. (2003). Nogo-A inhibits neurite outgrowth and cell spreading with three discrete regions. *J. Neurosci.*, 23:5393–5406.

Oertner, T. G. and Matus, A. (2005). Calcium regulation of actin dynamics in dendritic spines. *Cell Calcium*, 37:477–482.

Okamoto, K.-I., Nagai, T., Miyawaki, A., and Hayashi, Y. (2004). Rapid and persistent modulation of actin dynamics regulates postsynaptic reorganization underlying bidirectional plasticity. *Nat. Neurosci.*, 7:1104–1112.

O'Keefe, J. and Dostrovsky, J. (1971). The hippocampus as a spatial map. Preliminary evidence from unit activity in the freely-moving rat. *Brain Res.*, 34:171–175.

Ouyang, Y., Wong, M., Capani, F., Rensing, N., Lee, C.-S., Liu, Q., Neusch, C., Martone, M. E., Wu, J. Y., Yamada, K., Ellisman, M. H., and Choi, D. W. (2005). Transient decrease in F-actin may be necessary for translocation of proteins into dendritic spines. *Eur. J. Neurosci.*, 22:2995–3005.

Park, J. I., Frantz, M. G., Kast, R. J., Chapman, K. S., Dorton, H. M., Stephany, C.-É., Arnett, M. T., Herman, D. H., and McGee, A. W. (2014). Nogo receptor 1 limits tactile task performance independent of Basal anatomical plasticity. *PLoS One*, 9:1–13.

Peng, X., Kim, J., Zhou, Z., Fink, D. J., and Mata, M. (2011). Neuronal Nogo-A regulates glutamate receptor subunit expression in hippocampal neurons. *J. Neurochem.*, 119:1183–1193.

Puehringer, D., Orel, N., Lüningschrör, P., Subramanian, N., Herrmann, T., Chao, M. V., and Sendtner, M. (2013). EGF transactivation of Trk receptors regulates the migration of newborn cortical neurons. *Nat. Neurosci.*, 16:407–15.

Raiker, S. J., Lee, H., Baldwin, K. T., Duan, Y., Shrager, P., and Giger, R. J. (2010). Oligodendrocyte-myelin glycoprotein and Nogo negatively regulate activity-dependent synaptic plasticity. *J. Neurosci.*, 30:12432–12445.

Rajagopal, R. (2004). Transactivation of Trk Neurotrophin Receptors by G-Protein-Coupled Receptor Ligands Occurs on Intracellular Membranes. *J. Neurosci.*, 24:6650–6658.

Rebola, N., Lujan, R., Cunha, R. A., and Mulle, C. (2008). Adenosine A 2A Receptors Are Essential for Long-Term Potentiation of NMDA-EPSCs at Hippocampal Mossy Fiber Synapses. *Cell*, 57:121–134.

Rex, C. S., Chen, L. Y., Sharma, A., Liu, J., Babayan, A. H., Gall, C. M., and Lynch, G. (2009). Different Rho GTPase-dependent signaling pathways initiate sequential steps in the consolidation of long-term potentiation. *J. Cell Biol.*, 186:85–97.

Rex, C. S., Lin, C.-Y., Kramár, E. a., Chen, L. Y., Gall, C. M., and Lynch, G. (2007). Brain-derived neurotrophic factor promotes long-term potentiation-related cytoskeletal changes in adult hippocampus. *J. Neurosci.*, 27:3017–3029.

Rolls, E. T. (2013). The mechanisms for pattern completion and pattern separation in the hippocampus. *Front. Syst. Neurosci.*, 7:1–21.

Rösch, H., Schweigreiter, R., Bonhoeffer, T., Barde, Y.-A., and Korte, M. (2005). The neurotrophin receptor p75NTR modulates long-term depression and regulates the expression of AMPA receptor subunits in the hippocampus. *Proc. Natl. Acad. Sci. U. S. A.*, 102:7362–7367.

Rudy, J. W. (2014). Actin Dynamics and the evolution of the memory trace. *Brain Res.*, 1621:17–28.

Ruediger, S., Vittori, C., Bednarek, E., Genoud, C., Strata, P., Sacchetti, B., and Caroni, P. (2011). Learning-related feedforward inhibitory connectivity growth required for memory precision. *Nature*, 473:514–518.

Schwab, M. E. (2004). Nogo and axon regeneration. *Curr. Opin. Neurobiol.*, 14:118–24.

Schwab, M. E. (2010). Functions of Nogo proteins and their receptors in the nervous system. *Nat. Rev. Neurosci.*, 11:799–811.

Schwab, M. E. and Caroni, P. (1988). Oligodendrocytes and CNS myelin are nonpermissive substrates for neurite growth and fibroblast spreading in vitro. *J. Neurosci.*, 8:2381–2393.

Schwab, M. E. and Strittmatter, S. M. (2014). Nogo limits neural plasticity and recovery from injury. *Curr. Opin. Neurobiol.*, 27:53–60.

Scoville, W. B. and Milner, B. (1957). Loss of recent memory after bilateral hippocampal lesions. 1957. *J. Neurol. Neurosurg. Psychiatry*, 20:11–21.

Smith, M. L., Milner, B., Smiih, M. L., and Milnek, B. (1981). The role of the right hippocampus in the recall of spatial location. *Science*, 19:781–793.

Spiegel, S. and Milstien, S. (2002). Sphingosine 1-phosphate, a key cell signaling molecule. *J. Biol. Chem.*, 277:25851–4.

Squire, L. R. and Zola-Morgan, S. (1991). The medial temporal lobe memory system. *Science*, 253:1380–6.

Stoppini, L., Buchs, P.-A., and Muller, D. (1991). A simple method for organotypic cultures of nervous tissue. *J. Neurosci. Methods*, 37:173–182.

Syken, J. (2006). PirB Restricts Ocular-Dominance Plasticity in Visual Cortex. *Science*, 313:1795–1800.

Takesian, A. E. and Hensch, T. K. (2013). Balancing Plasticity/Stability Across Brain Development. *Prog. Brain Res.*, 207:3–34.

Teng, F. Y. H. and Bor, L. T. (2008). Cell autonomous function of Nogo and reticulons: The emerging story at the endoplasmic reticulum. *J. Cell. Physiol.*, 216:303–308.

Tews, B., Schönig, K., Arzt, M. E., Clementi, S., Rioult-Pedotti, M.-S., Zemmar, A., Berger, S. M., Schneider, M., Enkel, T., Weinmann, O., Kasper, H., Schwab, M. E., and Bartsch, D. (2013). Synthetic microRNA-mediated downregulation of Nogo-A in transgenic rats reveals its role as regulator of synaptic plasticity and cognitive function. *Proc. Natl. Acad. Sci. U. S. A.*, 110:6583–6588.

Thallmair, M., Metz, G. a., Z'Graggen, W. J., Raineteau, O., Kartje, G. L., and Schwab, M. E. (1998). Neurite growth inhibitors restrict plasticity and functional recovery following corticospinal tract lesions. *Nat. Neurosci.*, 1:124–131.

Tully, K. (2004). Distinct Intracellular Calcium Profiles Following Influx Through N- Versus L-Type Calcium Channels: Role of Ca2+-Induced Ca2+ Release. *J. Neurophysiol.*, 92:135–143.

Vanguilder, H. D., Bixler, G. V., Sonntag, W. E., and Freeman, W. M. (2012). Hippocampal expression of myelin-associated inhibitors is induced with age-related cognitive decline and correlates with deficits of spatial learning and memory. *J. Neurochem.*, 121:77–98.

Vargha Khadem, F., Gadian, D. G., Watkins, K. E., Connelly, A., van Paesschen, W., and Mishkin, M. (1997). Differential effects of early hippocampal pathology on episodic and semantic memory. *Science*, 277:376–380.

Venkatesh, K., Chivatakarn, O., Lee, H., Joshi, P. S., Kantor, D. B., Newman, B. a., Mage, R., Rader, C., and Giger, R. J. (2005). The Nogo-66 receptor homolog NgR2 is a sialic acid-dependent receptor selective for myelin-associated glycoprotein. *J. Neurosci.*, 25:808–822.

Voeltz, G. K., Prinz, W. a., Shibata, Y., Rist, J. M., and Rapoport, T. a. (2006). A class of membrane proteins shaping the tubular endoplasmic reticulum. *Cell*, 124:573–86.

von Schack, D., Casademunt, E., Schweigreiter, R., Meyer, M., Bibel, M., and Dechant, G. (2001). Complete ablation of the neurotrophin receptor p75NTR causes defects both in the nervous and the vascular system. *Nat. Neurosci.*, 4:977–978.

Wang, K. C., Kim, J. a., Sivasankaran, R., Segal, R., and He, Z. (2002a). P75 interacts with the Nogo receptor as a co-receptor for Nogo, MAG and OMgp. *Nature*, 420:74–78.

Wang, X., Chun, S.-j., Treloar, H., Vartanian, T., Greer, C. A., and Strittmatter, S. M. (2002b). Localization of Nogo-A and Nogo-66 Receptor Proteins at Sites of Axon-Myelin and Synaptic Contact. *J. Neurosci.*, 22:5505–5515.

Wills, Z. P., Mandel-Brehm, C., Mardinly, A. R., McCord, A. E., Giger, R. J., and Greenberg, M. E. (2012). The nogo receptor family restricts synapse number in the developing hippocampus. *Neuron*, 73:466–481.

Woo, N. H., Teng, H. K., Siao, C.-J., Chiaruttini, C., Pang, P. T., Milner, T. a., Hempstead, B. L., and Lu, B. (2005). Activation of p75NTR by proBDNF facilitates hippocampal long-term depression. *Nat. Neurosci.*, 8:1069–1077.

Xu, B., Gottschalk, W., Chow, A., Wilson, R. I., Schnell, E., Zang, K., Wang, D., Nicoll, R. a., Lu, B., and Reichardt, L. F. (2000). The role of brain-derived neurotrophic factor receptors in the mature hippocampus: modulation of long-term potentiation through a presynaptic mechanism involving TrkB. *J. Neurosci.*, 20:6888–6897.

Yamashita, T. and Tohyama, M. (2003). The p75 receptor acts as a displacement factor that releases Rho from Rho-GDI. *Nat. Neurosci.*, 6:461–467.

Yiu, G. and He, Z. (2006). Glial inhibition of CNS axon regeneration. *Nat. Rev. Neurosci.*, 7:617–27.

Yuste, R. (2013). Electrical compartmentalization in dendritic spines. *Annu. Rev. Neurosci.*, 36:429–49.

Zagrebelsky, M., Holz, A., Dechant, G., Barde, Y.-A., Bonhoeffer, T., and Korte, M. (2005). The p75 neurotrophin receptor negatively modulates dendrite complexity and spine density in hippocampal neurons. *J. Neurosci.*, 25:9989–9999.

Zagrebelsky, M. and Korte, M. (2014). Maintaining stable memory engrams: New roles for Nogo-A in the CNS. *Neuroscience*, 283:17–25.

Zagrebelsky, M., Schweigreiter, R., Bandtlow, C. E., Schwab, M. E., and Korte, M. (2010). Nogo-A stabilizes the architecture of hippocampal neurons. *J. Neurosci.*, 30:13220–13234.

Zemmar, A., Weinmann, O., Kellner, Y., Yu, X., Vicente, R., Gullo, M., Kasper, H., Lussi, K., Ristic, Z., Luft, A. R., Rioult-Pedotti, M., Zuo, Y., Zagrebelsky, M., and Schwab, M. E. (2014). Neutralization of nogo-a enhances synaptic plasticity in the rodent motor cortex and improves motor learning in vivo. *J. Neurosci.*, 34:8685–8698.

Zhou, Q., Homma, K. J., and Poo, M.-m. (2004). Shrinkage of dendritic spines associated with long-term depression of hippocampal synapses. *Neuron*, 44:749–57.

Zörner, B. and Schwab, M. E. (2010). Anti-Nogo on the go: from animal models to a clinical trial. *Ann. N. Y. Acad. Sci.*, 1198:22–34.